ФИЗИКА ЭЛЕМЕНТАРНЫХ ЧАСТИЦ И АТОМНОГО ЯДРА
2001. Т. 32. ВЫП. 3

УДК 514.763.4

TOWARDS AN ALGEBRAIC CLASSIFICATION OF CALABI–YAU MANIFOLDS

Study of $K3$ Spaces

F. Anselmo

INFN–Bologna, Bologna, Italy

J. Ellis

Theory Division, CERN, CH-1211 Geneva, Switzerland

D.V. Nanopoulos

Dept. of Physics, Texas A & M University, College Station, TX 77843-4242, USA,
HARC, The Mitchell Campus, Woodlands, TX 77381, USA,
and Academy of Athens, 28 Panepistimiou Avenue, Athens 10679, Greece

G. Volkov

Theory Division, CERN, CH-1211 Geneva, Switzerland
and Theory Division, Institute for High-Energy Physics,
Protvino, Russia

«ФИЗИКА ЭЛЕМЕНТАРНЫХ ЧАСТИЦ И АТОМНОГО ЯДРА»
2001, ТОМ 32, ВЫП. 3

УДК 514.763.4

TOWARDS AN ALGEBRAIC CLASSIFICATION OF CALABI–YAU MANIFOLDS
Study of $K3$ Spaces

F. Anselmo

INFN–Bologna, Bologna, Italy

J. Ellis

Theory Division, CERN, CH-1211 Geneva, Switzerland

D.V. Nanopoulos

Dept. of Physics, Texas A & M University, College Station, TX 77843-4242, USA,
HARC, The Mitchell Campus, Woodlands, TX 77381, USA,
and Academy of Athens, 28 Panepistimiou Avenue, Athens 10679, Greece

G. Volkov

Theory Division, CERN, CH-1211 Geneva, Switzerland
and Theory Division, Institute for High-Energy Physics,
Protvino, Russia

We present an inductive algebraic approach to the systematic construction and classification of generalized Calabi–Yau (CY) manifolds in different numbers of complex dimensions, based on Batyrev's formulation of CY manifolds as toric varieties in weighted complex projective spaces associated with reflexive polyhedra. We show how the allowed weight vectors in lower dimensions may be extended to higher dimensions, emphasizing the roles of projection and intersection in their dual description, and the natural appearance of Cartan–Lie algebra structures. The 50 allowed extended four-dimensional vectors may be combined in pairs (triples) to form 22 (4) chains containing 90 (91) $K3$ spaces, of which 94 are distinct, and one further $K3$ space is found using duality. In the case of CY_3 spaces, pairs (triples) of the 10270 allowed extended vectors yield 4242 (259) chains with $K3$ (elliptic) fibers containing 730 additional $K3$ polyhedra. A more complete study of CY_3 spaces is left for later work.

На основе формулировки Батырева многообразий Калаби–Яо (КЯ) как торических множеств во взвешенных комплексных проективных пространствах, ассоциированных с рефлексивными полиэдрами, предложен индуктивный алгебраический подход к систематическому построению и классификации обобщенных многообразий КЯ для различных комплексных размерностей. Показано, как допустимые весовые векторы в низших размерностях могут быть расширены для высших размерностей. При этом отмечена роль проектирования и пересечения в их дуальном описании и естественное появление алгебраических структур Картана–Ли. Пятьдесят допустимых расширенных четырехмерных векторов могут быть скомбинированы в пары (тройки), формирующие 22 (4) цепочки, содержащие 90 (91) $K3$-пространств, из которых 94 являются особыми, а одно $K3$-пространство находится с использованием дуальности. В случае пространств CY_3

пары (тройки) из 10270 допустимых расширенных векторов дают 4242 (259) цепочек с $K3$ (эллиптическими)-расслоениями, содержащими 730 дополнительных $K3$-полиэдров. Более полное изучение CY_3-пространств будет приведено в следующей работе.

1. INTRODUCTION

One of the outstanding issues in both string theory and phenomenology is the choice of vacuum. Recent dramatic advances in the nonperturbative understanding of strings have demonstrated that all string theories, thought previously to be distinct, are in fact related by various dualities, and can be regarded as different phases of a single underlying theory, called variously M and/or F theory [1]. This deeper nonperturbative understanding does not alter the fact that many classical string vacua appear equally consistent at the perturbative level. However, the new nonperturbative methods may provide us with new tools to understand transitions between these classical vacua, and perhaps eventually provide a dynamical criterion for deciding which vacuum is preferred physically [2, 3].

Consistent string vacua are constrained by the principles of quantum mechanics applied to extended objects. At the classical level, these are expressed in the conformal symmetry of the supersymmetric world-sheet field theory. Consistent quantization of the string must confront a possible anomaly in conformal symmetry, as manifested in a net nonzero central charge of the Virasoro algebra. Early studies of the quantum mechanics of extended objects indicated that strings could not survive in the familiar dimension $D = 3 + 1$ of our space-time. The way initially used to cancel the conformal anomaly was to choose appropriately the dimension of the ambient space-time, for example, $D = 25 + 1$ for bosonic strings and $D = 9 + 1$ for the supersymmetric and heterotic strings.

This suggested that the surplus $n = 6$ real dimensions should be compactified. The simplest possibility is on a Calabi–Yau manifold [4], which is defined by the following conditions:

- It has a complex structure, with $N = 3$ complex dimensions required for the $D = 9 + 1 \to 3 + 1$ case of most direct interest, though all the cases $N = 1, 2, 3, 4, ...$ have some interest.
- It is compact.
- It has a Kähler structure.
- It has holonomy group $SU(n)$ or $Sp(n)$, e.g., $SU(3)$ in the $N = 3$ case.

It has subsequently been realized that one could compactify on an orbifold [5], rather than a manifold, and also that generalized heterotic strings could be formulated directly in $D = 3+1$ dimensions, with extra world-sheet degrees of freedom replacing the surplus space coordinates. More recently, the nonperturbative formulation of the theory in eleven or twelve dimensions, as M or F theory, has opened up new possibilities [6]. However, Calabi–Yau compactifications continue to play a key role in the search for realistic four-dimensional string models, motivating us to revisit their classification.

One of the most important tools in the investigation of such complex manifolds is the feature that their singularities are connected with the structure of Lie algebras. Kaluza was the first to attempt to understand this circumstance, and used this idea to embark on the unification of all the gauge interactions known at that time, namely electromagnetism and gravitation. These ideas were subsequently extended to non-Abelian gauge theories, and string theory can be regarded as the latest stage in the evolution of this programme.

The three-complex-dimensional CY manifolds can be situated in a sequence of complex spaces of increasing dimensions: two-real- (one-complex-)dimensional tori T_2, the two-complex-dimensional $K3$ spaces, the three-complex-dimensional CY_3 themselves, four-complex-dimensional CY_4, etc., whose topological structure and classification become progressively more complicated. Their topologies may be described by the Betti–Hodge numbers which count the numbers of distinct one-, two-, three-dimensional, ... cycles (holes,...). The topological data of the different CY manifolds determine their physical properties, such as the different numbers of generations N_g (which are related to the Euler characteristics of CY_3 spaces), etc. This emphasizes the desirability of approaching systematically the problem of their classification and the relations between, e.g., CY_3 manifolds with different values of the Euler characteristic and hence the number of generations N_g. Since some nonperturbative tools now exist for studying transitions between different CY manifolds, one could hope eventually to find some dynamical criterion for determining N_g.

The topologies and classification of the lower-dimensional spaces in this sequence are better known: although our ultimate objective is deeper understanding of CY_3 spaces, in this paper we study as a warm-up problem the simpler case of the two-complex-dimensional $K3$ hypersurfaces. These are of considerable interest in their own right, since, for example, they may appear as fibrations of higher-dimensional CY_n spaces. It is well known that any two $K3$ spaces are diffeomorphic to each other. This can be seen, for example, by using the polyhedron techniques of Batyrev [7] discussed in Sections 2 and 3, to calculate the Betti–Hodge invariants for all the $K3$ hypersurfaces corresponding to the $\mathbf{k}_4$ vectors we found. It is easy to check that Batyrev's results yield the same Euler number 24 for all $K3$ manifolds [8].

The quasi-homogeneous polynomial equations (hereafter called CY equations) whose zeroes define the CY spaces as hypersurfaces in complex projective space are defined (2.6), (2.7), (2.8), (2.9) by projective vectors $\mathbf{k}$, whose components specify the exponents of the polynomials. The number of CY manifolds is large but finite, as follows from the property of reflexivity introduced in Section 2. The central problem in the understanding of classification of these manifolds may be expressed as that of understanding the set of possible projective vectors

$\mathbf{k} = (k_1, \ldots, k_{n+1})$, the corresponding Lie algebras and their representations. More precisely, the classification of all CY manifolds contains the following problems:

• To study the structure of the $K3, CY_3, ...$ projective vectors $\mathbf{k}_n$, in particular, to find the links with the projective vectors of lower dimensions: $D = n-1, n-2, ...$

• To establish the web of connections between all the projective vectors $\mathbf{k}_n$ of the same dimension.

• To find an algebraic description of the geometrical structure for all projective vectors, and calculate the corresponding Betti–Hodge invariants.

• To establish the connections between the projective vectors $\mathbf{k}_n$, the singularities of the corresponding CY hypersurfaces, the gauge groups and their matter representations, such as the number of generations, N_g.

• To study the duality symmetries and hypermodular transformations of the projective vectors $\mathbf{k}_n$.

In addition to the topological properties and gauge symmetries already mentioned, it is now well known that string vacua may be related by duality symmetries. This feature is familiar even from simple compactifications on S_1 spaces of radius R, which revealed a symmetry: $R \to 1/R$ [9]. In the case of compactifications on tori, there are known to be S, T, and U dualities that interrelate five string theories and play key roles in the formulations of M and F theories [10]. Compactifications on different types of CY manifolds have also been used extensively in verifying these string dualities [10]. For example, in proving the duality between type-II A and type-II B string theories, essential use was made of the very important observation that all CY manifolds have mirror partners [7,11–15]. Thus, duality in string theory found its origins in a duality of complex geometry.

Further information about string/M/F theory and its compactifications on CY manifolds can be obtained using the methods of *toric geometry*. The set of homogeneous polynomials of degree d in the complex projective space CP^n defined by the vector $\mathbf{k}_{n+1}$ with $d = k_1 + ...k_{n+1}$ defines a convex *reflexive* polyhedron *, whose intersection with the integer lattice corresponds to the polynomials of the CY equation. Therefore, instead of studying the complex hypersurfaces directly, one can study the geometry of polyhedrons. This method was first used to look for the solutions of the algebraic equations of degree five or more in terms of radicals [16]. Thus, the problem of classifying CY hypersurfaces is also connected with the problem of solving high-degree polynomial equations in terms of radicals. The solutions of quintic- and higher-degree algebraic equations in terms of radicals may be expressed using elliptic and hyperelliptic functions, respectively. Specifically, it is known that CY manifolds may be represented using double-periodic elliptic or multi-periodic hyperelliptic functions [17]. These functions

*The notion of a reflexive polyhedron is introduced and defined in Section 2.

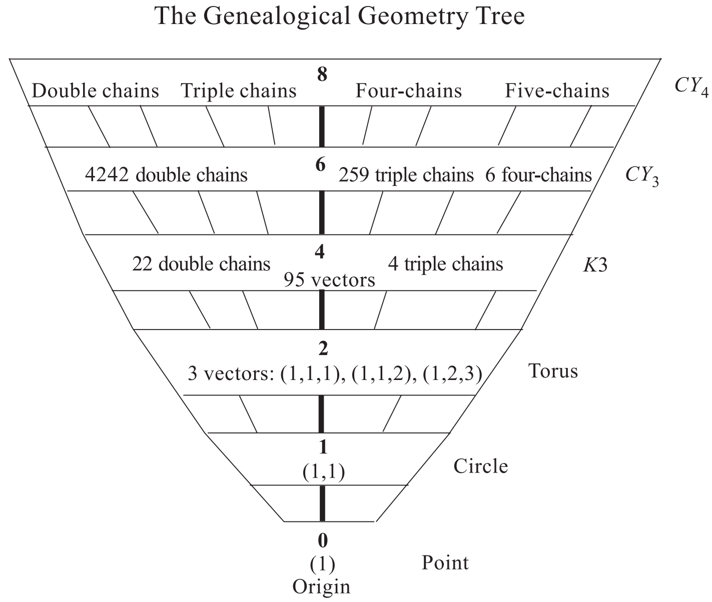

Fig. 1. The genealogical tree of reflexive projective vectors in different dimensions up to $d = 4$

have therefore been used to describe the behaviour of strings, and they should also be used to construct the ambient space-time in which strings move.

We embark here on a systematic classification of $K3$ manifolds, as a prelude to a subsequent classification of CY_3 manifolds, based on their construction in the framework of toric geometry. Within this approach, CY manifolds and their mirrors are toric varieties that can be associated with polyhedra in spaces of various dimensions. We propose here an inductive algebraic-geometric construction of the projective vectors **k** that define these polyhedra and the related $K3$ and CY spaces. This method has the potential to become exhaustive up to any desired complex dimensionality $d = 1, 2, 3, 4, 5, 6, ...$ (see Figure 1), limited essentially by the available computer power. As a first step in this programme, we present in this article a construction of $K3$ spaces, which is complete for those described by simple polynomial zeroes, and in principle for $K3$ spaces obtained as the complete intersections of pairs or triples of such polynomial zero loci. In the construction of projective vectors corresponding to hypersurfaces without an intersection with one internal point, the duality between a complex manifold and its mirror (which does contain an intersection) plays an important role. We discuss here also aspects of the CY_3 construction that are relevant for the classification of $K3$ spaces. We also indicate already how one may generate CY_3 manifolds with elliptic fibrations or $K3$ fibers. More aspects of our CY_3 construction are left for later work.

To get the flavour of our construction, which is based on the formalism reviewed in Sections 2 and 3 [7] and is discussed in more detail in Sections 4 *et seq.*, consider first CP^1 space. Starting from the trivial unit «vector» $\mathbf{k}_1 \equiv (1)$, we introduce two *singly-extended* basic vectors

$$\mathbf{k}_1^{ex'} = (0,1),\ \mathbf{k}_1^{ex''} = (1,0), \tag{1.1}$$

obtained by combining $\mathbf{k}_1$ with zero in the two possible ways. The basic vectors (1.1) correspond to the sets of polynomials

$$\begin{aligned} x^n \cdot y \ &\Longrightarrow\ \{\boldsymbol{\mu}_1\} = (n,\,1): \quad \boldsymbol{\mu}_1 \cdot \mathbf{k}_1^{ex'} = d = 1, \\ x \cdot y^m \ &\Longrightarrow\ \{\boldsymbol{\mu}_2\} = (1,\,m): \quad \boldsymbol{\mu}_2 \cdot \mathbf{k}_1^{ex''} = d = 1, \end{aligned} \tag{1.2}$$

respectively. The only polynomial common to these two sequences is xy, which may be considered as corresponding to the trivial «vector» $\mathbf{k}_1 = (1)$. Consider now the composite vector $\mathbf{k}_2 = (1,1)$, which can be constructed out of the basic vectors (1.1), and is easily seen to correspond to the following three monomials of two complex arguments (x,y):

$$\begin{aligned} \{x^2, x\cdot y,\, y^2\} \Longrightarrow \boldsymbol{\mu}|_{i=1,2,3} \ &=\ \{(2,0),(1,1),(0,2)\} \Longrightarrow \\ \boldsymbol{\mu}'|_{i=1,2,3} \equiv \boldsymbol{\mu}|_{i=1,2,3} - \mathbf{1} \ &=\ \{(1,-1),(0,0),(-1,+1)\}, \end{aligned} \tag{1.3}$$

where we have used the condition: $\boldsymbol{\mu}\cdot\mathbf{k}_2 = \mu_1\cdot 1 + \mu_2\cdot 1 = d = 2$, corresponding to $\boldsymbol{\mu}\,'\cdot\mathbf{k}_2 = 0$, and we denote by d the dimensionality of the projective vectors. It is convenient to parametrize (1.3) in terms of the new basis vector $\mathbf{e} = (-1,1)$:

$$\boldsymbol{\mu}'|_{i=1,2,3} \Longrightarrow (\mathbf{e})|_{i=1,2,3} = \{(-1),(0),(+1)\} \times \mathbf{e}. \tag{1.4}$$

The three points $(2,0),(1,1),(0,2)$ (or $-1,0,+1$) corresponding to the composite vector $k_2 = (1,1)$ may be considered as composing a degenerate linear polyhedron with two integer vertices $\{(2,0),(0,2)\}$ (± 1) and one central interior point $(1,1)$ (0). As we see in more detail later, this polyhedron is self-dual, or reflexive as defined in Section 2.

To describe CY_1 spaces in CP^2 projective space, via the analogous projective vectors $\mathbf{k}_3 = (1,1,1),(1,1,2),(1,2,3)$, that are associated with the corresponding polynomial zero loci, one may introduce the two following types of extended vectors: the *doubly-extended basic* vectors

$$\mathbf{k}_1^{ex} = (0,0,1),\ (0,1,0),\ (1,0,0) \tag{1.5}$$

obtained by adding zero to the two-dimensional basic vectors (1.1) in all possible ways, and the three simple extensions of the composite vector $\mathbf{k}_2 = (1,1)$:

$$\mathbf{k}_2^{ex} = (0,1,1),\ (1,0,1),\ (1,1,0). \tag{1.6}$$

Then, out of all the extended vectors (1.5) and (1.6) and the corresponding sets of monomials, one should consider only those pairs (triples) whose common monomials correspond to the composite vector $\mathbf{k}_2 = (1,1)$ (to the unit vector) which produces the reflexive linear polyhedron with three integer points (a single point). The condition of reflexivity restricted to the extended vector pairs (triples), ... will also be very important for constructing the closed sets of higher-dimensional projective vectors (again reflexive).

For example, consider one such 'good' pair,

$$\mathbf{k}_2^{ex} \;=\; (0,1,1) \;\Longleftrightarrow\; \mathbf{k}_1^{ex} \;=\; (1,0,0), \tag{1.7}$$

with the corresponding set of monomials,

$$\begin{aligned} \{x^m \cdot y^2\} &\;\Longrightarrow\; \boldsymbol{\mu} = (m,2,0), \\ \{x^n \cdot y \cdot z\} &\;\Longrightarrow\; \boldsymbol{\mu} = (n,1,1), \\ \{x^p \cdot z^2\} &\;\Longrightarrow\; \boldsymbol{\mu} = (p,0,2), \\ \boldsymbol{\mu}_i \cdot \mathbf{k}_2^{ex} &\;=\; 2, \end{aligned} \tag{1.8}$$

and

$$\begin{aligned} \{x \cdot y^k \cdot z^l\} &\;\Longrightarrow\; \boldsymbol{\mu} = (1,k,l), \\ \boldsymbol{\mu} \cdot \mathbf{k}_1^{ex} &\;=\; 1. \end{aligned} \tag{1.9}$$

The common action of these two extended vectors, (0,1,1) and (1,0,0), gives as results only the following three monomials:

$$\begin{aligned} &\{x \cdot y^2,\, x \cdot y \cdot z,\, x \cdot z^2\} \;\Longrightarrow \\ \boldsymbol{\mu}|_{i=1,2,3} &\;=\; \{(1,2,0),\, (1,1,1),\, (1,0,2)\} \;\Longrightarrow \\ \boldsymbol{\mu}|_{i=1,2,3} - \mathbf{1} &\;=\; \{(0,1,-1),\, (0,0,0),\, (0,-1,1)\} \;\Longrightarrow \\ \mathbf{e}|_{i=1,2,3} &\;=\; \{(-1),\, (0),\, (1)\} \end{aligned} \tag{1.10}$$

which correspond to the CP^1 case. Such pairs or triples may be termed «reflexive» pairs or triples, because of the vertices $\mathbf{e}|_{i=1,2,3}$ above a generate (degenerate) reflexive polyhedron.

Such pairs, triples and higher-order sets of projective vectors $\mathbf{k}_1$ may be used to define *chains* of integer-linear combinations, as explained in more detail in Subsection 4.1:

$$m_1\mathbf{k}_1 + m_2\mathbf{k}_2 + \ldots \tag{1.11}$$

We use the term *eldest vector* for the leading entry in any such chain, with minimal values of $m_1, m_2, \ldots$ In the above case, there are just two distinct types of «reflexive» pairs: $\{(0,0,1),(1,1,0)\}$ and $\{(0,1,1),(1,0,1)\}$, which give rise to two such chains: $\{(1,1,1),(1,1,2)\}$ and $\{(1,1,2),\ (1,2,3)\}$. There is only one useful «reflexive» triple: $\{(0,0,1),(0,1,0),(1,0,0)\}$ defining a non-trivial three-vector chain. Together, these chains can be used to construct all three projective $\mathbf{k}_2$ vectors. The second possible «reflexive» triple $\{(0,1,1),(1,0,1),(1,1,0)\}$ produces a chain that consists of only one projective $\mathbf{k}_3$ vector: $(1,1,1)$.

In addition to the zero loci of single polynomials, CY spaces may be found by higher-level contructions as the intersections of the zero loci of two or more polynomial loci. The higher-level CY_1 spaces found in this way are given in the last Section of this paper.

In the case of the $K3$ hypersurfaces in CP^3 projective space, our construction starts from the five possible types of extended vectors, with all their possible Galois groups of permutations. These types are the triply-extended basic vectors with the cyclic C_4 group of permutations,

$$\mathbf{k}_1^{ex} = (0,0,0,1): \ |C_4| = 4, \tag{1.12}$$

the doubly-extended composite vectors with the D_3 dihedral group of permutations,

$$\mathbf{k}_2^{ex} = (0,0,1,1): \ |D_3| = 6, \tag{1.13}$$

and the following singly-extended composite vectors with the cyclic C_4, alternating A_4 and symmetric S_4 groups of permutations, respectively:

$$\mathbf{k}_3^{ex} \ = \ (0,1,1,1): \ |C_4| = 4, \tag{1.14}$$
$$\mathbf{k}_3^{ex} \ = \ (0,1,1,2): \ |A_4| = 12, \tag{1.15}$$
$$\mathbf{k}_3^{ex} \ = \ (0,1,2,3): \ |S_4| = 24. \tag{1.16}$$

The A_4 and S_4 groups of permutations can be identified with the tetrahedral T and octahedral O rotation groups, respectively. Combining these 50 extended vectors in pairs, we find 22 pairs whose common actions correspond to reflexive polyhedra in the plane. These give rise to 22 chains (lattices parametrized by two positive integers), which together yield 90 $\mathbf{k}_4$ vectors based on such extended structures, that are discussed in more detail in Section 5. In addition, there exist just four triples constructed from the 10 extended vectors $(0,0,0,1)$ + permutations and $(0,0,1,1)$ + permutations whose common actions give a unique reflexive polyhedron on the line: $(-1),(0),(+1)$. The corresponding four triple chains (lattices parametrized by three positive integers) yield 91 $\mathbf{k}_4$ vectors, as discussed in Section 6. As also discussed there, it turns out that most of the $\mathbf{k}_4$ vectors obtained from the triple combinations are already included among those found in the double chains, so that the combined number of distinct vectors is just 94. The total number of vectors is, however, 95 (see Table 1), because there exists, in addition to the above enumeration, a single vector $\mathbf{k}_4 = (7, 8, 9, 12)$ which has only a trivial intersection consisting just of the zero point. This can be found within our approach using the nontrivial projection structure of its dual, which is an example of the importance of duality in our classification, as discussed in Section 7.

To find all CY manifolds, and thereby to close their algebra with respect the duality between *intersection* and *projection* that is described in more detail in Sections 3 and 4, one must consider how to classify the projective structures of CY manifolds. Some of the 22 chains are dual with respect to the «intersection-projection» structure, but more analysis is required to close the CY algebra. As discussed in Section 7, it is useful for this purpose to look for the so-called *invariant* directions. To find all such *invariant* directions in the case of $K3$ spaces, one should consider all triples selected from the following five extended vectors: $(0,0,0,1), (0,0,1,1), (0,1,1,1), (0,1,1,2), (0,1,2,3)$, and their possible permutations, whose intersections give the following five types of *invariant* directions defined by two monomials:

$$\begin{aligned}
\boldsymbol{\pi}_1^\alpha &= \{(1,1,1,1) \to (0,1,1,3)\}, \ \alpha = 1,\,2, \\
\boldsymbol{\pi}_2^\alpha &= \{(1,1,1,1) \to (0,0,0,3)\}, \ \alpha = 1,\,2,\,3,\,4, \\
\boldsymbol{\pi}_3^\alpha &= \{(1,1,1,1) \to (0,0,1,3)\}, \ \alpha = 1,\,2,\,3,\,4, \\
\boldsymbol{\pi}_4^\alpha &= \{(1,1,1,1) \to (0,0,0,4)\}, \ \alpha = 1,\,2,\,3,\,4, \\
\boldsymbol{\pi}_5^\alpha &= \{(1,1,1,1) \to (0,0,1,4)\}, \ \alpha = 1,
\end{aligned} \tag{1.17}$$

and the following three types of *invariant* directions defined by three monomials:

$$\begin{aligned}
\boldsymbol{\pi}_6^\alpha &= \{(0,2,1,1) \to (1,1,1,1) \to (2,0,1,1)\}, \ \alpha = 1,\,2, \\
\boldsymbol{\pi}_7^\alpha &= \{(0,0,1,2) \to (1,1,1,1) \to (2,2,1,0)\}, \ \alpha = 1,\,2,\,3,\,4, \\
\boldsymbol{\pi}_8^\alpha &= \{(0,0,0,2) \to (1,1,1,1) \to (2,2,2,0)\}, \ \alpha = 1,\,2,\,3,\,4,
\end{aligned} \tag{1.18}$$

respectively. Each double intersection of a pair of extended vectors from one of these triples gives the same «good» planar polyhedron whose intersection with the plane integer lattice Z_2 has just one interior point.

By this method, one can classify the projective vectors by projections, finding 78 projective vectors which can be characterized by their invariant directions. Taking into account the projective vectors with intersection-projection duality that have already been found by the double-intersection method, one can recover all 95 $K3$ projective vectors, including the exceptional vector $(7, 8, 9, 12)$ that was not found previously among the double and triple chains.

Table 1: **The algebraic structure of the 95 projective vectors characterizing $K3$ spaces. The numbers of points/vertices in the corresponding polyhedra (their duals) are denoted by N/V (N^*/V^*), and their Picard numbers are denoted by Pic (Pic*). In each case, we also list the double, triple chains and projective chains where the corresponding $K3$ vector may be found**

ℵ	$\mathbf{k}_4$	N	N^*	V	V^*	Pic	Pic*	Double chains	Triple chains	Projective chains
1	(1, 1, 1, 1)	35	5	4	4	1	19	I, VII, X, XII	I	$\boldsymbol{\pi}_3, \boldsymbol{\pi}_4, \boldsymbol{\pi}_6$
2	(1, 1, 1, 2)	34	6	6	5	2	18	I, IV, XI, XIV	I, II	$\boldsymbol{\pi}_1, \boldsymbol{\pi}_3, \boldsymbol{\pi}_5, \boldsymbol{\pi}_6, \boldsymbol{\pi}_7$
3	(1, 1, 1, 3)	39	6	4	4	1	19	I, V, XX	I, III	$\boldsymbol{\pi}_8$
4	(1, 1, 2, 2)	30	6	4	4	4	18	$II, IV, X,$ $XXI, XXII$	I, II, IV	$\boldsymbol{\pi}_2, \boldsymbol{\pi}_6, \boldsymbol{\pi}_7$
5	(1, 1, 2, 3)	31	8	7	6	4	16	$IV, XI, XIII, XV$	$I, II,$	$\boldsymbol{\pi}_1, \boldsymbol{\pi}_3, \boldsymbol{\pi}_6, \boldsymbol{\pi}_7$
6	(1, 1, 2, 4)	35	7	4	4	3	18	IV, V, VI, XVI	I, II, III	$\boldsymbol{\pi}_8$
7	(1, 1, 3, 4)	33	9	5	5	4	16	$XI, XVII$	I, II	$\boldsymbol{\pi}_2, \boldsymbol{\pi}_6$
8	(1, 1, 3, 5)	36	9	5	5	3	17	$V, XVIII$	I, III	$\boldsymbol{\pi}_8$
9	(1, 1, 4, 6)	39	9	4	4	2	18	V, XIX	I, III	
10	(1, 2, 2, 3)	24	8	6	5	7	16	$VII, VIII, XI,$ $XV, XXII$	I, II, IV	$\boldsymbol{\pi}_1, \boldsymbol{\pi}_3, \boldsymbol{\pi}_4, \boldsymbol{\pi}_7$
11	(1, 2, 2, 5)	28	8	4	4	6	18	V, IX, XVI	I, III	$\boldsymbol{\pi}_8$
12	(1, 2, 3, 3)	23	8	6	5	8	16	II, III, XIV, XV	I, II	$\boldsymbol{\pi}_1, \boldsymbol{\pi}_2, \boldsymbol{\pi}_7$
13	(1, 2, 3, 4)	23	11	7	6	8	13	$XII, XIII,$ $XV, XXII$	II, IV	$\boldsymbol{\pi}_1, \boldsymbol{\pi}_3, \boldsymbol{\pi}_7$
14	(1, 2, 3, 5)	24	13	8	7	8	12	$XIII, XIV, XV$	II	$\boldsymbol{\pi}_1, \boldsymbol{\pi}_3, \boldsymbol{\pi}_5, \boldsymbol{\pi}_7$
15	(1, 2, 3, 6)	27	9	4	4	7	16	VI, XV, XVI, XX	II, III	$\boldsymbol{\pi}_8$
16	(1, 2, 4, 5)	24	12	5	5	8	14	$XVII, XXI, XXII$	II, IV	$\boldsymbol{\pi}_1, \boldsymbol{\pi}_2$
17	(1, 2, 4, 7)	27	12	5	5	7	15	$XVI, XVIII$	III	$\boldsymbol{\pi}_8$
18	(1, 2, 5, 7)	26	17	6	6	8	12	$XVII$	II	$\boldsymbol{\pi}_1, \boldsymbol{\pi}_2$
19	(1, 2, 5, 8)	28	14	5	5	7	14	$XVI, XVIII$	III	$\boldsymbol{\pi}_8$
20	(1, 2, 6, 9)	30	12	4	4	6	16	XVI, XIX	III	
21	(1, 3, 4, 4)	21	9	4	4	10	16	$II, VIII$	I, II	$\boldsymbol{\pi}_2, \boldsymbol{\pi}_7$
22	(1, 3, 4, 5)	20	15	7	7	10	10	$XIII, XIV$	II	$\boldsymbol{\pi}_7$
23	(1, 3, 4, 7)	22	17	6	6	10	10	$XIII$	II	$\boldsymbol{\pi}_3, \boldsymbol{\pi}_7$
24	(1, 3, 4, 8)	24	12	5	5	9	14	VI, IX	II, III	$\boldsymbol{\pi}_8$
25	(1, 3, 5, 6)	21	15	5	5	10	12	$III, XVII$	II	
26	(1, 3, 5, 9)	24	15	5	5	9	13	$XVIII, XX$	III	$\boldsymbol{\pi}_8$
27	(1, 3, 7, 10)	24	24	4	4	10	10	$XVII$	II	$\boldsymbol{\pi}_2$
28	(1, 3, 7, 11)	25	20	5	5	9	11	$XVIII$	III	$\boldsymbol{\pi}_8$
29	(1, 3, 8, 12)	27	15	4	4	8	14	XIX	III	
30	(1, 4, 5, 6)	19	17	6	6	11	9	$VIII, XIII$	II	$\boldsymbol{\pi}_7$
31	(1, 4, 5, 10)	23	13	4	4	10	14	VI	II, III	$\boldsymbol{\pi}_8$
32	(1, 4, 6, 7)	19	20	6	6	11	9	$XVII$	II	
33	(1, 4, 6, 11)	22	20	6	6	10	10	$IX, XVIII$	III	
34	(1, 4, 9, 14)	24	24	4	4	10	10	$XVIII$	III	$\boldsymbol{\pi}_8$
35	(1, 4, 10, 15)	25	20	5	5	9	11	XIX	III	
36	(1, 5, 7, 8)	18	24	5	5	12	8	$XVII$	II	
37	(1, 5, 7, 13)	21	24	5	5	11	9	$XVIII$	III	
38	(1, 5, 12, 18)	24	24	4	4	10	10	XIX	III	
39	(1, 6, 8, 9)	18	24	5	5	12	8	$XVII$	II	
40	(1, 6, 8, 15)	21	24	5	5	11	9	$XVIII$	III	
41	(1, 6, 14, 21)	24	24	4	4	10	10	XIX	III	
42	(2, 2, 3, 5)	17	11	5	5	11	14	$VIII, XI$	I, II	$\boldsymbol{\pi}_4, \boldsymbol{\pi}_6, \boldsymbol{\pi}_7$
43	(2, 2, 3, 7)	19	11	5	5	10	16	V, IX	I, III	$\boldsymbol{\pi}_8$
44	(2, 3, 3, 4)	15	9	4	4	12	16	III, VII, XXI	I, IV	$\boldsymbol{\pi}_1, \boldsymbol{\pi}_2, \boldsymbol{\pi}_3, \boldsymbol{\pi}_4, \boldsymbol{\pi}_6$
45	(2, 3, 4, 5)	13	16	7	7	13	9	$XII, XIV, XXII$	II, IV	$\boldsymbol{\pi}_1, \boldsymbol{\pi}_3, \boldsymbol{\pi}_5, \boldsymbol{\pi}_7$
46	(2, 3, 4, 7)	14	18	6	6	13	10	$VIII, XIV$	II	$\boldsymbol{\pi}_1, \boldsymbol{\pi}_3, \boldsymbol{\pi}_4, \boldsymbol{\pi}_5, \boldsymbol{\pi}_7$
47	(2, 3, 4, 9)	16	14	5	5	12	13	IX, XVI, XX	III	$\boldsymbol{\pi}_8$
48	(2, 3, 5, 5)	14	11	6	5	14	14	II	I, II	$\boldsymbol{\pi}_2, \boldsymbol{\pi}_7$
49	(2, 3, 5, 7)	13	20	8	8	14	6	$XIII$	II	$\boldsymbol{\pi}_3, \boldsymbol{\pi}_5, \boldsymbol{\pi}_7$
50	(2, 3, 5, 8)	14	20	6	6	14	7	$XIII$	II	$\boldsymbol{\pi}_3, \boldsymbol{\pi}_7$
51	(2, 3, 5, 10)	16	14	5	5	13	12	VI	II, III	$\boldsymbol{\pi}_8$
52	(2, 3, 7, 9)	14	23	6	6	14	8	$XVII$	II	$\boldsymbol{\pi}_2$

Table 1: (cont.)

$\aleph$	$\mathbf{k}_4$	N	N^*	V	V^*	Pic	Pic*	Double chains	Triple chains	Projective chains
53	$(2,3,7,12)$	16	20	5	5	13	10	$XVIII$	III	$\boldsymbol{\pi}_8$
54	$(2,3,8,11)$	15	27	4	4	14	8	$XVII$	II	$\boldsymbol{\pi}_2$
55	$(2,3,8,13)$	16	23	5	5	13	9	$XVIII$	III	$\boldsymbol{\pi}_8$
56	$(2,3,10,15)$	18	18	4	4	12	12	XIX	III	
57	$(2,4,5,9)$	13	23	4	4	14	10	$VIII$	II	$\boldsymbol{\pi}_1, \boldsymbol{\pi}_4, \boldsymbol{\pi}_7$
58	$(2,4,5,11)$	14	19	5	5	13	11	IX, XVI	III	$\boldsymbol{\pi}_8$
59	$(2,5,6,7)$	11	23	5	5	15	7	$VIII$	II	$\boldsymbol{\pi}_3, \boldsymbol{\pi}_4, \boldsymbol{\pi}_7$
60	$(2,5,6,13)$	13	23	5	5	14	9	IX	III	$\boldsymbol{\pi}_8$
61	$(2,5,9,11)$	11	32	6	6	16	4	$XVII$	II	$\boldsymbol{\pi}_2$
62	$(2,5,9,16)$	13	29	5	5	15	6	$XVIII$	III	$\boldsymbol{\pi}_8$
63	$(2,5,14,21)$	15	27	4	4	14	8	XIX	III	
64	$(2,6,7,15)$	13	23	4	4	14	10	IX	III	$\boldsymbol{\pi}_8$
65	$(3,3,4,5)$	12	12	5	5	14	14	III	I	$\boldsymbol{\pi}_2, \boldsymbol{\pi}_3, \boldsymbol{\pi}_5, \boldsymbol{\pi}_6$
66	$(3,4,5,6)$	10	17	6	6	15	9	III, XII, XXI	IV	$\boldsymbol{\pi}_1, \boldsymbol{\pi}_2, \boldsymbol{\pi}_3$
67	$(3,4,5,7)$	9	24	7	8	16	4	XIV	II	$\boldsymbol{\pi}_3, \boldsymbol{\pi}_5, \boldsymbol{\pi}_7$
68	$(3,4,5,8)$	10	22	6	6	16	7	$VIII$	II	$\boldsymbol{\pi}_1, \boldsymbol{\pi}_3, \boldsymbol{\pi}_4, \boldsymbol{\pi}_7$
69	$(3,4,5,12)$	12	18	5	5	15	10	IX, XX	III	$\boldsymbol{\pi}_8$
70	$(3,4,7,10)$	10	26	5	6	17	3	$XIII$	II	$\boldsymbol{\pi}_3, \boldsymbol{\pi}_7$
71	$(3,4,7,14)$	12	18	5	5	16	10	VI	II, III	$\boldsymbol{\pi}_8$
72	$(3,4,10,13)$	10	35	5	5	17	3	$XVII$	II	$\boldsymbol{\pi}_2$
73	$(3,4,10,17)$	11	31	6	6	16	4	$XVIII$	III	$\boldsymbol{\pi}_8$
74	$(3,4,11,18)$	12	30	4	4	16	6	$XVIII$	III	$\boldsymbol{\pi}_8$
75	$(3,4,14,21)$	13	26	5	5	15	7	XIX	III	
76	$(3,5,6,7)$	9	21	5	5	16	8	III		$\boldsymbol{\pi}_1, \boldsymbol{\pi}_2$
77	$(3,5,11,14)$	9	39	4	4	18	2	$XVII$	II	$\boldsymbol{\pi}_2$
78	$(3,5,11,19)$	10	35	5	5	17	3	$XVIII$	III	$\boldsymbol{\pi}_8$
79	$(3,5,16,24)$	12	30	4	4	16	6	XIX	III	
80	$(3,6,7,8)$	9	21	4	4	16	10	III		$\boldsymbol{\pi}_1, \boldsymbol{\pi}_2, \boldsymbol{\pi}_3, \boldsymbol{\pi}_4$
81	$(4,5,6,9)$	8	26	5	6	17	4	XIV	II	$\boldsymbol{\pi}_3, \boldsymbol{\pi}_4, \boldsymbol{\pi}_5, \boldsymbol{\pi}_7$
82	$(4,5,6,15)$	10	20	5	5	16	9	XX	III	$\boldsymbol{\pi}_8$
83	$(4,5,7,9)$	7	32	5	6	18	2		II	$\boldsymbol{\pi}_3, \boldsymbol{\pi}_7$
84	$(4,5,7,16)$	9	27	5	5	17	6	IX	III	$\boldsymbol{\pi}_8$
85	$(4,5,13,22)$	9	39	4	4	18	2	$XVIII$	III	$\boldsymbol{\pi}_8$
86	$(4,5,18,27)$	10	35	5	5	17	3	XIX	III	
87	$(4,6,7,11)$	7	35	4	4	18	3	$VIII$	II	$\boldsymbol{\pi}_4, \boldsymbol{\pi}_5, \boldsymbol{\pi}_7$
88	$(4,6,7,17)$	8	31	5	5	17	4	IX	III	$\boldsymbol{\pi}_8$
89	$(5,6,7,9)$	6	30	5	6	18	2	III		$\boldsymbol{\pi}_2, \boldsymbol{\pi}_3, \boldsymbol{\pi}_5$
90	$(5,6,8,11)$	6	39	4	4	19	1		II	$\boldsymbol{\pi}_3, \boldsymbol{\pi}_7$
91	$(5,6,8,19)$	7	35	5	5	18	2	IX	III	$\boldsymbol{\pi}_8$
92	$(5,6,22,33)$	9	39	4	4	18	2	XIX	III	
93	$(5,7,8,20)$	8	28	4	4	18	6		III	$\boldsymbol{\pi}_8$
94	$(7,8,10,25)$	6	39	4	4	19	1		III	$\boldsymbol{\pi}_8$
95	$(7,8,9,12)$	5	35	4	4	19	1			$\boldsymbol{\pi}_2, \boldsymbol{\pi}_3, \boldsymbol{\pi}_4, \boldsymbol{\pi}_5$

Section 8 of this paper contains a systematic description how various gauge groups emerge associated with singularities in our construction of $K3$ spaces [18]. These are interesting because of their possible role in studies of F theory. Since this may be regarded as a decompactification of type-IIA string, understanding of duality between the heterotic string and type-IIA string in $D = 6$ dimensions can be used to help understand the duality between the heterotic string on T^2 and F theory on an elliptically-fibered $K3$ hypersurface [19]. The gauge group is directly defined by the ADE classification of the quotient singularities of hypersurfaces. The Cartan matrix of the Lie group in this case coincides up to a sign with the intersection matrix of the blown-down divisors. There are two different mechanisms leading to enhanced gauge groups on the F-theory side and on the heterotic side. On the F-theory side, the singularities of the CY hypersurface give rise to the gauge groups, but on the heterotic side the singularities can give an enhancement of the gauge group if «small» instantons of the gauge bundle lie on these singularities [20]. This question has been studied in terms of the numbers of instantons placed on a singularity of type G, where G is a simply-laced group. Studies of groups associated with singularities of $K3$ spaces are also interesting because elliptic CY_n ($n = 3, 4$) manifolds with $K3$ fibers can be considered to study F-theory dual compactifications of the $E_8 \times E_8$ or $SO(32)$ string theory. To do this in toric geometry, it is possible to consider the $K3$ polyhedron fiber as a subpolyhedron of the CY_n polyhedron, and the Dynkin diagrams of the gauge groups of the type-IIA string (F-theory) compactifications on the corresponding threefold (fourfold) can then be seen precisely in the polyhedron of this $K3$ hypersurface. By extension, one could consider the case of an elliptic CY_4 with CY_3 fiber, where the last is a CY hypersurface with $K3$ fiber. We give in Section 8 several detailed examples of group structures associated with chains of $K3$ spaces, which our algebraic approach equips us to study systematically.

Finally, Section 9 provides a brief discussion of CY_3 manifolds and describes how additional CY spaces can be constructed at higher levels as the intersections of multiple polynomial loci. This discussion is illustrated by the examples of higher-level CY_1 and $K3$ spaces obtained via our construction of lower-level $K3$ and CY_3 spaces. We find, for example, 7 new polyhedra describing CY_1 spaces given by «level-one» intersections of pairs of polynomial loci, and three new «level-two» polyhedra given by triple intersections of polynomial loci. In looking for higher-level $K3$ spaces, we start from 100 types of extended vectors in five dimensions, corresponding to 10270 distinct vectors when permutations are taken into account. We find that these give rise to 4242 two-vector chains of CY_3 spaces, 259 triple-vector chains and 6 quadruple-vector chains. Analyzing their internal structures, we find 730 new $K3$ polyhedra at level one, of which 146 can be obtained as intersections of polynomials corresponding to simple polyhedra (points, line segments, triangles and tetrahedra). A complete characterization of higher-level $K3$ spaces given by multiple intersections of polynomial loci lies beyond our present computing scope, and we leave their further study to later work.

2. CALABI–YAU SPACES AS TORIC VARIETIES

We recall that an n-dimensional complex manifold is a $2 \cdot n$-dimensional Riemannian space with a Hermitean metric

$$ds^2 = g_{i\bar{j}} \cdot dz^i \cdot d\bar{z}^{\bar{j}} : \quad g_{ij} = g_{\bar{i}\bar{j}} = 0, \quad g_{i\bar{j}} = \bar{g}_{\bar{j}i} \tag{2.1}$$

on its n complex coordinates z_i. Such a complex manifold is Kähler if the $(1,1)$ differential two-form

$$\Omega = \frac{1}{2} \cdot i \cdot g_{i\bar{j}} \cdot dz^i \Lambda d\bar{z}^{\bar{j}}, \tag{2.2}$$

is closed, i.e., $d\Omega = 0$. In the case of a Kähler manifold, the metric (2.1) is defined by a Kähler potential:

$$g_{i\bar{j}} = \frac{\partial^2 K(z^i, \bar{z}^{\bar{j}})}{\partial z^i \partial \bar{z}^{\bar{j}}}. \tag{2.3}$$

The Kähler property yields the following constraints on components of the Cristoffel symbols:

$$\begin{aligned} \Gamma^i_{\bar{j}k} &= \Gamma^{\bar{i}}_{j\bar{k}} = \Gamma^i_{\bar{j}k} = 0, \\ \Gamma^{\bar{i}}_{\bar{j}\bar{k}} &= \Gamma^{\bar{i}}_{jk} = g^{\bar{i}s} \cdot \frac{\partial g_{\bar{k}s}}{\partial \bar{z}^{\bar{j}}}, \end{aligned} \tag{2.4}$$

yielding in turn the following form

$$R_{\bar{i}j} = -\frac{\partial \Gamma^{\bar{k}}_{\bar{i}\bar{k}}}{\partial z^j} \tag{2.5}$$

for the Ricci tensor.

Since the only compact submanifold of C^n is a point [21], in order to find nontrivial compact submanifolds, one considers weighted complex projective spaces, $CP^n(k_1, k_2, ..., k_{n+1})$, which are characterized by $(n+1)$ quasi-homogeneous coordinates $z_1, ..., z_{n+1}$, with the identification:

$$(z_1, \dots, z_{n+1}) \sim (\lambda^{k_1} \cdot z_1, \dots, \lambda^{k_{n+1}} \cdot z_{n+1}). \tag{2.6}$$

The loci of zeroes of quasi-homogeneous polynomial equations in such weighted projective spaces yield compact submanifolds, as we explain in more detail in the rest of Section 2, where we introduce and review several of the geometric and algebraic techniques used in our subsequent classification. Other compact submanifolds may be obtained as the complete intersections of such polynomial zero constraints, as we discuss in more detail in Section 9.

2.1. The Topology of Calabi–Yau Manifolds in the Polyhedron Method. A CY variety X in a weighted projective space $CP^n(\mathbf{k}) = CP^n(k_1, ..., k_{n+1})$ is given by the locus of zeroes of a transversal quasi-homogeneous polynomial $\wp$ of degree $\deg(\wp) = d$, with $d = \sum_{j=1}^{n+1} k_j$ [7, 13–15, 21–29]:

$$X \equiv X_d(k) \equiv \{[x_1, ..., x_{n+1}] \in CP^n(k) | \wp(x_1, ..., x_{n+1}) = 0\}. \tag{2.7}$$

The general polynomial of degree d is a linear combination

$$\wp = \sum_{\boldsymbol{\mu}} c_{\boldsymbol{\mu}} x^{\boldsymbol{\mu}} \tag{2.8}$$

of monomials $x^{\boldsymbol{\mu}} = x_1^{\mu_1} x_2^{\mu_2} ... x_{r+1}^{\mu_{r+1}}$ with the condition:

$$\boldsymbol{\mu} \cdot \mathbf{k} \, = \, d. \tag{2.9}$$

We recall that the existence of a *mirror symmetry*, according to which each Calabi–Yau manifold should have a dual partner, was first observed pragmatically in the literature [11–14, 27]. Subsequently, Batyrev [7] found a very elegant way of describing any Calabi–Yau hypersurface in terms of the corresponding *Newton polyhedron*, associated with degree-d monomials in the CY equation, which is the convex hull of all the vectors $\boldsymbol{\mu}$ of degree d. The Batyrev description provides a systematic approach to duality and mirror symmetry.

To each monomial associated with a vector $\boldsymbol{\mu}$ of degree d, i.e., $\boldsymbol{\mu} \cdot \mathbf{k} = d$, one can associate a vector $\boldsymbol{\mu}' \equiv \boldsymbol{\mu} - \mathbf{e}_0 : \mathbf{e}_0 \equiv (1, 1, ..., 1)$, so that $\boldsymbol{\mu}' \cdot \mathbf{k} = 0$. Using the new vector $\boldsymbol{\mu}'$, hereafter denoted without the prime ($'$), it is useful to define the lattice Λ:

$$\Lambda = \{\boldsymbol{\mu} \in Z^{r+1} : \boldsymbol{\mu} \cdot \mathbf{k} = 0\} \tag{2.10}$$

with basis vectors e_i, and the dual lattice Λ^* with basis e_j^*, where $e_j^* \cdot e_i = \delta_{ij}$. Consider the polyhedron $\triangle$, defined to be the convex hull of $\{\boldsymbol{\mu} \in \Lambda : \mu_i \geqslant -1, \forall i\}$. Batyrev [7] showed that to describe a Calabi–Yau hypersurface*, such a polyhedron should satisfy the following conditions:

- The vertices of the polyhedron should correspond to the vectors $\boldsymbol{\mu}$ with integer components.
- There should be only one interior integer point, called the centre.
- The distance of any face of this polyhedron from the centre should be equal to unity.

Such an integral polyhedron $\triangle$ is called *reflexive*, and the only interior point of $\triangle(k_1 + ... + k_{r+1} = d)$ may be taken as the origin $(0, ..., 0)$. Batyrev [7] showed that the mirror polyhedron

$$\triangle^* \equiv \{\boldsymbol{\nu} \in \Lambda^* : \boldsymbol{\nu} \cdot \boldsymbol{\mu} \geqslant -1, \forall \boldsymbol{\mu} \in \triangle\} \tag{2.11}$$

of any reflexive integer polyhedron is also reflexive, i.e., is also integral and contains one interior point only. Thus Batyrev proved the existence of dual pairs of hypersurfaces M and M' with dual Newton polyhedra, $\triangle$ and $\triangle^*$.

*I.e., with trivial canonical bundle and at worst Gorenstein canonical singularities only.

Following Batyrev [7], to obtain all the topological invariants of the $K3, CY_3$, etc., manifolds, one should study the reflexive regular polyhedra in three, four, etc., dimensions. For this purpose, it is useful to recall the types of polyhedra and their duality properties. In three dimensions, the Descartes–Euler polyhedron formula relates the numbers of vertices, N_0, the number of edges, N_1 and numbers of faces, N_2:

$$1 - N_0 + N_1 - N_2 + 1 = 0. \tag{2.12}$$

This formula yields:

$$\begin{aligned} 1 - 4 + 6 - 4 + 1 &= 0 \Rightarrow \{3,3\} : \text{Tetrahedron} \\ 1 - 8 + 12 - 6 + 1 &= 0 \Rightarrow \{3,4\} : \text{Cube} \\ 1 - 6 + 12 - 8 + 1 &= 0 \Rightarrow \{4,3\} : \text{Octahedron} \\ 1 - 20 + 30 - 12 + 1 &= 0 \Rightarrow \{5,3\} : \text{Dodecahedron} \\ 1 - 12 + 30 - 20 + 1 &= 0 \Rightarrow \{3,5\} : \text{Icosahedron} \end{aligned} \tag{2.13}$$

in the particular cases of the five Platonic solids, with the duality relations $T \leftrightarrow T$, $C \leftrightarrow O, D \leftrightarrow I$.

As we shall see later when we consider the $K3$ classification, it is interesting to recall the link between the classification of the five ADE simply-laced Cartan–Lie algebras and the finite rotation groups in three dimensions, namely, the cyclic and dihedral groups and the groups of the tetrahedron, octahedron (cube) and icosahedron (dodecahedron): $G_M \equiv C_n, D_n, T, O, I$, corresponding to the A_n, D_n series and the exceptional groups $E_{6,7,8}$, respectively [30]. Any cyclic group C_n of order n may be represented as the rotations in a plane around an axis $0x$ through angles $(2 \cdot m \cdot \pi)/n$ for $m = 0, 1, 2, ..., n-1$. This symmetry is realized by the group of symmetries of an oriented regular n-gon. The dihedral group D_n consists of the transformations in C_n and in addition n rotations through angles π around axes lying in planes orthogonal to $0x$, crossing $0x$ and making angles with one another that are multiples of $(2 \cdot \pi)/n$. This group has order $2 \cdot n$. In the case of three-dimensional space, there are three exceptional examples T, O, I of finite groups, related to the corresponding regular polyhedra. The order of the corresponding G_M is equal to the product of the number of the vertexes of the regular polyhedra with the number of edges leaving the vertex:

$$\begin{aligned} |T| &= |A_4| = 12, \\ |O| &= |S_4| = 24, \\ |I| &= |A_5| = 60. \end{aligned} \tag{2.14}$$

The dual polyhedron, whose vertices are the midpoints of the faces of the corresponding polyhedron, has the same group of symmetry, G_M. The finite groups of orthogonal transformations in three-dimensional space do not consist only of rotations. It is remarkable to note that every finite group of rotations of three-space that preserves the sphere centred at the origin can be interpreted as a fractional-linear transformation of the Riemann sphere of a complex variable.

Finally, we recall that all $K3$ hypersurfaces have the following common values of the topological invariants: the Hodge number $h_{1,1}$ is 20, the Betti number $b_2 = 22$, and we have

$$Pic = h_{1,1} - (l(\Delta) - 4 - \sum_{\theta\in\Delta} l'(\theta)) \leqslant 20 \tag{2.15}$$

for the Picard number, where $l(\Delta)$ is the number of integer points in the polyhedron and $l'(\theta)$ is the number of integer interior points on the facets.

In the case of the CY_3 classification, a corresponding important role will be played by the structure and the duality properties of the four regular polyhedra known in four-dimensional Euclidean space [31]. The Descartes–Euler formulae for these cases become:

$$\begin{aligned}
1-5+10-10+5-1=0 \quad &\Rightarrow \quad \{3,3,3\} : \text{Pentahedroid}\\
1-16+32-24+8-1=0 \quad &\Rightarrow \quad \{3,3,4\} : \text{Hypercube}\\
1-8+24-32+16-1=0 \quad &\Rightarrow \quad \{4,3,3\} : \text{16-hedroid}\\
1-24+96-96+24-1=0 \quad &\Rightarrow \quad \{3,4,3\} : \text{24-hedroid}\\
1-600+1200-720+120-1=0 \quad &\Rightarrow \quad \{3,3,5\} : \text{120-hedroid}\\
1-120+720-1200+600-1=0 \quad &\Rightarrow \quad \{5,3,3\} : \text{600-hedroid}
\end{aligned} \tag{2.16}$$

with the duality relations $P\leftrightarrow P$, $H\leftrightarrow$16-hedroid, 24-hedroid$\leftrightarrow$24-hedroid, 120-hedroid$\leftrightarrow$600-hedroid.

We do not discuss these relations further in this paper, but do recall that each mirror pair of CY spaces, M_{CY} and M^*_{CY} has Hodge numbers that satisfying the mirror symmetry relation [7, 15]:

$$\begin{aligned}
h_{1,1}(M) &= h_{d-1,1}(M^*),\\
h_{d-1,1}(M) &= h_{1,1}(M^*).
\end{aligned} \tag{2.17}$$

This means that the Hodge diamond of M^*_{CY} is a mirror reflection through a diagonal axis of the Hodge diamond of M_{CY}. The existence of mirror symmetry is a consequence of the dual properties of CY manifolds. A pair of reflexive polyhedra $(\triangle, \triangle^*)$ gives a pair of mirror CY manifolds and the following identities for the Hodge numbers for $n \geqslant 4$:

$$\begin{aligned} h_{1,1}(\triangle) &= h_{d-1,1}(\triangle^*) = \\ &= l(\triangle^*) - (d+2) - \sum_{\mathrm{codim}\Theta^*=1} l^{'}(\Theta^*) + \\ &+ \sum_{\mathrm{codim}\Theta^*=2} l'(\Theta^*) l^{'}\Theta, \end{aligned} \tag{2.18}$$

$$\begin{aligned} h_{1,1}(\triangle^*) &= h_{d-1,1}(\triangle) = \\ &= l(\triangle) - (d+2) - \sum_{\mathrm{codim}\Theta=1} l'(\Theta) + \\ &+ \sum_{\mathrm{codim}\Theta=2} l'(\Theta) l'(\Theta^*), \end{aligned} \tag{2.19}$$

$$h_{p,1} = \sum_{\mathrm{codim}\Theta^*=p+1} l^{'}(\Theta) \cdot l^{'}(\Theta^*), \;\; 1 < p < d-1. \tag{2.20}$$

Here, the quantities $l(\Theta)$ and $l'(\Theta)$ are the numbers of integer points on a face Θ of $\triangle$ and in its interior, and similarly for Θ^* and $\triangle^*$. An l-dimensional face Θ can be defined by its vertices $(v_{i_1} = ... = v_{i_k})$, and the dual face defined by $\Theta^* = \{m \in \triangle^* : (m, v_{i_1}) =, ..., = (m, v_{i_k}) = -1\}$ is an $(n-l-1)$-dimensional face of $\triangle^*$. Thus, we have a duality between the l-dimensional faces of $\triangle$ and the $(n-l-1)$-dimensional faces of $\triangle^*$. The last terms in (2.18), (2.19) correspond to the «twisted» contributions, and the last term corresponds to $d = 4$. In this case, if the manifold has $SU(4)$ group holonomy, then $h_{2,0} = h_{1,0} = 0$, and the remaining nontrivial Hodge number $h_{2,2}$ is determined by:

$$h_{2,2} = 2[22 + 2h_{1,1} + h_{3,1} - h_{2,1}]. \tag{2.21}$$

Some further comments about CY_3 spaces are made in Section 9.

2.2. The Web of CY Manifolds in the Holomorphic-Quotient Approach to Toric Geometry. It is well known that weighted projective spaces are examples of *toric varieties* [32]. The complex weighted projective space CP^n can be defined as

$$CP^n \equiv \frac{C^{n+1} - \mathbf{0}}{C^*}, \tag{2.22}$$

with the action C^*:

$$(x_1, ..., x_{n+1}) \Rightarrow (\lambda^{k_1} \cdot x_1, ..., \lambda^{k_{n+1}} \cdot x_{n+1}), \quad \lambda \in C \backslash 0. \tag{2.23}$$

The generalization of the projective space CP^n to a toric variety can be expressed in the following form:

$$\mho \equiv \frac{C^n \, - \, Z_\Sigma}{(C^*)^p}, \tag{2.24}$$

where, instead of removing the origin, as in the case of a simple projective space, here one removes a point set Z_Σ, and one takes the quotient by a suitable set of C^* actions. Thus, to understand the structure of certain geometrical spaces in the framework of toric geometry, one must specify the combinatorical properties of the Z_Σ and the actions C^*.

In the toric-geometry approach, algebraic varieties are described by a dual pair of lattices M and N, each isomorphic to Z^n, and a fan Σ^* [32] defined on N_R, the real extension of the lattice N. In the toric-variety description, the equivalence relations of projective vectors can be considered as diagrams in the lattice N, in which some vectors $\mathbf{v}_i$ satisfy linear relations (see later some examples in $P^2(1,1,1)$, $P^2(1,1,2)$, $P^2(1,2,3)$ projective spaces). The complex dimension of the variety coincides with the dimension of the lattice N. To determine the structure of a toric variety in higher dimensions $d > 2$, it is useful to introduce the notion of a fan [32, 33]. A fan Σ^* is defined as a collection of r-dimensional ($0 \leqslant r \leqslant d$) convex polyhedral cones with apex in 0, with the properties that with every cone it contains also a face, and that the intersection of any two cones is a face of each one.

In the holomorphic-quotient approach of Batyrev [7] and Cox [29], a single homogeneous coordinate is assigned to the system $\mho_\Sigma$ of varieties, in a way similar to the usual construction of P^n. This holomorphic-quotient construction gives immediately the usual description in terms of projective spaces, and turns out to be more natural in the descriptions of the elliptic, $K3$ and other fibrations of higher-dimensional CY spaces.

One can assign a coordinate $z_k : k = 1, ..., N$ to each one-dimensional cone in Σ. The integer points of $\Delta^* \cap N$ define these one-dimensional cones

$$(v_1, ..., v_N) = {\Sigma_1}^* \tag{2.25}$$

of the fan Σ^*. The one-dimensional cones span the vector space N_R and satisfy $(N - n)$ linear relations with nonnegative integer coefficients:

$$\sum_l k_j^l v_l = 0, \;\; k_j^l \geqslant 0. \tag{2.26}$$

These linear relations can be used to determine equivalence relations on the space $C^N \backslash Z_{\Sigma^*}$. A variety $\mho_{\Sigma^*}$ is the space $C^N \backslash Z_{\Sigma^*}$ modulo the action of a group which is the product of a finite Abelian group and the torus $(C^*)^{(N-n)}$:

$$(z_1, ..., z_N) \sim (\lambda^{k_j^1} z_1, ..., \lambda^{k_j^N} z_N), \;\; j = 1, ..., N - n. \tag{2.27}$$

The set Z_{Σ^*} is defined by the fan in the following way:

$$Z_{\Sigma^*} \equiv \bigcup_I ((z_1, ..., z_N)|z_i = 0, \forall i \in I), \tag{2.28}$$

where the union is taken over all index sets $I = (i_1, ..., i_k)$ such that $(v_{i_1}, ..., v_{i_k})$ do not belong to the same maximal cone in Σ^*, or several z_i can vanish simultaneously only if the corresponding one-dimensional cones v_i are from the same cone. It is clear from the above definitions that toric varieties can have often singularities, which will be very important for understanding the link between the topological properties of Calabi–Yau hypersurfaces and Cartan–Lie algebras: see the more systematic discussion in Section 8. The method of blowing up (blowing down) these singularities was developed in algebraic geometry: it consists of replacing the singular point or curve by a higher-dimensional (lower-dimensional) variety. The structure of the fan Σ^* determines what kind of singularities will appear in Calabi–Yau hypersurfaces. For example, if the fan Σ^* is simplicial, one can get only orbifold singularities in the corresponding variety [33].

The elements of Σ^*_1 are in one-to-one correspondence with divisors

$$D_{v_i} = \mho_{\Sigma^*_{1i}}, \tag{2.29}$$

which are subvarieties given simply by $z_i = 0$. This circumstance was used [34] to give a simple graphic explanation of Cartan–Lie algebra (CLA) diagrams, whose Coxeter number could be identified with the intersections of the divisors D_{v_i}.

Two divisors, D_{v_i} and D_{v_j}, can intersect only when the corresponding one-dimensional cones v_i and v_j lie in a single higher-dimensional cone of the fan Σ^*. The divisors D_{v_i} form a free Abelian group $\mathrm{Div}\,(\mho_{\Sigma^*})$. In general, a divisor $D \in \mathrm{Div}\,(\mho_{\Sigma^*})$ is a linear combination of some irreducible hypersurfaces with integer coefficients:

$$qD = \sum a_i \cdot D_{v_i}. \tag{2.30}$$

If $a_i \geqslant 0$ for every i, one can say that $D > 0$. For a meromorphic function f on a toric variety, one can define a principal divisor

$$(f) \equiv \sum_i \mathrm{ord}_{D_i}(f) \cdot D_i, \tag{2.31}$$

where $\mathrm{ord}_{D_i}(f)$ is the order of the meromorphic function f at D_i. One can further define the zero divisor $(f)_0$ and the polar divisor $(f)_{\mathrm{inf}}$ of the meromorphic function f, such that

$$(f) = (f)_0 - (f)_{\mathrm{inf}}. \tag{2.32}$$

Any two divisors D_1, D_2 are linearly equivalent: $D_1 \sim D_2$, if their difference is a principal divisor, $D_1 - D_2 = (f)$ for some appropriate f. The quotient of all divisors $\mathrm{Div}(\mho_{\Sigma^*})$ by the principal divisors forms the Picard group.

The points of $\Delta \cap M$ are in one-to-one correspondence with the monomials in the homogeneous coordinates z_i. A general polynomial is given by

$$\wp = \sum_{m \in \Delta \cap M} c_m \prod_{l=1}^{N} z_l^{\langle v_l, m\rangle + 1}. \tag{2.33}$$

The equation $\wp = 0$ is well defined and $\wp$ is holomorphic if the condition

$$\langle v_l, m\rangle \geqslant -1 \ \forall\ l \tag{2.34}$$

is satisfied. The c_m parametrize a family M_Δ of CY surfaces defined by the zero locus of $\wp$.

2.3. Three Examples of CY_1 Spaces. As discussed in Section 1, three CY_1 spaces may be obtained as simple loci of polynomial zeroes associated with reflexive polyhedra. For a better understanding of the preceding formalism, we consider as warm-up examples the three elliptic reflexive polyhedron pairs Δ_i and Δ_i^*, which define the CY_1 surfaces $P^2(1,1,1)[3]$, $P^2(1,1,2)[4]$, and $P^2(1,2,3)[6]$*. The first polyhedron $\Delta_I \equiv \Delta(P^2(1,1,1)[3])$ consists of the following ten integer points:

$$\begin{aligned}
z^3 &\implies \mu_1^{(I)} = (-1,2),\\
xz^2 &\implies \mu_2^{(I)} = (-1,1),\\
x^2z &\implies \mu_3^{(I)} = (-1,0),\\
x^3 &\implies \mu_4^{(I)} = (-1,-1),\\
yz^2 &\implies \mu_5^{(I)} = (0,1),\\
xyz &\implies \mu_6^{(I)} = (0,0),\\
x^2y &\implies \mu_7^{(I)} = (0,-1),\\
y^2z &\implies \mu_8^{(I)} = (1,0),\\
xy^2 &\implies \mu_9^{(I)} = (1,-1),\\
y^3 &\implies \mu_{10}^{(I)} = (2,-1)
\end{aligned} \tag{2.35}$$

*Here and subsequently, we use the conventional notation for such surfaces in n-dimensional projective space: $P^n(k_1, k_2, ...)[k_1 + k_2 + ...]$.

and the mirror polyhedron $\Delta_I^* \equiv \equiv \Delta^*(P^2(1,1,1)[3])$ consists of one interior point and three one-dimensional cones:

$$v_1^{(I)} = (0,1),$$
$$v_2^{(I)} = (1,0),$$
$$v_3^{(I)} = (-1,-1). \quad (2.36)$$

We use as a basis the exponents of the following monomials:

$$y^2z \implies \mathbf{e}_1 = (-1,1,0),$$
$$yz^2 \implies \mathbf{e}_2 = (-1,0,1), \quad (2.37)$$

where the determinant of this lattice coincides with the dimension of the projective vector $\mathbf{k} = (1,1,1)$ (see Figure 2):

$$\det\{\mathbf{e}_1, \mathbf{e}_2, \mathbf{e}_0\} = \dim(\mathbf{k}) = 3, \quad (2.38)$$

where $\mathbf{e}_0$ is the unit vector (1,1,1).

For this projective vector there exist 27 possibilities of choosing two monomials for constructing the basis. Of course, all these bases are equivalent, i.e., they are connected by the $SL(2,Z)$ modular transformations:

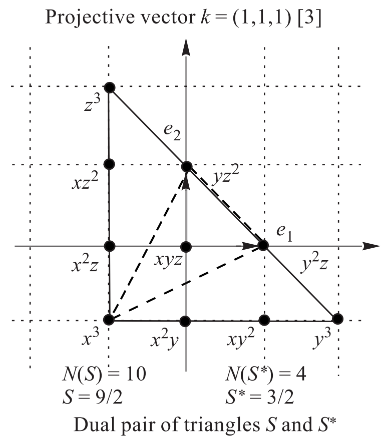

Fig. 2. The dual pair of reflexive plane polyhedra defined by the projective vector $(1,1,1)$ with $N(S) = 10$ and $N(S^*) = 4$ integer points, respectively. $SL(2,Z)$ transformations produce an infinite number of dual-pair triangles, conserving the areas $S = 9/2$ and $S^* = 3/2$, respectively

$$L_{i,j} = \begin{pmatrix} a & b \\ c & d \end{pmatrix},$$

where $a, b, c, d \in Z$ and $ad - bc = 1$. For the mirror polyhedron obtained from this vector, the basis should correspond to a lattice with determinant three times greater than (2.38), namely nine, for example:

$$\mathbf{e}_1 = (-1,2,-1),$$
$$\mathbf{e}_2 = (-1,-1,2), \quad (2.39)$$

with

$$\det\{\mathbf{e}_1, \mathbf{e}_2, \mathbf{e}_0\} = \dim(\mathbf{k}) = 9, \quad (2.40)$$

where $\mathbf{e}_0$ is again the unit vector (1,1,1).

To describe this toric curve, one should embed it in the toric variety

$$P^2 = (C^3\backslash 0)/(C\backslash 0), \quad (2.41)$$

where the equivalence relation

$$(x_1, x_2, x_3) \sim (\lambda x_1, \lambda x_2, \lambda x_3) \text{ for } \lambda \in C\backslash 0 \qquad (2.42)$$

is a consequence of the equation:

$$q_1 \cdot v_1^{(I)} + q_2 \cdot v_2^{(I)} + q_3 \cdot v_3^{(I)} = 0, \qquad (2.43)$$

where the $q_i = 1$, $i = 1, 2, 3$ are the exponents of λ. The corresponding general polynomial describing a CY surface is (setting $z_l \equiv x_l$):

$$\begin{aligned} \wp_I &= x_1^3 + x_2^3 + x_3^3 + x_1x_2x_3 + x_1^2x_2 + \\ &+ x_1^2x_3 + x_2^2x_1 + x_2^2x_3 + x_3^2x_1 + x_3^2x_2, \end{aligned} \qquad (2.44)$$

and the Weierstrass equation can be written in the following form:

$$y^2 \cdot z = x^3 + a \cdot x \cdot y^3 + b \cdot z^3, \qquad (2.45)$$

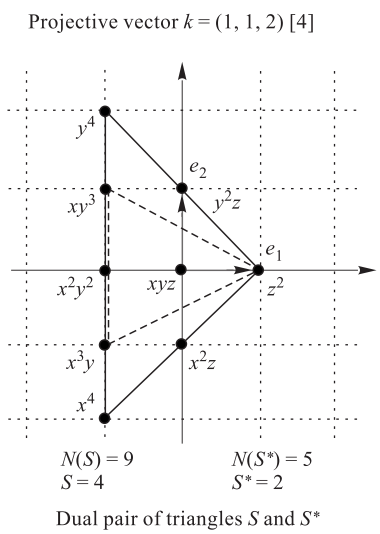

Fig. 3. The dual pair of reflexive plane polyhedra defined by the projective vector $(1, 1, 2)$ with $N(S) = 9$ and $N(S^*) = 5$ integer points, respectively. $SL(2, Z)$ transformations produce an infinite number of dual-pair triangles, conserving the areas $S = 4$ and $S^* = 2$, respectively

where we have set $x_1 = x, x_2 = y, x_3 = z$.

The second dual pair of triangle polyhedra $\Delta_{II} \equiv \Delta(P^2(1, 1, 2)[4])$ and its mirror $\Delta^*_{II} \equiv \Delta^*(P^2(1, 1, 2)[4])$ have nine points

$$\begin{aligned} y^4 &\implies \mu_1^{(II)} = (-1, 2), \\ xy^3 &\implies \mu_2^{(II)} = (-1, 1), \\ x^2y^2 &\implies \mu_3^{(II)} = (-1, 0), \\ x^3y &\implies \mu_4^{(II)} = (-1, -1), \\ x^4 &\implies \mu_5^{(II)} = (-1, -2), \\ y^2z &\implies \mu_6^{(II)} = (0, 1), \\ xyz &\implies \mu_7^{(II)} = (0, 0), \\ x^2z &\implies \mu_8^{(II)} = (0, -1), \\ z^2 &\implies \mu_9^{(II)} = (1, 0), \end{aligned} \qquad (2.46)$$

and five points, respectively (see Figure 3).

We use as a basis the exponents of the following monomials:

$$\begin{aligned} z^2 &\implies \mathbf{e}_1 = (-1, -1, 1), \\ y^2z &\implies \mathbf{e}_2 = (-1, 1, 0), \end{aligned} \qquad (2.47)$$

where the determinant of this lattice coincides with the dimension of the projective vector $\mathbf{k} = (1, 1, 2)$:

$$\det\{\mathbf{e}_1, \mathbf{e}_2, \mathbf{e}_0\} = \dim(\mathbf{k}) = 4, \tag{2.48}$$

where $\mathbf{e}_0$ is again the unit vector (1,1,1).

To get the mirror polyhedron with five integer points, four on the edges and one interior point, one should find a basis with lattice determinant twice (2.48), namely eight, for example:

$$\begin{aligned} \mathbf{e}_1 &= (-1, -1, 1), \\ \mathbf{e}_2 &= (-2, 2, 0). \end{aligned} \tag{2.49}$$

The following four points define four one-dimensional cones in $\Sigma_1(\Delta^*_{II})$:

$$\begin{aligned} v_1^{(3)} &= (1, 0), \\ v_2^{(3)} &= (-1, 0), \\ v_3^{(3)} &= (-1, -1), \\ v_4^{(3)} &= (-1, 1). \end{aligned} \tag{2.50}$$

Using the linear relations between the four one-dimensional cones, the corresponding $(C^*)^2$ is seen to be given by ($z_l \equiv \chi_l$):

$$(\chi_1, \chi_2, \chi_3, \chi_4) \Longrightarrow (\lambda\mu^2\chi_1, \lambda\chi_2, \mu\chi_3, \mu\chi_4), \tag{2.51}$$

and the general polynomial has the following nine terms:

$$\begin{aligned} \wp_{II} &= \chi_2^2\chi_3^4 + \chi_2^2\chi_3^3\chi_4 + \chi_2^2\chi_3^2\chi_4^2 + \chi_2^2\chi_3\chi_4^3 + \chi_2^2\chi_4^4 + \\ &+ \chi_1\chi_2\chi_3^2 + \chi_1\chi_2\chi_3\chi_4 + \chi_1\chi_2\chi_4^2 + \chi_1^2 \end{aligned} \tag{2.52}$$

in this case.

The vectors $\mathbf{k} = (1, 1, 1)$ and $\mathbf{k} = (1, 1, 2)$ have three common monomials and a related reflexive segment-polyhedron, corresponding to the projective vector $\mathbf{k}_2 = (1, 1)$ of CP^1. This circumstance can be used further in the construction of the projective algebra in which these two vectors appear in the same chain.

The last CY_1 example involves the plane of the projective vector $\mathbf{k} = (1, 2, 3)$, whose polyhedron $\Delta_{III} \equiv \Delta(P^2(1, 2, 3)[6])$ and its mirror partner $\Delta^*_{III} \equiv$ $\equiv \Delta^*(P^2(1, 2, 3)[6])$ both have seven self-dual points, and one can check the

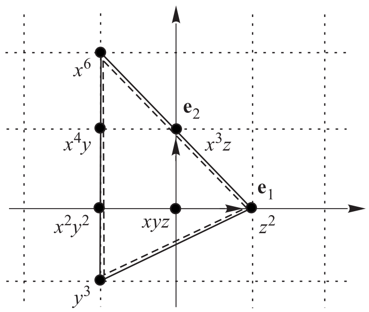

Fig. 4. The self-dual pair of reflexive plane polyhedra defined by the projective vector (1,2,3) with $N(S) = = 7$ and $N(S^*) = 7$ integer points. $SL(2, Z)$ transformations produce an infinite number of the dual-pair triangles, conserving the areas $S = 3$ and $S^* = 3$, respectively

existence of the following six one-dimensional cones (see Figure 4):

$$\begin{aligned} z^2 &\Longrightarrow v_1^{(III)} = (1,0), \\ x^2y^2 &\Longrightarrow v_2^{(III)} = (-1,0), \\ x^3z &\Longrightarrow v_3^{(III)} = (0,1), \\ y^3 &\Longrightarrow v_4^{(III)} = (-1,-1), \\ x^4y &\Longrightarrow v_5^{(III)} = (-1,1), \\ x^6 &\Longrightarrow v_6^{(III)} = (-1,2). \end{aligned} \tag{2.53}$$

We use as a basis the exponents of the following monomials:

$$\begin{aligned} z^2 &\Longrightarrow \mathbf{e}_1 = (-1,-1,1), \\ x^3z &\Longrightarrow \mathbf{e}_2 = (2,-1,0), \end{aligned} \tag{2.54}$$

where the determinant of this lattice coincides with the dimension of the projective vector $\mathbf{k} = (1,2,3)$:

$$\det\{\mathbf{e}_1, \mathbf{e}_2, \mathbf{e}_0\} = \dim(\mathbf{k}) = 6. \tag{2.55}$$

As in the case of the two projective vectors $\mathbf{k} = (1,1,1)$ and $\mathbf{k} = (1,1,2)$, the vectors $\mathbf{k} = (1,1,2)$ and $\mathbf{k} = (1,2,3)$ also have three common monomials, corresponding to the reflexive segment polyhedron described by the vector $\mathbf{k}_2 = (1,1)$ in CP^1 projective space. Hence these vectors will appear in the second chain of the plane projective algebra.

Thus one can see that, with these three plane projective vectors, $\mathbf{k} = (1,1,1)$, $\mathbf{k} = (1,1,2)$, $\mathbf{k} = (1,2,3)$, one finds only triangle reflexive polyhedra intersecting the integer planar lattice in $10+4^*$, $9+5^*$, $7+7^*$ points. Of course, on the plane one can find other reflexive polyhedra, whose intersection with the integer plane lattice will give new CP^1 surfaces corresponding to different polygons with more than three vertices, such as a reflexive pair of square and rhombus. These new figures can be obtained using the techniques of extended vectors.

In the following, we will go on to study reflexive polyhedron pairs in three-dimensional space. The corresponding general polynomial can be expressed in terms of six variables, and contains seven monomials:

$$\begin{aligned} \wp_{III} &= z_1^2z_3 + z_2^2z_3z_4^2z_5^2z_6^2 + z_1z_2z_3^2z_5^2z_6^3 + z_2^2z_4^3z_5 + \\ &+ z_2^2z_3^2z_4z_5^3z_6^4 + z_2^2z_3^3z_5^4z_6^6 + z_1z_2z_3z_4z_5z_6. \end{aligned} \tag{2.56}$$

The C^{*4} action is determined by the following linear relations:

$$\begin{aligned} v_1^{(III)} \;+\; v_2^{(III)} &= 0, \\ 2v_1^{(III)} \;+\; v_4^{(III)} \;+\; v_5^{(III)} &= 0, \\ v_1^{(III)} \;+\; v_3^{(III)} \;+\; v_4^{(III)} &= 0, \\ 3v_1^{(III)} \;+\; 2v_4^{(III)} \;+\; v_6^{(III)} &= 0 \end{aligned} \tag{2.57}$$

between the elements of $\Sigma_1(\Delta^*_{III})$, and is given by

$$(z_1, z_2, z_3, z_4, z_5, z_6) \longrightarrow (\lambda\mu^2\nu\rho^3 z_1, \lambda z_2, \nu z_3, \mu\nu\rho^2 z_4, \mu z_5, \rho z_6). \tag{2.58}$$

One can introduce the following birational map between $P^2(1,2,3)[6]$ and $\mho_{\Sigma^*}$:

$$z_1^2 z_3 \;=\; y_3^2, \tag{2.59}$$

$$z_2^2 z_4^3 z_5 \;=\; y_2^3, \tag{2.60}$$

$$z_2^2 z_3^3 z_5^4 z_6^6 \;=\; y_1^6. \tag{2.61}$$

Then, a dimensionally-reduced example of a CY manifold embedded in a toric variety is described by the weight vector $k = (1,2,3)$ and the zero locus of the Weierstrass polynomial

$$\wp_{III} = y_1^6 \;+\; y_2^3 \;+\; y_3^2 \;+\; y_1 y_2 y_3 + \; y_1^4 y_2 \;+\; y_1^2 y_2^2 \;+\; y_1^3 y_3. \tag{2.62}$$

The elliptic Weierstrass equation can be written in the weighted projective space $P^2(1,2,3)[6]$ as

$$y^2 = x^3 \;+\; a \cdot x \cdot z^4 \;+\; b \cdot z^6 \tag{2.63}$$

with the following equivalence relation

$$(x, y, z) \;\sim\; (\lambda^2 x, \lambda^3 y, \lambda z), \quad \lambda \in C\backslash 0 \tag{2.64}$$

in this case.

These examples illustrate how toric varieties can be defined by the quotient of $C^k\backslash Z_\Sigma$, and not only by a group $(C\backslash 0)^{k-n}$. One should divide $C^k\backslash Z_\Sigma$ also by a finite Abelian group $G(v_1, ..., v_k)$, which is determined by the relations between the D_{v_i} divisors. In this case, the toric varieties can often have orbifold singularities, $C^k\backslash G$. For example, the toric variety defined by (2.63) looks near the points $y = z = 0$ and $x = z = 0$ locally like $C^2\backslash Z_2$ (related to the $SU(2)$ algebra) and $C^2\backslash Z_3$ (related to the $SU(3)$ algebra), respectively, as seen in Figure 5.

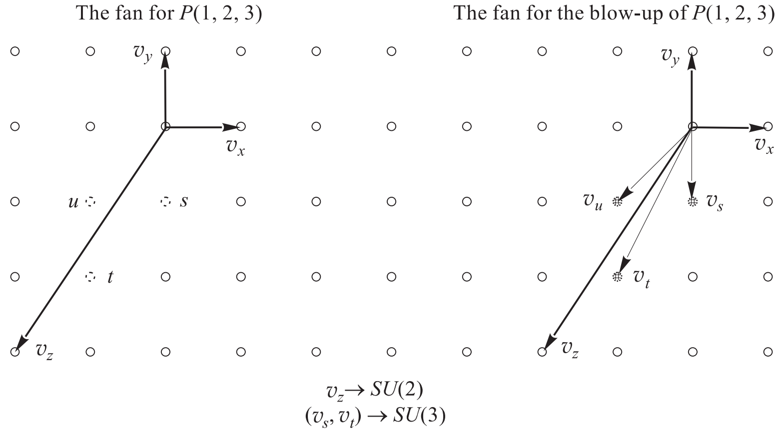

Fig. 5. The toric variety $P(1,2,3)$ with two orbifold singularities at the points $y = z = 0$ and $x = z = 0$ can be blown up by extra divisors $D(v_u)$ and $D(v_s)$, $D(v_t)$, respectively

3. GAUGE GROUP IDENTIFICATIONS FROM TORIC GEOMETRY

3.1. Calabi–Yau Spaces as Toric Fibrations. As discussed in Section 2, any Calabi–Yau manifold can be considered as a hypersurface in a toric variety, with a corresponding reflexive polyhedron Δ with a positive-integer lattice Λ, associated with a dual polyhedron Δ^* in the dual lattice Λ^*. The toric variety is determined by a fan Σ^*, consisting of the cones which are given by a triangulation of Δ^*. A large subset of reflexive polyhedra and their corresponding Calabi–Yau manifolds can be classified in terms of their fibration structures. In this way, it is possible, as we discuss later, to connect the structures of all the projective vectors of the one dimensionality with the projective vectors of other dimensionalities, and thereby construct a new algebra in the set of all «reflexive» projective vectors that gives the full set of CY_d hypersurfaces in all dimensions: $d = 1, 2, 3, \ldots$

In order to embark on this programme, it is useful first to review two key operations, *intersection* and *projection*, which can give possible fibration structures for reflexive polyhedra [34]:

• There may exist a projection operation $\pi : \Lambda \to \Lambda_{n-k}$, where Λ_{n-k} is an $(n-k)$-dimensional sublattice, and $\pi(\Delta)$ is also a reflexive polyhedron, and

• there may exist an intersection projection J through the origin of a reflexive polyhedron, such that $J(\Delta)$ is again an $(n-l)$-dimensional reflexive polyhedron, and

• these operations may exhibit the following duality properties:

$$\begin{aligned} \Pi(\Delta) \quad &\Leftrightarrow \quad J(\Delta^*) \\ J(\Delta) \quad &\Leftrightarrow \quad \Pi(\Delta^*). \end{aligned} \tag{3.1}$$

For a reflexive polyhedron Δ with fan Σ over a triangulation of the facets of Δ^*, the CY hypersurface in variety $\mho_\Sigma$ is given by the zero locus of the polynomial:

$$\wp = \sum_{\mu \in \Delta \cap M} c_{\boldsymbol{\mu}} \cdot \prod_{i=1}^{N} z_i^{\langle \mathbf{v}_i \cdot \boldsymbol{\mu} \rangle + 1}. \tag{3.2}$$

One can consider the variety $\mho_\Sigma$ as a fibration over the base $\mho_{\Sigma_{\rm base}}$ with generic fiber $\mho_{\Sigma_{\rm fiber}}$. This fibration structure can be written in terms of homogeneous coordinates. The fiber as an algebraic subvariety is determined by the polyhedron $\Delta^*_{\rm fiber} \subset \Delta^*_{\rm CY}$, whereas the base can be seen as a projection of the fibration along the fiber. The set of one-dimensional cones in $\Sigma_{\rm base}$ (the primitive generator of a cone is zero or $\tilde{v}_i$) is the set of images of one-dimensional cones in $\Sigma_{\rm CY}$ (with primitive generator v_j) that do not lie in $N_{\rm fiber}$. The image $\Sigma_{\rm base}$ of $\Sigma_{\rm CY}$ under $\Pi : N_{\rm CY} \to N_{\rm base}$ gives us the following relation:

$$\Pi v_i \ = \ r_i^j \cdot \tilde{v}_j, \tag{3.3}$$

if Πv_i is in the set of one-dimensional cones determined by $\tilde{v}_j$ $r_i^j \in N$, otherwise $r_i^j = 0$.

Similarly, the base space is the weighted projective space with the torus transformation:

$$(\tilde{x}_1, ..., \tilde{x}_{\tilde{N}}) \ \sim (\lambda^{\tilde{k}_j^1} \cdot \tilde{x}_1, ..., \lambda^{\tilde{k}_j^{\tilde{N}}} \cdot \tilde{x}_{\tilde{N}}), \ \ j = 1, ..., \tilde{N} - \tilde{n}, \tag{3.4}$$

where the $\tilde{k}_j^i$ are integers such that $\sum_j \tilde{k}_i^j \tilde{v}_j = 0$. The projection map from the variety $\mho_\Sigma$ to the base can be written as

$$\tilde{x}_i = \prod_j x_j^{r_j^i}, \tag{3.5}$$

corresponding to the following redefinitions of the torus transformation for $\tilde{x}_i$:

$$\Pi : \tilde{x}_i \to \lambda^{k_l^j \cdot r_j^i} \cdot \tilde{x}_i, \ \ \sum k_l^j \cdot r_j^i \cdot \tilde{v}_i = 0. \tag{3.6}$$

In the toric description of $K3$ surfaces with elliptic fibers, denoted by $\Delta^*{}_{\rm fiber}$, one can consider the following divisors: $D_{\rm fiber}$, $D_{\rm section}$, D_{v_a} and D_{v_b}. The last pair of divisors correspond to lattice points of Δ^* that are «above» or «below» the fiber, respectively. Let us consider the case when all divisors D_{v_a} (or D_{v_b}) shrink to zero size. In this case, there appears a $K3$ hypersurface with two point singularities, which belong to the ADE classification. The process of blowing up these singularities gives the primordial $K3$ manifold, and its intersection structure is given by the structure of the edges. The Cartan–Lie algebra (CLA) diagrams of the gauge groups that appear when the exceptional fibers are blown down to points are nothing but the edge diagrams of the upper and lower parts of Δ^* without vertices, respectively. A simple well-known example with elliptic fiber and with base P^1 is given by the following Weierstrass equation for the fiber:

$$y^2 = x^3 \,+\, f(z_1, z_2) \cdot x \cdot z^4 \,+\, g(z_1, z_2) \cdot z^6, \tag{3.7}$$

where the coefficients $f(z_1, z_2), g(z_1, z_2)$ are functions on the base.

In the following parts of this Section, we discuss some examples of $K3$ spaces from our general classification, and explain the identification of their corresponding gauge groups.

3.2. Examples of $K3$ Toric Fibrations with $J = \Pi$ Weierstrass Structure. As a first example, we consider the case of the elliptic $K3$ hypersurface with elliptic fiber $P^2(1,2,3)[6]$ defined by the integer positive lattice with basis (we explain this lattice basis later in terms of our algebraic description):

$$\begin{pmatrix} \mathbf{e}_1 \\ \mathbf{e}_2 \\ \mathbf{e}_3 \end{pmatrix} = \begin{pmatrix} -m & n & 0 & 0 \\ -2 & -2 & 1 & 0 \\ -1 & -1 & -1 & 1 \end{pmatrix},$$

where we consider the following 12 pairs of integer numbers (m, n) which are taken from the numbers: $1, 2, 3, 4, 5, 6,$

$$\{\, (1,1),\, (1,2),\, (1,3),\, (1,4),\, (1,5),\, (1,6),\, (2,3),\, (2,5)\, (3,4),\, (4,5),\, (5,6)\}.$$

With this choice of the pairs, the basis above determines a self-dual set of 12 projective $\mathbf{k}_4$ vectors:

$$\begin{aligned}
m &= 1, n = 1 \implies \mathbf{k}_4 = (1,1,4,\ 6\ )[12], \iff (5,6,22,33)\\
m &= 1, n = 2 \implies \mathbf{k}_4 = (1,2,6,\ 9\ )[18], \iff (3,5,16,24)\\
m &= 1, n = 3 \implies \mathbf{k}_4 = (1,3,8,\ 12)[24], \iff (2,5,14,21)\\
m &= 1, n = 4 \implies \mathbf{k}_4 = (1,4,10,15)[30], \iff DI^{'}\\
m &= 1, n = 5 \implies \mathbf{k}_4 = (1,5,12,16)[36], \iff \text{self-dual}\\
m &= 1, n = 6 \implies \mathbf{k}_4 = (1,6,14,21)[42], \iff \text{self-dual}\\
m &= 2, n = 3 \implies \mathbf{k}_4 = (2,3,10,15)[30], \iff \text{self-dual}\\
m &= 2, n = 5 \implies \mathbf{k}_4 = (2,5,14,21)[42], \iff (1,3,8,12)\\
m &= 3, n = 4 \implies \mathbf{k}_4 = (3,4,14,21)[42], \iff DI^{''}\\
m &= 3, n = 5 \implies \mathbf{k}_4 = (3,5,16,24)[48], \iff (1,2,6,9)\\
m &= 4, n = 5 \implies \mathbf{k}_4 = (4,5,18,27)[54], \iff DI^{'''}\\
m &= 5, n = 6 \implies \mathbf{k}_4 = (5,6,22,33)[66], \iff (1,1,4,6).
\end{aligned} \tag{3.8}$$

Later this set will emerge as the intersection-projection symmetric XIX chain ($J = \Pi$) of our algebraic classification. In this example, one can see that the projective vectors corresponding to the tetrahedra produce a self-dual set. We also show in (3.8) the duality relations between six other vectors and some of the vectors from Table 1.

However, three of the projective vectors in (3.8), $\mathbf{k}_4 = (1,4,10,15)[30]$, $(3,4,14,21)[42]$ and $(4,5,18,27)[54]$, correspond to polyhedra with five vertices, and their duals can be found among higher-level $K3$ spaces. They are found by double intersections (DI) among the five-dimensional extensions of the $K3$ vectors shown in Table 1:

$$\begin{aligned}
\mathbf{k}_4 = (1,4,10,15)[30] &\overset{DI'}{\Longleftrightarrow} \{\mathbf{k}_5^{ex} = (0,1,6,8,15)[30]\} \bigcap \\
&\bigcap \{\mathbf{k}_5^{ex} = (6,1,0,14,21)[42]\}, \\
\mathbf{k}_4 = (3,4,14,21)[42] &\overset{DI''}{\Longleftrightarrow} \{\mathbf{k}_5^{ex} = (2,1,0,6,9)[18]\} \bigcap \\
&\bigcap \{\mathbf{k}_5^{ex} = (0,1,2,4,7)[14]\}, \\
\mathbf{k}_4 = (4,5,18,27)[54] &\overset{DI'''}{\Longleftrightarrow} \{\mathbf{k}_5^{ex} = (1,0,1,4,6)[12]\} \bigcap \\
&\bigcap \{\mathbf{k}_5^{ex} = (0,1,1,3,5)[10]\}
\end{aligned} \tag{3.9}$$

as discussed in more detail in Section 6.

The ascending Picard numbers for polyhedra in this chain include:

$$\begin{aligned}
(\Delta(P^3(1,6,14,21)[42]) : \aleph &= 24(24^*),\ \mathrm{Pic} = 10(10^*) \\
\approx (\Delta(P^3(1,5,12,18)[36]) : \aleph &= 24(24^*),\ \mathrm{Pic} = 10(10^*) \\
\subset (\Delta(P^3(1,4,10,15)[30]) : \aleph &= 25(20^*),\ \mathrm{Pic} = 9(11^*) \\
\subset (\Delta(P^3(1,3,8,12)[24]) : \aleph &= 27(15^*),\ \mathrm{Pic} = 8(14^*) \\
\subset (\Delta(P^3(1,2,6,9)[18]) : \aleph &= 30(12^*),\ \mathrm{Pic} = 6(16^*) \\
\subset (\Delta(P^3(1,1,4,6)[12]) : \aleph &= 39(9),\ \mathrm{Pic} = 2(18^*) \subset ....
\end{aligned} \tag{3.10}$$

In the case of the mirror polyhedron chain, there is the inverse property: $\Delta^*(P^3(1,6,14,21)[42])$ corresponds to the maximal member of the set of mirror polyhedra. These Picard numbers are listed in Table 1, together with those of the other $K3$ spaces.

In the chain (3.8), the mirror polyhedra, Δ^*, have an intersection plane H^*_{fiber} through the interior point which defines an elliptic-fiber triangle with seven integer points, $P^2(1,2,3)[6]$ (see Figures 6,7):

$$\Delta^*_{\mathrm{fiber}} = \Delta^* \bigcap H^*_{\mathrm{fiber}}. \tag{3.11}$$

The dual pair of projective vectors $k = (1, 1, 4, 6)$ [12] and $k = (5, 6, 22, 33)$ [66]

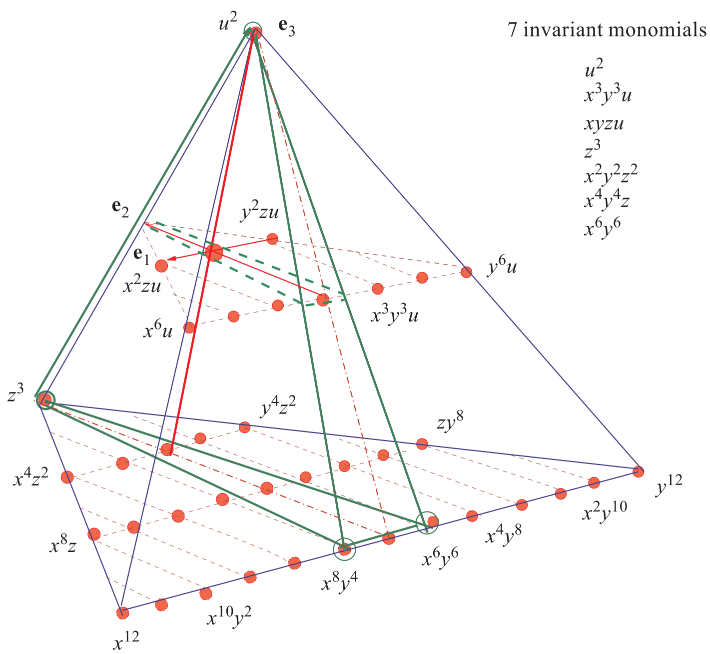

The dual pair of reflexive polyhedra S and S^*: $N(S) = 39$ $V(S) = 12$ $N(S^*) = 9$ $V(S^*) = 2$

Fig. 6. The dual pair of reflexive planar polyhedra defined by the eldest projective vector (1,1,4,6) with $N(S) = 39$ and the youngest projective vector (5,6,22,33) with $N(S^*)$=9 integer points (marked by circles), respectively. $SL(3,Z)$ transformations produce an infinite number of dual pairs of tetrahedra, conserving the volumes Vol $(S) = 12$, Vol $(S^*) = 6$, respectively

By mirror symmetry in the polyhedron Δ, a projection operator π can be defined: $\pi : M \to M_{n-1}$, where M_{n-1} is an $(n-1)$-dimensional sublattice, such that $\pi(\Delta)$ is a reflexive polyhedron in M_{n-1}. This reflexive polyhedron also consists of seven points, so it is self-dual. Also, one can find a planar intersection H through Δ and through the interior point, which also produces the reflexive polyhedron with seven points, namely the fiber $P^2(1,2,3)[6]$ (see Figures 6,7):

$$\Delta_{\text{fiber}} = \Delta \bigcap H_{\text{fiber}}. \tag{3.12}$$

The dual pair of tetrahedra $\Delta(P^3(1,1,4,6)[12])$ and $\Delta(P^3(5,6,22,33)[66])$ consist of 39 and 9 points, respectively, as seen in Figure 6. They are the biggest and smallest polyhedra in the chain (3.8), and all other tetrahedra in this chain can

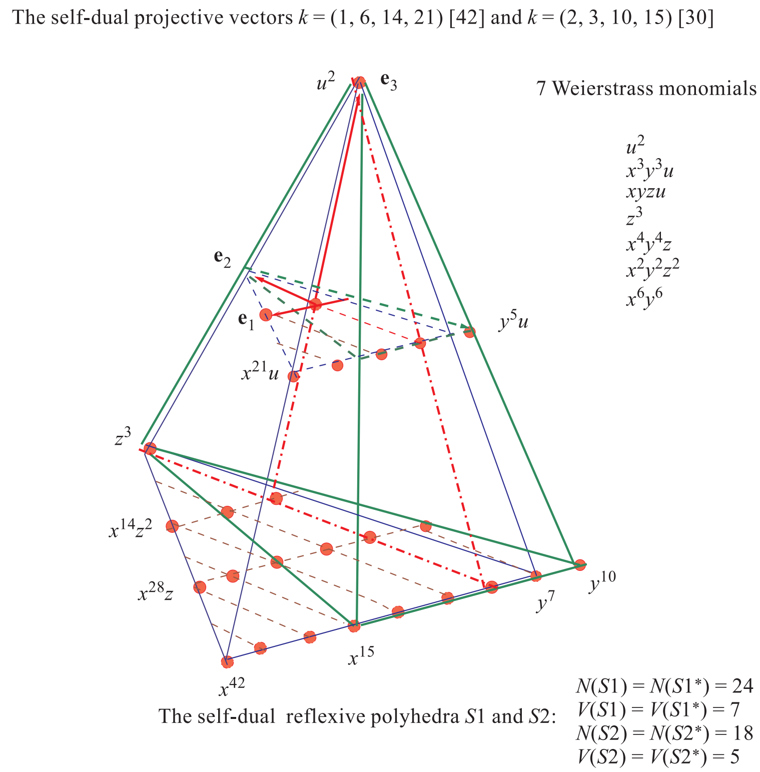

Fig. 7. The self-dual polyhedra in the chain XIX determined by projective vector (1,6,14,21) with $N(S1) = 24$ and vector (2,3,10,15) with $N(S2) = 18$ integer points, respectively. $SL(3, Z)$ transformations produce an infinite number of dual pairs of tetrahedra, conserving the volumes $\mathrm{Vol}\,(S1) = 7$ and $\mathrm{Vol}\,(S2) = 5$, respectively

be found in this Figure. This contains, in particular, the two self-dual polyhedra $\Delta(P^3(1,6,14,21)[42])$ and $\Delta(P^3(2,3,10,15)[30])$ consisting of $24 + 24^*$ and $18 + 18^*$ points, respectively, as seen in Figure 7:

$$\begin{aligned}&(0,0,1),\ (0,1,-1),\ (-1,-2,-1),\ (6,-2,-1),\\&(0,0,1),\ (0,1,-1),\ (-2,-2,-1),\ (3,-2,-1).\end{aligned} \tag{3.13}$$

We now consider the intersection of the three-dimensional polyhedron $\Delta(P^3(1,6,14,21)[42])$ with the two-dimensional plane H through the interior point. The intersection of this plane with the polyhedron, $H \bigcap \Delta$, forms a reflexive polyhedron fiber $P^2(1,2,3)$ with seven points. The equation of this plane in canonical coordinates μ_1, μ_2, μ_3 is: $m_1 = 0$. The fiber consists of the following polyhedron points:

$$\begin{aligned} v_0 &= (0, \underline{0, 0}), \\ v_1 &= (0, \underline{-1, 0}), \\ v_2 &= (0, \underline{0, 1}), \\ v_3 &= (0, \underline{1, -1}), \\ v_4 &= (0, \underline{0, -1}), \\ v_5 &= (0, \underline{-1, -1}), \\ v_6 &= (0, \underline{-2, -1}). \end{aligned} \tag{3.14}$$

Here and subsequently, the components of the vector corresponding to the fiber are underlined.

With respect to this fiber, the base is one-dimensional: P^1, and its fan F_2 consists of the divisors corresponding to the interior point and two divisors corresponding to two rays, $R_1 = +\mathbf{e}_1$ and $R_2 = -\mathbf{e}_1$, with directions from the point $(0, -2, -1)$ to the point $(6, -2, -1)$ and from the point $(0, -2, -1)$ to $(-1, -2, -1)$, respectively. The points of $\pi_B^{-1}(R_i)$ (i.e., the points projected onto R_i by π_B) for the rays R_i, $(i = 1 = +, i = 2 = -)$ are of the form $(\pm..., b, c)$, where $(0, b, c)$ is the point of the fiber.

The 16 points of $\pi_B^{-1}(R_1)$ are listed in Table 2: they correspond to the divisors D_{v_i}, which produce the E_8 algebra [34]. Also, from this Table one can easily read the Coxeter numbers/weights. There is only one point in $\pi_B^{-1}(R_2)$, namely

$$\tilde{v}_1^1 = (-1, \underline{-2, -1}) \tag{3.15}$$

which therefore does not correspond to any nontrivial group.

Table 2. The points of $\pi_B^{-1}(R_1)$

Coxeter #	$v_6^{(i)}$	$v_5^{(i)}$	$v_1^{(i)}$	$v_4^{(i)}$	$v_0^{(i)}$
1	$(1, \underline{-2, -1})$	$(1, \underline{-1, -1})$	$(1, \underline{-1, 0})$	$(1, \underline{0, -1})$	$(1, \underline{0, 0})$
2	$(2, \underline{-2, -1})$	$(2, \underline{-1, -1})$	$(2, \underline{-1, 0})$	$(2, \underline{0, -1})$	$---$
3	$(3, \underline{-2, -1})$	$(3, \underline{-1, -1})$	$(3, \underline{-1, 0})$	$---$	$---$
4	$(4, \underline{-2, -1})$	$(4, \underline{-1, -1})$	$---$	$---$	$---$
5	$(5, \underline{-2, -1})$	$---$	$---$	$---$	$---$
6	$(6, \underline{-2, -1})$	$---$	$---$	$---$	$---$

3.3. Example of Gauge-Group Identification. Consider again the toric variety determined by the dual pair of polyhedra $\Delta(P^3(1,1,4,6)[12])$ and its dual Δ^* shown in Figure 6. The mirror polyhedron contains the intersection H^* through the interior point, the elliptic fiber $P^2(1,2,3)$. For all integer points of Δ^* (apart from the interior point), one can define in a convenient basis the corresponding complex variables:

$$\begin{aligned} v_1 &= (0,\underline{-2,-3}) \to z_1, \\ v_2 &= (0,\underline{-1,-2}) \to z_2, \\ v_3 &= (0,\underline{-1,-1}) \to z_3, \\ v_4 &= (0,\underline{0,-1}) \to z_4, \\ v_0 &= (0,\underline{0,0}), \\ v_6 &= (0,\underline{1,0}) \to z_6, \\ v_7 &= (0,\underline{0,1}) \to z_7, \end{aligned} \tag{3.16}$$

and

$$\begin{aligned} &v_8 = (-1,\underline{-4,-6}) \to z_8, \\ &v_9 = (1,\underline{0,0}) \to z_9. \end{aligned} \tag{3.17}$$

There are some linear relations between integer points inside the fiber:

$$\begin{aligned} v_1 + 2v_6 + 3v_7 &= 0, \\ v_2 + v_6 + 2\cdot v_7 &= 0, \\ v_3 + v_6 + v_7 &= 0, \\ v_4 + v_6 + v_7 &= 0 \end{aligned} \tag{3.18}$$

and also the following relation between points in Δ^*:

$$v_8 + v_9 + 4v_6 + 6v_7 = 0. \tag{3.19}$$

The polyhedron $\Delta(P^3(1,1,4,6))$ contains 39 points, which can be subdivided as follows. There are seven points in the fiber $P^2(1,2,3)$, determined by the intersection of the plane $m_1 + 2m_2 + 3m_3 = 0$ and the positive integer lattice. This plane separates the remaining 32 points in 16 «left» and 16 «right» points.

These «left» and «right» points define singularities of the E_{8_L} and E_{8_R} types, respectively, which may be illustrated as follows. The plane

$H(\Delta) = m_1 + 2m_2 + 3m_3$ contains the following seven points:

$$
\begin{aligned}
t_1 &= (5, \underline{-1, -1}) \to (z_8^6 z_9^6) \cdot (\underline{z_1^6 z_2^4 z_3^3 z_4^2}),\\
t_2 &= (3, \underline{0, -1}) \to (z_8^4 z_9^4) \cdot (\underline{z_1^4 z_2^3 z_3^3 z_4^2 z_6}),\\
t_3 &= (2, \underline{-1, 0}) \to (z_8^3 z_9^3) \cdot (\underline{z_1^3 z_2^2 z_3^2 z_4 z_7}),\\
t_4 &= (1, \underline{1, -1}) \to (z_8^2 z_9^2) \cdot (\underline{z_1^2 z_2^2 z_3 z_4^2 z_6^2}),\\
t_5 &= (0, \underline{0, 0}) \to (z_8 z_9) \cdot (\underline{z_1^6 z_2^4 z_3^3 z_4^2}),\\
t_6 &= (-1, \underline{2, -1}) \to (\underline{z_2 z_4^2 z_6^3}),\\
t_7 &= (-1, \underline{-1, 1}) \to (\underline{z_3 z_7^2}).
\end{aligned}
\tag{3.20}
$$

The Weierstrass equation for the E_{8_L} group based on the polyhedron $\Delta(P^3(1,1,4,6))$ can be written in the form:

$$
\begin{aligned}
&\underline{z}_6^3 + \underline{z}_6^2 \cdot (a_2^{(1)} z_8 z_9^3 + a_2^{(2)} z_9^4) +\\
&+\underline{z}_1^4 \cdot \underline{z}_6 \cdot (a_4^{(1)} z_8^3 z_9^5 + a_4^{(2)} z_8^2 z_9^6 + a_4^{(3)} z_8 z_9^7 + \ a_4^{(4)} z_9^8) +\\
&+\underline{z}_1^6 \cdot (a_6^{(1)} z_8^5 z_9^7 \ + a_6^{(2)} z_8^4 z_9^8 + a_6^{(3)} z_8^3 z_9^9 + a_6^{(4)} z_8^2 z_9^{(10)} + a_6^{(5)} z_8 z_9^{(11)} + a_6^{(6)} z_9^{(12)}) =\\
&= \underline{z}_7^2 + a_1 \cdot \underline{z}_6 \underline{z}_7 \cdot z_9^2 + \underline{z}_7 \cdot (a_3^{(1)} z_8^2 z_9^4 + a_3^{(2)} z_8 z_9^{(5)}).
\end{aligned}
\tag{3.21}
$$

The second Weierstrass equation for the E_{8_R} group can be obtained from this equation by interchanging the variables desrcibing the base: $z_8 \leftrightarrow z_9$*. The Weierstrass triangle equation can be presented in the following general form, where we denote $\underline{z}_6 = x$, $\underline{z}_7 = y$:

$$
y^2 \, + \, a_1 \cdot x \cdot y \, + \, a_3 \cdot y = x^3 \, + \, a_2 \cdot x^2 \, + \, a_4 \cdot x \, + \, a_6, \tag{3.22}
$$

where the a_i are polynomial functions on the base. The Weierstrass equation can be written in more simplified form as:

$$
y^2 \, = \, x^3 \, + \, x \cdot f \, + \, g, \tag{3.23}
$$

with discriminant

$$
\Delta \, = \, 4f^3 \, + \, 27g^2. \tag{3.24}
$$

In the zero locus of the discriminant, some divisors D_i define the degeneration of the torus fiber.

In addition to the method [34] described above, there is a somewhat different way to find the singularity type [35]. As we saw in the above example, the

*The coefficients a_i correspond to the notations of [35].

polynomials f and g can be homogeneous of orders 8 and 12, respectively, with a fibration that is degenerate over 24 points of the base. For this form of Weierstrass equation, there exists the ADE classification of degenerations of elliptic fibers. In this approach, the type of degeneration of the fiber is determined by the orders of vanishing of the functions f, g and δ. In the case of the general Weierstrass equation, a general algorithm for the ADE classification of elliptic singularities was considered by Tate [36]. For convenience, we repeat in Table 3 some results of Tate's algorithm, from which one can recover the $E_8 \times E_8$ type of Lie-algebra singularity for the (1,1,4,6) polyhedron.

Table 3. Lie algebras obtained from Tate's algorithm [36]: $a_{j;k} = a_j/\sigma^k$

Type	Group	$k(a_1)$	$k(a_2)$	$k(a_3)$	$k(a_4)$	$k(a_6)$	$k(\Delta)$
I_0	—	0	0	0	0	0	0
I_1	—	0	0	1	1	1	1
I_2	$SU(2)$	0	0	1	1	1	1
I_{2k}^{ns}	$Sp(2k)$	0	0	k	k	$2k$	$2k$
I_{2k}^{s}	$SU(2k)$	0	1	k	k	$2k$	$2k$
I_{2k+1}^{s}	$SU(2k+1)$	0	1	k	$k+1$	$2k+1$	$2k+1$
III	$SU(2)$	1	1	1	1	2	3
IV_s	$SU(3)$	1	1	1	2	3	4
I_0^{*ns}	G_2	1	1	2	2	3	6
I_1^{*s}	$SO(10)$	1	1	2	3	5	7
I_{2k-3}^{*ns}	$SO(4k+1)$	1	1	k	$k+1$	$2k$	$2k+3$
I_{2k-3}^{*s}	$SO(4k+2)$	1	1	k	$k+1$	$2k+1$	$2k+3$
I_{2k-2}^{*ns}	$SO(4k+3)$	1	1	$k+1$	$k+1$	$2k+1$	$2k+4$
I_{2k-2}^{*s}	$SO(4k+4)$	1	1	$k+1$	$k+1$	$2k+1$	$2k+4$
IV^{*ns}	F_4	1	2	2	3	4	8
IV^{*s}	E_6	1	2	2	3	5	8
III^*	E_7	1	2	3	3	5	9
II^*	E_8	1	2	3	4	5	10

4. THE COMPOSITE STRUCTURE OF PROJECTIVE VECTORS

We now embark in more detail on our construction of the projective vectors $\mathbf{k}$ which determine CY hypersurfaces, as previewed briefly in the Introduction and based on the polyhedron technique and the concept of duality [7] reviewed in Section 2. We develop this construction inductively, studying the structure of these vectors initially in low dimensions and then proceeding to higher ones.

4.1. Initiation to the Dual Algebra of CY Projective Vectors. Our starting point is the trivial zero-dimensional «vector»,

$$\mathbf{k}_1 = (1), \tag{4.1}$$

which defines the trivial self-dual polyhedron comprising a single point, with the simplest possible associated monomial:

$$x \Rightarrow \mu_1 = 1 \Rightarrow \mu_1' = (0). \tag{4.2}$$

The next step is to consider the only polyhedron on the line R^1 which is also self-dual, and whose intersection with the integer lattice on the line contains three integer points:

$$\mu_1' = (-1), \, \mu_1' = (0), \, \mu_1' = (+1). \tag{4.3}$$

The projective vector corresponding to this linear polyhedron is

$$\mathbf{k}_2 = (1, 1), \tag{4.4}$$

which can be constructed from the $\mathbf{k}_1$ vector, by the following procedure.

We extend the vector $\mathbf{k}_1$ to a two-dimensional vector in CP_1, by inserting a zero component in all possible ways:

$$\begin{aligned} \mathbf{k}_1^{ex'} &= (0, 1) \\ \mathbf{k}_1^{ex''} &= (1, 0). \end{aligned} \tag{4.5}$$

The following monomials correspond to these «extended» vectors:

$$\begin{aligned} \mu^{'} &= (\nu, 1) \Rightarrow x^{\nu} \cdot y \\ \mu^{''} &= (1, \xi) \Rightarrow x \cdot y^{\xi} \end{aligned} \tag{4.6}$$

with the arbitrary integer numbers ν, ξ. From all the possible $\mathbf{k}$ pairs:

$$(\mathbf{k}^{ex'} \Leftrightarrow \mathbf{k}^{ex'}), \; (\mathbf{k}^{ex''} \Leftrightarrow \mathbf{k}^{ex''}), \; (\mathbf{k}^{ex'} \Leftrightarrow \mathbf{k}^{ex''}), \tag{4.7}$$

we select only those whose intersections give a reflexive polyhedron. In this simple two-dimensional case, only a single pair is so selected, namely $\mathbf{k}_1^{ex'}$ and $\mathbf{k}_1^{ex''}$:

$$\mathbf{k}_1^{ex'} \bigcap \mathbf{k}_1^{ex''} = 1, \tag{4.8}$$

and the reflexive polyhedron comprises just a single point. The corresponding monomial is $x \cdot y$, whose degree is unity for both variables: $\deg_x = 1$ and $\deg_y = 1$.

We now introduce a second operation on these «extended» vectors $\mathbf{k}^{'\cdots}$, which is «dual» to the intersection, namely the «sum» operation:

$$\mathbf{k}_1^{ex'} \bigcup \mathbf{k}_1^{ex''} = \mathbf{k}_2 = (0,1) + (1,0) = (1,1). \tag{4.9}$$

In this simple case, one has three quadratic monomials:

$$\begin{aligned} x^2 \Rightarrow \mu_1 &= (2,0) \Rightarrow \mu_1' = (-1); \\ x \cdot y \Rightarrow \mu_2 &= (1,1) \Rightarrow \mu_2' = (0); \\ y^2 \Rightarrow \mu_3 &= (0,2) \Rightarrow \mu_3' = (+1). \end{aligned} \tag{4.10}$$

If a projective vector is multiplied by a positive integer number $m \in Z^+$, it still determines the same hypersurface. Therefore, we should also consider sums of such vectors, characterized by two positive integer numbers, $m,\ n$:

$$m \cdot \mathbf{k}_1^{ex'} + n \cdot \mathbf{k}_1^{ex''}. \tag{4.11}$$

It turns out that, in order to get a reflexive polyhedron with only one interior point, the numbers m and n have to be lower than certain maximal values: $m_{\max}$ and $n_{\max}$, respectively. In our first trivial example, we find that

$$m_{\max} = 1,\ \ n_{\max} = 1. \tag{4.12}$$

In general, the set of all pairs (m,n) with $m \leqslant m_{\max}$ and $n \leqslant n_{\max}$ generate a «chain» of possible reflexive polyhedra, which happens to be trivial in this simple case.

Following the previous procedure, to construct all possible vectors on the plane we should start from two vectors, $\mathbf{k}_1$ and $\mathbf{k}_2$, «extended» to dimension three in CP_2 space:

$$\begin{aligned} &\mathbf{k}_1^{ex'} = (0,0,1),\, \mathbf{k}_1^{ex''} = (0,1,0),\ \mathbf{k}_1^{ex'''} = (1,0,0), \\ &\mathbf{k}_2^{ex'} = (0,1,1),\, \mathbf{k}_2^{ex''} = (1,1,0),\ \mathbf{k}_2^{ex'''} = (1,0,1). \end{aligned} \tag{4.13}$$

The next step consists in finding all possible pairs of these three-dimensional vectors whose intersection gives the only reflexive polyhedron of dimension two, which corresponds to the polyhedron projective vector $\mathbf{k}_2 = (1,1)$. Only two pairs (plus cyclic permutations) satisfy this constraint:

$$[\mathbf{k}_1^{ex'}(0,0,1)] \bigcap [\mathbf{k}_2^{ex''}(1,1,0)] = [\mathbf{k}_2(1,1)]_J \tag{4.14}$$

and

$$[\mathbf{k}_2^{ex'}(0,1,1)] \bigcap [\mathbf{k}_2^{ex''}(1,1,0)] \;=\; [\mathbf{k}_2(1,1)]_J. \tag{4.15}$$

In these two cases, the corresponding monomials are:

$$\begin{aligned} x^2 \cdot z \Rightarrow \mu_1 = (2,0,1) \;&\Rightarrow\; (-1),\\ x \cdot y \cdot z \Rightarrow \mu_2 = (1,1,1) \;&\Rightarrow\; (0),\\ y^2 \cdot z \Rightarrow \mu_3 = (0,2,1) \;&\Rightarrow\; (+1), \end{aligned} \tag{4.16}$$

and

$$\begin{aligned} x^2 \cdot z^2 \Rightarrow \mu_1 = (2,0,2) \;&\Rightarrow\; (-1),\\ x \cdot y \cdot z \Rightarrow \mu_2 = (1,1,1) \;&\Rightarrow\; (0),\\ y^2 \Rightarrow \mu_3 = (0,2,0) \;&\Rightarrow\; (+1), \end{aligned} \tag{4.17}$$

respectively. These lead to the two following chains:

$$\begin{aligned} I. \qquad \mathbf{k}_3(1) \;&=\; 1\cdot\mathbf{k}_1^{ex'} \,+\, 1\cdot\mathbf{k}_2^{ex''} \;=\; (1,1,1);\; m=1,\, n=1,\\ \mathbf{k}_3(2) \;&=\; 2\cdot\mathbf{k}_1^{ex'} \,+\, 1\cdot\mathbf{k}_2^{ex''} \;=\; (1,1,2);\; m=2,\, n=1,\\ m_{\max} \;&=\; \dim(\mathbf{k}_2^{ex''}) = 2, \quad n_{\max} = \dim(\mathbf{k}_1^{ex'}) = 1 \end{aligned} \tag{4.18}$$

and

$$\begin{aligned} II. \qquad \mathbf{k}_3(2) \;&=\; 1\cdot\mathbf{k}_2^{ex'} \,+\, 1\cdot\mathbf{k}_2^{ex'''} \;=\; (1,1,2);\; m=1,\, n=1,\\ \mathbf{k}_3(3) \;&=\; 2\cdot\mathbf{k}_2^{ex'} \,+\, 1\cdot\mathbf{k}_2^{ex'''} \;=\; (1,2,3);\; m=2,\, n=1,\\ m_{\max} \;&=\; \dim(\mathbf{k}_2^{ex''}) = 2, \quad n_{\max} = \dim(\mathbf{k}_2^{ex'}) = 2. \end{aligned} \tag{4.19}$$

Where the eldest vectors are given on the first lines of the two preceding equations, and we note that the vector $(1,1,2)$ is common to both chains.

It turns out that, also in higher dimensions, some $\mathbf{k}$ vectors are common to more than one chain. Thus it is possible to make a transition from one chain to another by passing through the common vectors. The algebra of projective vectors with the two operations $\bigcap$ and $\bigcup$ should be closed under duality symmetry:

$$J \iff \Pi, \tag{4.20}$$

where the symbols J and Π denote two dual conjugate operations: *intersection* and *projection*, respectively. In this way, all vectors $\mathbf{k}_d$ can be found. This structure underpins the idea of a web of transitions between all Calabi–Yau manifolds.

4.2. General Formulation of Calabi–Yau Algebra. In the spirit of the simple constructions of the previous subsection, we can also construct the corresponding closed $\mathbf{k}_4$ algebra in the case of $K3$ hypersurfaces. However, before giving the results, we first briefly formulate a theorem underlying the construction of a $\mathbf{k}_{d+1}$ projective vector, determining an associated reflexive $d+1$-dimensional polyhedron and CY_d hypersurface, starting from $\mathbf{k}_d$ projective vectors, which determine a d-dimensional reflexive polyhedron with one interior point and a corresponding CY_{d-1} hypersurface. This theorem underlies our systematic inductive algebraic construction of CY manifolds.

The theorem is based on two general points:

• First: from the vector $\mathbf{k}_d$, we construct the «extended» vectors $\mathbf{k}_{d+1}^{ex}$ using the rule:

$$(*) \quad \mathbf{k}_d = (k_1, ..., k_2) \overset{\pi^{-1}}{\Longrightarrow} \mathbf{k}_{d+1}^{ex(i)} = (k_1, ..., 0^i, ..., k_d). \tag{4.21}$$

• Second: we consider only those pairs of all possible «extended» vectors, $\mathbf{k}_{d+1}^{ex(i)}$ and $\mathbf{k}_{d+1}^{ex(j)}$ with $0 \leqslant i, j \leqslant d$, whose intersection gives the reflexive polyhedron of dimension d with only one interior point. We denote this operation by:

$$(**) \qquad \mathbf{k}_{d+1}^{ex(i)} \bigcap \mathbf{k}_{d+1}^{ex(j)} \ = \ [\mathbf{k}_d]_J. \tag{4.22}$$

The statement of the theorem is:

• If by the rule (*) one can get, from the projective $\mathbf{k}_d$ vector, a set of «extended» vectors $\mathbf{k}_{d+1}^{ex(i)}$, $0 \leqslant i \leqslant d$, and for any pair of such «extended» $\mathbf{k}_{d+1}^{ex(i)}$-vectors the conditions (**) are fulfilled, then the sum of these two «extended» vectors will give an eldest projective vector $\mathbf{k}_{d+1}$, which determines a reflexive polyhedron with only one interior point.

• Two finite positive integer numbers, $n_{\max}, m_{\max} \in Z_+$, exist such that any linear combination of two vectors $\mathbf{k}_{d+1}^{i,j}(n,m)$, with integer coefficients $m \leqslant m_{\max}$; $n \leqslant n_{\max}$ produce a CY hypersurface. We call «chain» the set of vectors generated by any such pair of «extended» vectors:

$$\begin{aligned} p \cdot \mathbf{k}_{d+1}^{i,j}(n,m) &= m \cdot \mathbf{k}_{d+1}^{ex(i)} \ + n \cdot \mathbf{k}_{d+1}^{ex(j)}, \\ \mathbf{k}_{d+1}^{i,j}(1,1) &= \mathbf{k}_{d+1}^{i,j}(\mathrm{eld}). \end{aligned} \tag{4.23}$$

• The intersection of the vector $\mathbf{k}_{d+1}^{i,j}(m,n)$ with the vector $\mathbf{k}_{d+1}^{ex(i)}$ is equal to the intersection of this vector with the vector $\mathbf{k}_{d+1}^{ex(j)}$:

$$[\mathbf{k}_{d+1}^{i,j}(m,n)] \bigcap [\mathbf{k}_{d+1}^{ex(j)}] = [\mathbf{k}_{d+1}^{i,j}(m,n)] \bigcap [\mathbf{k}_{d+1}^{ex(i)}]. \tag{4.24}$$

We can also formulate a converse theorem:

- If one can decompose a reflexive projective vector $\mathbf{k}_{d+1}$ as the sum of two reflexive projective vectors $\mathbf{k}'_{d+1}$ and $\mathbf{k}''_{d+1}$, then there exists the intersection of the vector $\mathbf{k}_{d+1}$ with either of these two vectors, which defines a projective vector $\mathbf{k}_d$ and a reflexive polyhedron with only one interior point.

The above theorem provides a description of all CY_{d+1} hypersurfaces with d-dimensional fibers in terms of two positive-integer parameters. Similarly, one can also consider the intersections of three (or more) «doubly-extended» vectors $\mathbf{k}_{d+1}^{ex(')}$, $\mathbf{k}_{d+1}^{ex('')}$, $\mathbf{k}_{d+1}^{ex(''')}$ (by «doubly-extended» we mean that they may be obtained by inserting two zero components in $\mathbf{k}_{d-1}$ vectors). One should check that this intersection gives a reflexive polyhedron in the $d-2$ space:

$$[\mathbf{k}_{d-1}^{ex(2')}] \bigcap [\mathbf{k}_{d-1}^{ex(2'')}] \bigcap [\mathbf{k}_{d-1}^{ex(2''')}] = [\mathbf{k}_{d-1}]_J. \tag{4.25}$$

In this way, one may obtain a $3, 4, ..., \leqslant d$ positive-integer parameter description of the $(d+1)$-dimensional polyhedra with $(d-1), (d-2), ...$-dimensional fiber sections:

$$p \cdot \mathbf{k}_{d+1} = m \cdot \mathbf{k}_{d-1}^{ex(2')} + n \cdot \mathbf{k}_{d-1}^{ex(2'')} + l \cdot \mathbf{k}_{d-1}^{ex(2''')}. \tag{4.26}$$

Finally, one can obtain additional lists of $\mathbf{k}_{d+1}$ vectors by using three «extended» vectors, $\mathbf{k}_d^{ex^r}$, $\mathbf{k}_d^{ex^i}$ $\mathbf{k}_d^{ex^j}$ (and similarly using four $\mathbf{k}_{...}^{ex}$, etc.), and a special algebra of summing these vectors only if the following three conditions are fulfilled:

$$\begin{aligned} &1. [\mathbf{k}_d^{ex^r}] \bigcap [\mathbf{k}_d^{ex^i}] = [\mathbf{k}_{d-1}]'_J, \\ &2. [\mathbf{k}_d^{ex^i}] \bigcap [\mathbf{k}_d^{ex^j}] = [\mathbf{k}_{d-1}]''_J, \\ &3. [\mathbf{k}_d^{ex^j}] \bigcap [\mathbf{k}_d^{ex^r}] = [\mathbf{k}_{d-1}]'''_J. \end{aligned} \tag{4.27}$$

In this way, one may obtain a complete description of the positive-integer lattice which defines all reflexive $\mathbf{k}$ vectors.

5. TWO-VECTOR CHAINS OF $K3$ SPACES

We now embark on a parametrization of the $\mathbf{k}_4$ vectors defining $K3$ hypersurfaces with fiber sections. Our description of $K3$ hypersurfaces is based on the above understanding of the composite and dual structure of the projective $\mathbf{k}_4$ vectors. As already mentioned, we find a link between this structure and the finite subgroups of the group of rotations of three-space, namely the cyclic and dihedral groups and the symmetry groups of the Platonic solids — the tetrahedron, the octahedron-cube and the icosahedron-dodecahedron:

- $C_n : n = 1, 2, 3, ...$ — the cyclic group of finite rotations in the plane around an axis «1» by the angles $\alpha = 2\pi/n$;
- $D_n : n = 2, 3, 4, ...$ — the dihedral group, comprising all these rotations together with all the reflections of a second axis «n» lying in this plane, which is orthogonal to the axis «l», and producing with respect to each other the angle $\alpha/2$;
- T — the finite group of the transformations leaving invariant the regular tetrahedron, with 12 parameters;
- O — the finite group of the transformations leaving invariant the regular cube and octahedron, with 24 parameters;
- I — the finite group of the transformations leaving invariant the regular icosahedron and dodecahedron, with 60 parameters.

We use the polyhedron technique introduced in the previous Section, taking into account all its duality, intersection and projection properties to study the projective-vector classification of $K3$ spaces.

5.1. Two-Dimensional Integer Chains of $K3$ Hypersurfaces. In the $K3$ case, as already foreshadowed in the Introduction, the classification can start from a basis of five types of «extended» vectors. We recall that the structure of the three «planar» projective vectors $\mathbf{k}_3 = (1, 1, 1), (1, 1, 2), (1, 2, 3)$ can easily be understood on the basis of the doubly-extended vector $\mathbf{k}_1^{ext} = (0, 0, 1)$ and the singly-extended vector $\mathbf{k}_2^{ext} = (0, 1, 1)$. The structure of the underlying composite vector $\mathbf{k}_2 = (1, 1)$ is also obvious. The full list of $K3$ projective vectors is obtainable from the algebra of the following five extended vectors: the maximally-extended vector of the form

$$\mathbf{k}_C^{\text{ext}} = (0, 0, 0, 1) \tag{5.1}$$

with its 4 cyclic permutations, the doubly-extended dihedral vector of the form

$$\mathbf{k}_D^{\text{ext}} = (0, 0, 1, 1) \tag{5.2}$$

with its 6 dihedral permutations, the singly-extended tetrahedral vector of the form

$$\mathbf{k}_T^{\text{ext}} = (0, 1, 1, 1) \tag{5.3}$$

with its 4 cyclic permutations, the extended octahedral vector of the form

$$\mathbf{k}_O^{\text{ext}} = (0, 1, 1, 2) \tag{5.4}$$

with its 12 permutations, and finally the extended icosahedral vector of the form

$$\mathbf{k}_I^{\text{ext}} = (0, 1, 2, 3) \tag{5.5}$$

with its 24 permutations, for a total of 50 extended vectors.

Using the algebra of combining pairs of these 50 extended $\mathbf{k}^i$ vectors, we obtain 90 distinct $\mathbf{k}_4$ vectors in 22 double chains with a regular planar k-gon intersection: $k > 3$ with only one interior point, as seen in Table 1. Combining three extended $\mathbf{k}^i$ vectors, we obtain four triple chains with self-dual line-segment intersection-projections and one interior point, which contain 91 distinct vectors, of which only four $\mathbf{k}_4$ vectors are different from the 90 vectors found previously, as also seen in Table 1. Of course, there are some vectors which have a regular planar k-gon in their intersection and no line-segment intersection. Further, as we see later in Section 7, there is just one vector, $\mathbf{k}_4 = (7, 8, 9, 12)$, which has only a single point intersection, i.e., the intersection consists of the zero point alone, and can be determined by the intersection-projection

$$J(\Delta) \leftrightarrow \Pi(\Delta^*), \qquad \Pi(\Delta) \leftrightarrow J(\Delta^*) \tag{5.6}$$

duality, where the polyhedra Δ and Δ^* determine a dual pair of $K3$ hypersurfaces. We recall that the sum of the integer points in intersection, $J(\Delta)$, and in projection, $\Pi(\Delta^*)$, is equal to $14 = 4 + 10, 5 + 9, 6 + 8, 7 + 7, 8 + 6, 9 + 5, 10 + 4$ for the plane intersection-projection and $6 = 3 + 3$ for the line-segment intersection-projection. This duality plays a very important role in our description. Eleven of the 22 two-vector chains found previously satisfy directly the following condition:

$$\begin{aligned} J(\Delta^n) &= \Pi(\Delta^n) = \Delta^{n-1}, \\ \Pi(\Delta^{n*}) &= J(\Delta^{n*}) = \Delta^{n-1^*}, \end{aligned} \tag{5.7}$$

which means that the number of integer points in the intersection of the polyhedron (mirror polyhedron) forming the reflexive polyhedron of lower dimension is equal to the number of projective lines crossing these integer points of the polyhedron (mirror). The projections of these lines on a plane in the polyhedron and a plane in its mirror polyhedron reproduce, of course, the reflexive polyhedra of lower dimension. Only for self-dual polyhedra one can have

$$J(\Delta^n) = \Pi(\Delta^n) = \Pi(\Delta^{n*}) = J(\Delta^{n*}) = \Delta^{n-1} = \Delta^{n-1^*}, \tag{5.8}$$

namely the most symmetrical form of these relations.

Following the recipe presented as our central Theorem in Section 4, we present Table 4, which lists all the $\mathbf{k}_4$ projective vectors derived from *pairs* of extended vectors of lower dimension, which fall into the 22 chains listed. In each case, we list the maximum integers m, n in the chains, which are determined by the dimensions of the extended $\mathbf{k}_i$ vectors. This Table includes all the 90 projective $\mathbf{k}_4$ vectors found using our construction. All of these $\mathbf{k}_4$ vectors define $K3$ hypersurfaces which could be obtained using the Z^n symmetry coset action*.

*They may also be used to construct higher-level CY_1 spaces as the intersections of polynomial loci, as discussed in Section 9.

Table 4. The 22 chains of $K3$ obtained using pairs of $\mathbf{k}_4$ projective vectors. The number of $K3$ spaces in each chain is denoted by N

Chain	$\mathbf{k}_i \bigcap \mathbf{k}_j$	$\Delta_{\rm Int}, \Delta^*_{\rm Int}$	$\mathbf{k}(K3) = m \cdot \mathbf{k}_i + n \cdot \mathbf{k}_j$	$\sum m + \sum n$	$\max(m, n)$	N
I	$(0001) \bigcap (1110)$	$(10, 4)$	(n, n, n, m)	$1 \cdot m + 3 \cdot n$	$m = 1, n = 3$	3
IV	$(0001) \bigcap (1120)$	$(9, 5)$	$(n, n, 2n, m)$	$1 \cdot m + 4 \cdot n$	$m = 1, n = 4$	4
XV	$(0001) \bigcap (1230)$	$(7, 7)$	$(n, 2n, 3n, m)$	$1 \cdot m + 6 \cdot n$	$m = 1, n = 6$	6
X	$(0011) \bigcap (1100)$	$(9, 5)$	(n, n, m, m)	$2 \cdot m + 2 \cdot n$	$m = 2, n = 2$	4
XI	$(0011) \bigcap (1101)$	$(9, 5)$	$(n, n, m, m + n)$	$2 \cdot m + 3 \cdot n$	$m = 3, n = 2$	6
V	$(0011) \bigcap (1102)$	$(9, 5)$	$(n, n, m, m + 2n)$	$2 \cdot m + 4 \cdot n$	$m = 4, n = 2$	6
$XXII$	$(0011) \bigcap (1210)$	$(7, 7)$	$(n, 2n, m + n, m)$	$2 \cdot m + 4 \cdot n$	$m = 3, n = 3$	6
XVI	$(0011) \bigcap (1203)$	$(7, 7)$	$(n, 2n, m, m + 3n)$	$2 \cdot m + 6 \cdot n$	$m = 6, n = 2$	9
II	$(0111) \bigcap (1011)$	$(10, 4)$	$(n, m, m + n, m + n)$	$3 \cdot m + 3 \cdot n$	$m = 3, n = 3$	4
$XIII$	$(0111) \bigcap (1012)$	$(8, 6)$	$(n, m, m + n, m + 2n)$	$3 \cdot m + 4 \cdot n$	$m = 4, n = 3$	9
III	$(0111) \bigcap (3012)$	$(4, 10)$	$(3n, m, m + n, m + 2n)$	$3 \cdot m + 6 \cdot n$	$m = 6, n = 2$	9
$XVII$	$(0111) \bigcap (1023)$	$(7, 7)$	$(n, m, m + 2n, m + 3n)$	$3 \cdot m + 6 \cdot n$	$m = 6, n = 3$	12
VI	$(0112) \bigcap (1012)$	$(9, 5)$	$(n, m, n + m, 2m + 2n)$	$4 \cdot m + 4 \cdot n$	$m = 4, n = 4$	6
$VIII$	$(0112) \bigcap (1120)$	$(5, 9)$	$(n, m + n, m + 2n, 2m)$	$4 \cdot m + 4 \cdot n$	$m = 3, n = 4$	9
VII	$(0112) \bigcap (2110)$	$(9, 5)$	$(2n, m + n, m + n, 2m)$	$4 \cdot m + 4 \cdot n$	$m = 3, n = 1$	3
$XVIII$	$(0112) \bigcap (1023)$	$(7, 7)$	$(n, m, m + 2n, 2m + 3n)$	$4 \cdot m + 6 \cdot n$	$m = 6, n = 4$	16
XIV	$(0112) \bigcap (2130)$	$(6, 8)$	$(2n, m + n, m + 3n, 2m)$	$4 \cdot m + 6 \cdot n$	$m = 5, n = 3$	8
IX	$(0112) \bigcap (2103)$	$(5, 9)$	$(2n, m + n, m, 2m + 3n)$	$4 \cdot m + 6 \cdot n$	$m = 6, n = 3$	12
XIX	$(0123) \bigcap (1023)$	$(7, 7)$	$(n, m, 2m + 2n, 3m + 3n)$	$6 \cdot m + 6 \cdot n$	$m = 6, n = 6$	12
XX	$(0123) \bigcap (2103)$	$(7, 7)$	$(2n, m + n, 2m, 3m + 3n)$	$6 \cdot m + 6 \cdot n$	$m = 3, n = 3$	12
XXI	$(0123) \bigcap (3120)$	$(7, 7)$	$(3n, m + n, 2m + 2n, 3n)$	$6 \cdot m + 6 \cdot n$	$m = 2, n = 2$	4
XII	$(0123) \bigcap (3210)$	$(5, 9)$	$(3n, m + 2n, 2m + n, 3m)$	$6 \cdot m + 6 \cdot n$	$m = 2, n = 2$	4

For illustration, we give in Table 5 the eldest vectors in each chain, i.e., the first members of all 22 chains, which have $m = 1, n = 1$. As one can see, some vectors are common to more than one chain. Using our understanding of the origins of the intersections, and duality, we can classify these 22 chains in five classes, as indicated by the groupings in Table 5, which correspond to the intersections, as indicated.

It should be noted, however, that the above doubly-extended vector structure does not exhaust the full list of possible $K3$ projective vectors. The projective vectors

$$\begin{aligned}
(\mathbf{k}_4)_{91} &= (4, 5, 7, 9), \\
(\mathbf{k}_4)_{92} &= (5, 6, 8, 11), \\
(\mathbf{k}_4)_{93} &= (5, 7, 8, 20), \\
(\mathbf{k}_4)_{94} &= (7, 8, 10, 25), \\
(\mathbf{k}_4)_{95} &= (7, 8, 9, 12)
\end{aligned} \tag{5.9}$$

Table 5. The eldest vectors $\mathbf{k}_i$ in the 22 $K3$ chains which have $m = n = 1$

Chain	d	$\mathbf{k}_i$	$\mathbf{k}_i$	(Δ, Δ^*)	$(\Delta_{\text{Int}}, \Delta^*_{\text{Int}})$
I	$d = 1 \cdot m + 3 \cdot n$	(n, n, n, m)	$(1, 1, 1, 1)$	$(35, 5)$	$(10, 4)$
II	$d = 3 \cdot m + 3 \cdot n$	$(n, m, m + n, m + n)$	$(1, 1, 2, 2)$	$(30, 6)$	$(10, 4)$
III	$d = 3 \cdot m + 6 \cdot n$	$(3n, m, m + n, m + 2n)$	$(1, 2, 3, 3)$	$(23, 8)$	$(4, 10)$
IV	$d = 1 \cdot m + 4 \cdot n$	$(n, n, 2n, m)$	$(1, 1, 1, 2)$	$(34, 6)$	$(9, 5)$
V	$d = 2 \cdot m + 2 \cdot n$	(n, n, m, m)	$(1, 1, 1, 1)$	$(35, 5)$	$(9, 5)$
VI	$d = 2 \cdot m + 3 \cdot n$	$(n, n, m, m + n)$	$(1, 1, 1, 2)$	$(34, 6)$	$(9, 5)$
VII	$d = 2 \cdot m + 4 \cdot n$	$(n, n, m, m + 2n)$	$(1, 1, 1, 3)$	$(39, 6)$	$(9, 5)$
$VIII$	$d = 4 \cdot m + 4 \cdot n$	$(n, m, m + n, 2m + 2n)$	$(1, 1, 2, 4)$	$(35, 7)$	$(9, 5)$
IX	$d = 4 \cdot m + 4 \cdot n$	$(2n, m + n, m + n, 2m)$	$(1, 1, 1, 1)$	$(35, 5)$	$(9, 5)$
X	$d = 4 \cdot m + 4 \cdot n$	$(n, m + n, m + 2n, 2m)$	$(1, 2, 2, 3)$	$(24, 8)$	$(5, 9)$
XI	$d = 4 \cdot m + 6 \cdot n$	$(2n, m + n, m, 2m + 3n)$	$(1, 2, 2, 5)$	$(28, 8)$	$(5, 9)$
XII	$d = 6 \cdot m + 6 \cdot n$	$(3n, m + 2n, 2m + n, 3m)$	$(1, 1, 1, 1)$	$(35, 5)$	$(5, 9)$
$XIII$	$d = 3 \cdot m + 4 \cdot n$	$(n, m, m + n, m + 2n)$	$(1, 1, 2, 3)$	$(31, 8)$	$(8, 6)$
XIV	$d = 4 \cdot m + 6 \cdot n$	$(2n, m + n, m + 3n, 2m)$	$(1, 1, 1, 2)$	$(34, 6)$	$(6, 8)$
XV	$d = 1 \cdot m + 6 \cdot n$	$(n, 2n, 3n, m)$	$(1, 1, 2, 3)$	$(31, 8)$	$(7, 7)$
XVI	$d = 2 \cdot m + 6 \cdot n$	$(m, n, 2n, 3n + m)$	$(1, 1, 2, 4)$	$(35, 7)$	$(7, 7)$
$XVII$	$d = 3 \cdot m + 6 \cdot n$	$(n, m, m + 2n, , m + 3n)$	$(1, 1, 3, 4)$	$(33, 9)$	$(7, 7)$
$XVIII$	$d = 4 \cdot m + 6 \cdot n$	$(n, m, m + 2n, 2m + 3n)$	$(1, 1, 3, 5)$	$(36, 9)$	$(7, 7)$
XIX	$d = 6 \cdot m + 6 \cdot n$	$(n, m, 2m + 2n, 3m + 3n)$	$(1, 1, 4, 6)$	$(39, 9)$	$(7, 7)$
XX	$d = 6 \cdot m + 6 \cdot n$	$(2n, m + n, 2m, 3m + 3n)$	$(1, 1, 1, 3)$	$(39, 6)$	$(7, 7)$
XXI	$d = 6 \cdot m + 6 \cdot n$	$(3n, m + n, 2m + 2n, 3m)$	$(2, 3, 3, 4)$	$(15, 9)$	$(7, 7)$
$XXII$	$d = 2 \cdot m + 4 \cdot n$	$(n, 2n, m + n, m)$	$(1, 1, 2, 2)$	$(30, 6)$	$(7, 7)$

have no planar reflexive polyhedron intersections, and therefore were not included in this list. To obtain most of the additional $\mathbf{k}_4$ vectors (5.10), one must consider chains constructed from three extended vectors of the type $\mathbf{k}^{ex} = (0, 0, 1)$ and $\mathbf{k}^{ex} = (0, 1, 1)$, with all possible permutations, having in the intersection the line-segment polyhedron consisting of three integer points. All these chains will be $J_1 - \Pi_1$ self-dual: $J_1 = \Pi_1 = 3$. It is easy to see that only four different such triple chains can be built, as discussed in Section 6. These chains are much longer than the previous two-vector chains, although their total number, 91, is also less than the full number of all $K3$ vectors. The projective vectors

$$\begin{aligned}
(\mathbf{k}_4)_{12} &= (3, 5, 6, 7), \\
(\mathbf{k}_4)_{13} &= (3, 6, 7, 8), \\
(\mathbf{k}_4)_{14} &= (5, 6, 7, 9), \\
(\mathbf{k}_4)_{95} &= (7, 8, 9, 12)
\end{aligned} \tag{5.10}$$

are not involved in these chains. However, the union of the doubly-extended and triply-extended vector chains gives a total of 94 $\mathbf{k}_4$ projective vectors. Only the $\mathbf{k}_4 = (7, 8, 9, 12)$ vector has just a point-intersection structure, and is not found by either the double- or triple-vector constructions, as discussed in more detail in Section 7.

To preview how it arises, note that, by $J - \Pi$ duality, we know that to $\mathbf{k} = (1, 1, 1, 1)$, which has three intersection planes (1,1,1) with ten points, there must correspond a $\mathbf{k}$ which has three different π projections with four points. Since it should have a nontrivial projection structure, namely a four-point planar polyhedron with one interior point in three independent directions, its external points should satisfy the following condition:

$$\frac{1}{4}\{M_1 + M_2 + M_3 + M_4\} = M_0 = (1, 1, 1, 1). \tag{5.11}$$

In three-space, these points can only be taken as:

$$\begin{aligned} M_1 &= (4, 1, 0, 0),\ M_2 = (0, 3, 1, 0), \\ M_3 &= (0, 0, 4, 0),\ M_4 = (0, 0, 0, 3). \end{aligned} \tag{5.12}$$

One can easily check that this polyhedron has three projections: π_{x_1}, π_{x_2}, π_{x_3}, with four points giving the $(1, 1, 1)$ planar polyhedron. The four points M_i (5.12) give the exceptional vector $\mathbf{k} = (7, 8, 9, 12)$. By projection, one can see that the five integer points of this polyhedron produce the $(1, 1, 1)$ planar polyhedron with four points.

5.2. Invariant Monomials and the $J - \Pi$ Structure of Calabi–Yau Equations. The experience provided by working with $K3$ hypersurfaces can aid in the classification of Calabi–Yau manifolds. Also for this more complicated case, one should use the duality conditions: one must be prepared to study the intersection structures of polyhedra and their mirrors and/or to study the projection structures for polyhedra and mirror polyhedra.

This «intersection-projection» structure of the $\mathbf{k}_4$ vectors from doubly-, triply- and quadruply-extended vectors allows us to introduce the concept of *invariant* monomials in the CY equations. These invariant monomials are homogeneous under the action of the extended vectors, i.e., if

$$\mathbf{z}' = \lambda^{\mathbf{k}_j^{ex}} \cdot \mathbf{z}, \quad j = 1, 2, 3, ..., \tag{5.13}$$

then

$$\mathbf{z}'^{\boldsymbol{\mu}} = \lambda^{\mathbf{k}_j^{ex} \cdot \boldsymbol{\mu}} \cdot \mathbf{z}^{\boldsymbol{\mu}} = \lambda^{d_j} \cdot \mathbf{z}^{\boldsymbol{\mu}}, \tag{5.14}$$

where $d_j = \dim(\mathbf{k}_j^{ex})$ and $j = 1, 2, 3, ...$ is the number of extended $\mathbf{k}_j^{ex}$ vectors. The invariant monomials, $\wp_i$, correspond to the reflexive polyhedra produced by the invariant set Ψ_{inv} which is the same for all the chains.

These extended vectors can be formed from the following five familiar types of projective vectors of lower dimensions:

$$\begin{aligned} &\mathbf{k}_1 = (0,0,1),\\ &\mathbf{k}_2 = (0,1,1), \qquad (5.15)\\ &\mathbf{k}_3 = (1,1,1),\ \mathbf{k}_3 = (1,1,2),\ \mathbf{k}_3 = (1,2,3). \end{aligned}$$

A chain of $\mathbf{k}_4$ projective vectors can be generated from the linear sums of extended vectors, for example, for $j = 1,2$ one can get:

$$\begin{aligned} &\mathbf{k}_4(m,n) = m \cdot \mathbf{k}_1^{ex} \,+\, n \cdot \mathbf{k}_2^{ex}\\ &\text{if } \mathbf{k}_1^{ex} \bigcap \mathbf{k}_2^{ex} = \{\wp_i : \wp_i \in \Sigma_{\text{inv}}\}. \end{aligned} \qquad (5.16)$$

The invariant monomials are universal for all the $\mathbf{k}_4$ vectors in this chain.

To construct the $\mathbf{k}_4$ vectors determining $K3$ hypersurfaces, i.e., determining the corresponding polyhedra with the property of reflexivity, one has to give a correct set of invariant monomials. We have constructed the 22 sets of invariant monomials corresponding to the doubly-extended vector structures among the $\mathbf{k}_4$ projective vectors. In this case, these sets of the invariant monomials give in the intersection reflexive polyhedra of lower dimensions. The number of invariant monomials for this doubly-extended vector structure is given by

$$31 \,=\, 1 \,+\, 4 \times 2 \,+\, 22, \qquad (5.17)$$

where the last number corresponds to the Betti number for $K3$ hypersurfaces: $b_2 = 22$. The structure of the $\mathbf{k}_4$ projective vectors obtained from the triply-extended vectors, namely $\mathbf{k}^{ex} = (0,0,0,1)$ and $\mathbf{k}^{ex} = (0,0,1,1)$, is given by the following four types of invariant monomials:

$$\begin{aligned} &\Psi_{I_3} : (2,0,1,1),\, (0,2,1,1),\, (1,1,1,1,) \Rightarrow x^2 \cdot z \cdot u,\, y^2 \cdot z \cdot u,\, x \cdot y \cdot z \cdot u,\\ &\Psi_{II_3} : (2,2,1,0),\, (0,0,1,2),\, (1,1,1,1,) \Rightarrow x^2 \cdot y^2 \cdot z,\, z \cdot u^2,\, x \cdot y \cdot z \cdot u,\\ &\Psi_{III_3} : (2,2,2,0),\, (0,0,0,2),\, (1,1,1,1,) \Rightarrow x^2 \cdot y^2 \cdot z^2,\, u^2,\, x \cdot y \cdot z \cdot u,\\ &\Psi_{IV_3} : (2,0,0,2),\, (0,2,2,0),\, (1,1,1,1,) \Rightarrow x^2 \cdot u^2,\, y^2 \cdot z^2,\, x \cdot y \cdot z \cdot u. \end{aligned} \qquad (5.18)$$

The four chains corresponding to these sets of invariant monomials are (see Tables 4,5,6, and 7):

$$
\begin{aligned}
\mathbf{k}_4(\Psi_{I_3}) = M \cdot (1,1,0,0) + N \cdot (0,0,1,0) + \\
+L \cdot (0,0,0,1) = (M,M,N,L), \\
\mathbf{k}_4(\Psi_{II_3}) = M \cdot (1,0,0,1) + N \cdot (0,1,0,1) + \\
+L \cdot (0,0,1,0) = (M,N,L,M+N), \\
\mathbf{k}_4(\Psi_{III_3}) = M \cdot (1,0,0,1) + N \cdot (0,1,0,1) + \\
+ L \cdot (0,0,1,1) = (M,N,L,M+N+L), \\
\mathbf{k}_4(\Psi_{IV_3}) = M \cdot (1,0,1,0) + N \cdot (0,1,0,1) + \\
+ L \cdot (0,0,1,1) = (M,N,M+L,N+L).
\end{aligned}
\tag{5.19}
$$

In these chains*, the sets of projective vectors are subject to the following additional projective restrictions:

$$
\begin{aligned}
\mathbf{k}_4(\Psi_{I_3}) \cdot \mathbf{e}_I &= 0, \quad \mathbf{e}_I = (-1,1,0,0), \\
\mathbf{k}_4(\Psi_{II_3}) \cdot \mathbf{e}_{II} &= 0, \quad \mathbf{e}_{II} = (-1,-1,0,1), \\
\mathbf{k}_4(\Psi_{III_3}) \cdot \mathbf{e}_{III} &= 0, \quad \mathbf{e}_{III} = (-1,-1,-1,1), \\
\mathbf{k}_4(\Psi_{IV_3}) \cdot \mathbf{e}_{IV} &= 0, \quad \mathbf{e}_{IV} = (1,-1,-1,1).
\end{aligned}
\tag{5.20}
$$

Corresponding to these chains, the following triple intersections

$$
\mathbf{k}_M^{ex} \bigcap \mathbf{k}_N^{ex} \bigcap \mathbf{k}_L^{ex} = \Psi_{I_3},\, \Psi_{II_3},\, \Psi_{III_3},\, \Psi_{IV_3}. \tag{5.21}
$$

have the above-mentioned invariant monomials.

The $K3$ algebra has the interesting consequence that all the $\{1+4+22\}$ invariant monomials that give «good» planar reflexive polyhedra in the 22 two-vector chains also can be found by triple constructions. Therefore it is interesting to list now the 22 types of invariant monomials whose origin is also connected with the triple intersections of all types of projective vectors, the triply-extended vectors $\mathbf{k}_1^{ex} = (0,0,0,1)$, the doubly-extended vectors $\mathbf{k}_2^{ex} = (0,0,1,1)$, and the singly-extended vectors, $\mathbf{k}_3^{ex} = (0,1,1,1), (0,1,1,2), (0,1,2,3)$.

These monomials, $\mathbf{z}^{\boldsymbol{\mu}}$, are invariant under action of the extended vectors

$$
\begin{aligned}
\mathbf{k}_i^{ex} \cdot \boldsymbol{\mu} = \dim(\mathbf{k}_i^{ex}), \\
\mathbf{k}_j^{ex} \cdot \boldsymbol{\mu} = \dim(\mathbf{k}_j^{ex}), \\
\mathbf{k}_l^{ex} \cdot \boldsymbol{\mu} = \dim(\mathbf{k}_l^{ex}).
\end{aligned}
\tag{5.22}
$$

*There is in fact another «good» triple intersection of the extended vectors $(1,1,0,0)$, $(0,0,1,1)$, $(0,0,0,1)$, but the chain $I_3' = (M,M,N,N+L)$ it produces has the same three invariant monomials, $(0,2,1,1)+(2,0,1,1)+(1,1,1,1)$ as the I_3 chain, which includes all its projective vectors.

The directions of the possible projections Π are determined[*] by the degenerate monomial $(x \cdot y \cdot z \cdot u) \Rightarrow \boldsymbol{\mu} = (1,1,1,1)$ and by the exponents of the following 22 invariant monomials, $\mu = (\mu_1, \mu_2, \mu_3, \mu_4)$:

$$\begin{aligned}
&\underline{(3,0,0,0),\ (3,1,0,0),\ (3,1,1,0),}\,(3,2,0,0),\\
&(3,2,1,0),\ (3,3,0,0),\ (3,3,1,0),\\
&\underline{(4,0,0,0),\ (4,1,0,0),}\,(4,1,1,0),\ (4,2,0,0),\\
&(4,2,1,0),(4,3,0,0),\ (4,3,1,0),\ (4,4,0,0),\ (4,4,1,0),\\
&(6,0,0,0),\ (6,1,0,0),\ (6,2,0,0),\ (6,3,0,0),\\
&(6,4,0,0),\ (6,6,0,0),
\end{aligned} \tag{5.23}$$

where the underlines pick out those triple intersections where the intersections of pairs of vectors also specify reflexive polyhedra, which will be important later. The four other types of possible projections were already defined above.

The algebraic-geometry sense of $(J,\Pi)(\Delta) \leftrightarrow (\Pi, J)(\Delta^*)$ duality for $K3$ hypersurfaces can be interpreted through the invariant monomials: the list of the invariant monomials for the two-extended-vector classification and the list of all of the three-extended-vector classification are the same, and the total number of them is equal to $31 = 1 + 4 \times 2 + 22$. The $J(\Delta, \Delta^*) \leftrightarrow \Pi(\Delta^*, \Delta)$ duality can be interpreted at a deeper level for $J = \Pi$ chains: the invariant monomials are identical for corresponding CY equation and for its mirror equation. The projection–projection structure gives additional information about the form of the corresponding CY equation. For example, this structure determines the subset of monomials corresponding to the invariant monomials. As a result, the homogeneous CY equation can be written in according in terms of the intersection–projection structure of the projective $\mathbf{k}$ vectors:

$$\wp(\mathbf{z}) = \sum_{i}^{J} \mathbf{z}^{\mathbf{m}_0^i} \{ \sum_{p}^{\Pi} a^p_{\mathbf{m}_0^i}\, \mathbf{z}^{n_p \cdot \mathbf{e}^\Pi} \} = 0. \tag{5.24}$$

Here the $\mathbf{z}^{\mathbf{m}_0^i}$ are the invariant monomials which are defined by intersection structure, the vector $\mathbf{e}^\Pi$ is the direction of the projection, and the n_p are integer numbers.

6. THREE-VECTOR CHAINS OF $K3$ SPACES

As already mentioned, one can find additional chains of $K3$ projective vectors $\mathbf{k}_4$ if one considers systems of three extended vectors of the type $\mathbf{k}_1^{ex} = (0,0,0,1)$

[*] Additional constraints on the invariant monomials are given in Section 7, reducing their number to 9 = 1 + 3 + 5.

Table 6. The 18 $K3$ hypersurfaces in the three-vector chain I_3: $\mathbf{k} = (M, M, N, L) = = M \cdot (1,1,0,0) + N \cdot (0,0,1,0) + L \cdot (0,0,0,1)$. Here and subsequently, the symbol ℵ in the first column denotes the location of the corresponding vector in Table 1. The numbers in the last columns indicate their locations in the corresponding chains

ℵ	M	M	N	L	$[d]$	(Δ, Δ^*)	I	II	IV	V	VII	X	XI	III
$J(\Delta)$	–	–	–	–	–	–	10	10	9	9	9	9	9	–
$\pi(\Delta^*)$	–	–	–	–	–	–	4	4	5	5	5	5	5	–
$\pi(\Delta)$	–	–	–	–	–	–	–	10	–	–	$9'$	–	–	–
$J(\Delta^*)$	–	–	–	–	–	–	–	4	–	–	$5'$	–	–	–
1	1	1	1	1	[4]	$(35, 5^*)$	1	–	–	–	1	1	–	–
2	1	1	1	2	[5]	$(34, 6^*)$	2	–	1	–	–	–	1	–
3	1	1	1	3	[6]	$(39, 6^*)$	3	–	–	1	–	–	–	–
4	1	1	2	2	[6]	$(30, 6^*)$	–	1	2	–	–	2	–	–
5	1	1	2	3	[7]	$(31, 8^*)$	–	–	3	–	–	–	2	–
6	1	1	2	4	[8]	$(35, 7^*)$	–	–	4	2	–	–	–	–
7	1	1	3	4	[9]	$(33, 9^*)$	–	–	–	–	–	–	4	–
8	1	1	3	5	[10]	$(36, 9^*)$	–	–	–	3	–	–	–	–
9	1	1	4	6	[12]	$(39, 9^*)$	–	–	–	5	–	–	–	–
10	2	2	1	3	[8]	$(24, 8^*)$	–	–	–	–	2	–	3	–
11	2	2	1	5	[10]	$(28, 8^*)$	–	–	–	4	–	–	–	–
42	2	2	3	5	[12]	$(17, 11^*)$	–	–	–	–	–	–	5	–
43	2	2	3	7	[14]	$(19, 11^*)$	–	–	–	6	–	–	–	–
12	3	3	1	2	[9]	$(23, 8^*)$	–	2	–	–	–	–	–	–
44	3	3	2	4	[12]	$(15, 9^*)$	–	–	–	–	3	–	–	–
65	3	3	4	5	[15]	$(12, 12^*)$	–	–	–	–	–	–	–	1
21	4	4	1	3	[12]	$(21, 9^*)$	–	3	–	–	–	–	–	–
48	5	5	2	3	[15]	$(14, 11^*)$	–	4	–	–	–	–	–	–

and $\mathbf{k}_2^{ex} = (0, 0, 1, 1)$, which have in their intersections only three integer points or only three invariant monomials. As also already remarked, there are only four different chains, corresponding to the four kinds of invariant monomial triples. We have also commented that these new chains yield only four additional $K3$ vectors, whilst the remaining vector, $\mathbf{k}_4 = (7, 8, 9, 12)$, can be constructed out of four extended vectors, as discussed in the following Section. The relationship between the two- and three-vector constructions, and their substantial overlap, is the subject of this Section.

6.1. The Three-Vector Chain I_3: $\mathbf{k}_4 = (M, M, N, L)$. In this chain, the dimension $(d = 2M + N + L)$ and the eldest vector is $\mathbf{k}_{\text{eld}} = (1, 1, 1, 1)$, whose invariant monomials are $(2, 0, 1, 1) + (0, 2, 1, 1)$. The relations between this three-vector chain and the previously-discussed two-vector chains can easily be found.

We consider the first three vectors in Table 6, which also form the two-vector chain I:

$$\begin{aligned} I: \quad & m \cdot (1,1,1,0) + n \cdot (0,0,0,1) = (m,m,m,n) \rightarrow \\ & M = N = m = [\dim]\{(0,0,0,1)\} = 1, \\ & L = n \leqslant [\dim]\{(1,1,1,0)\} = 3. \end{aligned} \tag{6.1}$$

Similarly, one can consider four vectors $(2,2,1,1)$, $(3,3,1,2)$, $(4,4,1,3)$, and $(5,5,2,3)$, which form the two-vector chain II:

$$\begin{aligned} II: \quad & m \cdot (1,1,1,0) + n \cdot (1,1,0,1) = (m+n, m+n, m, n) \rightarrow \\ & N = m \leqslant [\dim]\{(1,1,0,1)\} = 3, \\ & L = n \leqslant [\dim]\{(1,1,1,0)\} = 3, \\ & M = m + n < 6. \end{aligned} \tag{6.2}$$

The four vectors $(1,1,2,1)$, $(1,1,2,2)$, $(1,1,2,3)$, and $(1,1,2,4)$ from the two-vector chain IV have the following relations with this triple chain:

$$\begin{aligned} IV: \quad & m \cdot (1,1,2,0) + n \cdot (0,0,0,1) = (m,m,2m,n) \rightarrow \\ & M = m \leqslant [\dim]\{(0,0,0,1)\} = 1, \\ & N = 2m = 2, \\ & L = n \leqslant [\dim]\{(1,1,2,0)\} = 4. \end{aligned} \tag{6.3}$$

The six vectors $(1,1,1,3)$, $(1,1,2,4)$, $(1,1,3,5)$, $(1,1,4,6)$, $(2,2,1,5)$, and $(2,2,3,7)$ in Table 6 correspond to the two-vector chain V:

$$\begin{aligned} V: \quad & m \cdot (1,1,0,2) + n \cdot (0,0,1,1) = (m,m,n,2m+n) \rightarrow \\ & M = m \leqslant [\dim]\{(0,0,1,1)\} = 2, \\ & N = n \leqslant [\dim]\{(1,1,0,2)\} = 4, \\ & L = 2m + n <= 8. \end{aligned} \tag{6.4}$$

The next three vectors $(1,1,1,1)$, $(3,3,2,4)$, and $(2,2,1,3)$ from the two-vector chain VII have the following connection to this triple chain:

$$\begin{aligned} VII: \quad & m \cdot (1,1,2,0) + n \cdot (1,1,0,2) = (m+n, m+n, 2m, 2n) \rightarrow \\ & M = m + n < 4, \\ & N = 2m < 4, \\ & L = 2n < 4. \end{aligned} \tag{6.5}$$

Two vectors $(1,1,1,1)$ and $(1,1,2,2)$ correspond to the two-vector chain X:

$$\begin{aligned} X: \quad & m\cdot(1,1,0,0) + n\cdot(0,0,1,1) = (m,m,n,n) \rightarrow \\ & M = m \leqslant 2, \\ & N = n \leqslant 2, \\ & L = n \leqslant 2. \end{aligned} \tag{6.6}$$

Finally, the values of M, N, L of the five projective vectors $(1,1,1,2)$, $(1,1,2,3)$, $(1,1,3,4)$, $(2,2,1,3)$, and $(2,2,3,5)$ correspond to the fact that they are also from the two-vector chain XI:

$$\begin{aligned} XI: \quad & m\cdot(1,1,0,1) + n\cdot(0,0,1,1) = (m,m,n,m+n) \rightarrow \\ & M = m \leqslant 2, \\ & N = n \leqslant 3, \\ & L = m+n \leqslant 5. \end{aligned} \tag{6.7}$$

6.2. The Three-Vector Chain II_3: $\mathbf{k}_4 = (M, N, L, M+N)$. In this chain, shown in Table 7, the dimension $d = 2M + 2N + L$, there is a symmetry: $M \leftrightarrow N$, the eldest vector $\mathbf{k}_{\text{eld}} = (1,1,1,2)$, and the invariant monomials are $(2,2,1,0)+(0,0,1,2)$. Comparing this chain with the previous two-vector chains, one can see clearly the possible values of M, N, L for the projective vectors $(M, N, L, M+N)$. For example, if one compares the four vectors $(1,1,2,2)$, $(1,2,3,3)$, $(1,3,4,4)$, and $(2,3,5,5)$ in this triple chain with their structure in the two-vector chain II, one finds the following relations:

$$\begin{aligned} II: \quad & m\cdot(1,0,1,1) + n\cdot(0,1,1,1) = (m,n,m+n,m+n) \rightarrow \\ & M = m \leqslant [\dim]\{(0,1,1,1)\} = 3, \\ & N = n \leqslant [\dim]\{(1,0,1,1)\} = 3, \\ & L = m + n < 6. \end{aligned} \tag{6.8}$$

Similarly, we find the following relations between the values of M, N, L in the triple chain and the values of m, n for double chains:

$$\begin{aligned} IV: \quad & m\cdot(1,1,0,2) + n\cdot(0,0,1,0) = (m,m,n,2m) \rightarrow \\ & M = N = m \leqslant [\dim]\{(0,0,1,0)\} = 1, \\ & L = n \leqslant [\dim]\{(1,1,0,2)\} = 4. \end{aligned} \tag{6.9}$$

$$\begin{aligned} VI: \quad & m\cdot(1,0,2,1) + n\cdot(0,1,2,1) = (m,n,2m+2n,m+n) \rightarrow \\ & M = m \leqslant [\dim]\{(0,1,2,1)\} = 4, \\ & N = n \leqslant [\dim]\{(1,0,2,1)\} = 4, \\ & L = 2m + 2n < 8. \end{aligned} \tag{6.10}$$

$$\begin{aligned} VIII: \quad & m\cdot(1,0,2,1)\,+\,n\cdot(1,1,0,2)\,=\,(m+n,n,2m,m+2n)\,\rightarrow \\ & M=m+n\,\leqslant\,8, \\ & N=n\,\leqslant\,[\dim]\{(1,0,2,1)\}=4, \\ & L=2m\,\leqslant\,2[\dim]\{(1,1,0,2)\}=8. \end{aligned} \tag{6.11}$$

$$\begin{aligned} XI: \quad & m\cdot(1,0,1,1)\,+\,n\cdot(0,1,0,1)\,=\,(m,n,m,m+n)\,\rightarrow \\ & M=m\,\leqslant\,[\dim]\{(0,1,0,1)\}=2, \\ & N=n\,\leqslant\,[\dim]\{(1,0,1,1)\}=3, \\ & L=m. \end{aligned} \tag{6.12}$$

$$\begin{aligned} XIII: \quad & m\cdot(1,0,2,1)\,+\,n\cdot(0,1,1,1)\,=\,(m,n,2m+n,m+n)\,\rightarrow \\ & M=m\,\leqslant\,[\dim]\{(0,1,1,1)\}=3, \\ & N=n\,\leqslant\,[\dim]\{(1,0,2,1)\}=4, \\ & L=2m+n. \end{aligned} \tag{6.13}$$

$$\begin{aligned} XIV: \quad & m\cdot(1,0,2,1)\,+\,n\cdot(1,2,0,3)\,=\,(m+n,2n,2m,m+3n)\,\rightarrow \\ & M=m+n, \\ & N=2n\,\leqslant\,2[\dim]\{(1,0,2,1)\}=8, \\ & L=2m\,\leqslant\,2[\dim]\{(1,2,0,3)\}=12. \end{aligned} \tag{6.14}$$

$$\begin{aligned} XV: \quad & m\cdot(1,2,0,3)\,+\,n\cdot(0,0,1,0)\,=\,(m,2m,n,3m)\,\rightarrow \\ & M=m\leqslant\,[\dim]\{(0,0,1,0)\}=1, \\ & N=2m\,\leqslant\,2[\dim]\{(0,0,1,0)\}=2, \\ & L=n\,\leqslant\,[\dim]\{(1,2,0,3)\}=6. \end{aligned} \tag{6.15}$$

$$\begin{aligned} XVII: \quad & m\cdot(1,2,0,3)\,+\,n\cdot(0,1,1,1)\,=\,(m,2m+n,n,3m+n)\,\rightarrow \\ & M=m\leqslant\,[\dim]\{(0,1,1,1)\}=3, \\ & N=2m+n, \\ & L=n\,\leqslant\,[\dim]\{(1,2,0,3)\}=6. \end{aligned} \tag{6.16}$$

$$\begin{aligned} XXII: \quad & m\cdot(1,0,2,1)\,+\,n\cdot(0,1,0,1)\,=\,(m,n,2m,m+n)\,\rightarrow \\ & M=m\,\leqslant\,[\dim]\{(0,1,0,1)\}=2, \\ & N=n\,\leqslant\,[\dim]\{(1,0,2,1)\}=6, \\ & L=2m. \end{aligned} \tag{6.17}$$

Table 7. The 45 $K3$ hypersurfaces in the II_3 chain: $\mathbf{k} = (M, N, L, Q = N + M) = = M \cdot (1, 0, 0, 1) + N \cdot (0, 1, 0, 1) + L \cdot (0, 0, 1, 0)$

ℵ	M	N	L	Q	$[d]$	(Δ, Δ^*)	II	IV	VI	$VIII$	XI	$XIII$	XIV	XV	$XVII$	$XXII$
–	–	–	–	–	–	$J(\Delta)$	10	9	9	5	9	8	6	7	7	7
–	–	–	–	–	–	$\pi(\Delta^*)$	4	5	5	9	5	6	8	7	7	7
–	–	–	–	–	–	$\pi(\Delta)$	10	–	9	$5'$	–	–	–	–	7	–
–	–	–	–	–	–	$J(\Delta^*)$	4	–	5	$9'$	–	–	–	–	7	–
2	1	1	1	2	[5]	$(34, 6^*)$		1			1		1			
4	1	1	2	2	[6]	$(30, 6^*)$	1	2								1
5	1	1	3	2	[7]	$(31, 8^*)$		3			2	1		1		
6	1	1	4	2	[8]	$(35, 7^*)$		4	1							
10	1	2	2	3	[8]	$(24, 8^*)$				1	3			2		2
12	1	2	3	3	[9]	$(23, 8^*)$	2						2	3		
13	1	2	4	3	[10]	$(23, 11^*)$						2		4		3
14	1	2	5	3	[11]	$(24, 13^*)$						3	3	5		
15	1	2	6	3	[12]	$(27, 9^*)$			2					6		
7	1	3	1	4	[12]	$(33, 9^*)$					4				1	
21	1	3	4	4	[12]	$(21, 9^*)$	3			3						
24	1	3	8	4	[16]	$(24, 12^*)$			3							
16	1	4	2	5	[12]	$(24, 12^*)$									2	4
22	1	4	3	5	[13]	$(20, 15^*)$						4	5			
31	1	4	10	5	[20]	$(23, 13^*)$			4							
25	1	5	3	6	[15]	$(21, 15^*)$									3	
30	1	5	4	6	[16]	$(19, 17^*)$				4		5				
32	1	6	4	7	[18]	$(19, 20^*)$									4	
36	1	7	5	8	[21]	$(18, 24^*)$									5	
39	1	8	6	9	[24]	$(18, 24^*)$									6	
42	2	3	2	5	[12]	$(17, 11^*)$				2	5					
45	2	3	4	5	[14]	$(13, 16^*)$							4			5
48	2	3	5	5	[15]	$(14, 11^*)$	4									
51	2	3	10	5	[20]	$(16, 14^*)$			5							
18	2	5	1	7	[15]	$(26, 17^*)$									7	
49	2	5	3	7	[17]	$(13, 20^*)$						7				
59	2	5	6	7	[20]	$(11, 23^*)$				7						
52	2	7	3	9	[21]	$(14, 23^*)$									9	
61	2	9	5	11	[27]	$(11, 32^*)$									13	
23	3	4	1	7	[15]	$(22, 17^*)$						6				
46	3	4	2	7	[16]	$(14, 18^*)$				5			6			
67	3	4	5	7	[19]	$(9, 24^*)$							7			
71	3	4	14	7	[28]	$(12, 18^*)$			6							
50	3	5	2	8	[18]	$(14, 20^*)$						8				
68	3	5	4	8	[20]	$(10, 22^*)$				8						
27	3	7	1	10	[21]	$(24, 24^*)$									8	
70	3	7	4	10	[24]	$(10, 26^*)$						9				
54	3	8	2	11	[24]	$(15, 27^*)$									10	
72	3	10	4	13	[30]	$(10, 35^*)$									11	
77	3	11	5	14	[33]	$(9, 39^*)$									12	
57	4	5	2	9	[20]	$(13, 23^*)$				6						
81	4	5	6	9	[24]	$(8, 26^*)$							8			
83	4	5	7	9	[25]	$(7, 32^*)$										
87	4	7	6	11	[28]	$(7, 35^*)$				9						
90	5	6	8	11	[30]	$(6, 39^*)$										

6.3. The Three-Vector Chain III_3: $\mathbf{k}_4 = (M, N, L, M + N + L)$. In this chain, shown in Table 8, the dimension $d = 2M + 2N + 2L$, there is $M \leftrightarrow N \leftrightarrow L$

symmetry, the eldest vector $\mathbf{k}_{\rm eld} = (1,1,1,3)$, and the invariant monomials are $(2,2,2,0)+(0,2,2,2)$. We see in the Table the appearance of the following two-vector chains

$$\begin{aligned} V: \quad & m\cdot(1,1,0,2) \,+\, n\cdot(0,0,1,1) \,=\, (m,m,n,2m+n) \,\rightarrow \\ & M=N=m \,\leqslant\, [\dim]\{(0,0,1,1)\}=2, \\ & L=n \,\leqslant\, [\dim]\{(1,1,0,2)\}=4. \end{aligned} \tag{6.18}$$

$$\begin{aligned} VI: \quad & m\cdot(1,0,1,2) \,+\, n\cdot(0,1,1,2) \,=\, (m,n,m+n,2m+2n) \,\rightarrow \\ & M=m \,\leqslant\, [\dim]\{(0,1,1,2)\}=4, \\ & N=n \,\leqslant\, [\dim]\{(1,0,1,2)\}=4, \\ & L=m+n. \end{aligned} \tag{6.19}$$

$$\begin{aligned} IX: \quad & m\cdot(1,0,1,2) \,+\, n\cdot(0,2,1,3) \,=\, (m,2n,m+n,2m+3n) \,\rightarrow \\ & M=m \,\leqslant\, [\dim]\{(0,2,1,3)\}=6, \\ & N=2n \,\leqslant\, 2[\dim]\{(1,0,1,2)\}=8, \\ & L=m+n. \end{aligned} \tag{6.20}$$

$$\begin{aligned} XVI: \quad & m\cdot(1,0,2,3) \,+\, n\cdot(0,1,0,1) \,=\, (m,n,2m,3m+n) \,\rightarrow \\ & M=m \,\leqslant\, [\dim]\{(0,1,0,1)\}=2, \\ & N=n \,\leqslant\, [\dim]\{(1,0,2,3)\}=6, \\ & L=2m. \end{aligned} \tag{6.21}$$

$$\begin{aligned} XVIII: \quad & m\cdot(1,0,1,2) \,+\, n\cdot(0,1,2,3) \,=\, (m,n,m+2n,2m+3n) \,\rightarrow \\ & M=m \,\leqslant\, [\dim]\{(0,1,2,3)\}=6, \\ & N=n \,\leqslant\, [\dim]\{(1,0,1,2)\}=4, \\ & L=m+2n. \end{aligned} \tag{6.22}$$

$$\begin{aligned} XIX: \quad & m\cdot(1,0,2,3) \,+\, n\cdot(0,1,2,3) \,=\, (m,n,2m+2n,3m+3n) \,\rightarrow \\ & M=m \,\leqslant\, [\dim]\{(0,2,1,3)\}=6, \\ & N=n \,\leqslant\, [\dim]\{(1,0,2,3)\}=6, \\ & L=2m+2n. \end{aligned} \tag{6.23}$$

$$\begin{aligned} XX: \quad & m\cdot(2,0,1,3) \,+\, n\cdot(0,2,1,3) \,=\, (2m,2n,m+n,3m+3n) \,\rightarrow \\ & M=2m \,\leqslant\, 2[\dim]\{(0,2,1,3)\}=12, \\ & N=2n \,\leqslant\, 2[\dim]\{(2,0,1,3)\}=12, \\ & L=m+n. \end{aligned} \tag{6.24}$$

Table 8. The 48 $K3$ hypersurfaces in the III_3 chain: $\mathbf{k} = (M, N, L, Q = N{+}M{+}L) = = M \cdot (1,0,0,1) + N \cdot (0,1,0,1) + L \cdot (0,0,1,1)$

$\aleph$	M	N	L	Q	$[d]$	(Δ, Δ^*)	V	VI	IX	XVI	$XVIII$	XIX	XX
–	–	–	–	–	–	$J(\Delta)$	9	9	5	7	7	7	7
–	–	–	–	–	–	$\pi(\Delta^*)$	5	5	9	7	7	7	7
–	–	–	–	–	–	$\pi(\Delta)$	–	9	–	–	7	7	7
–	–	–	–	–	–	$J(\Delta^*)$	–	5	–	–	7	7	7
3	1	1	1	3	[6]	$(39, 6^*)$	1						1
6	1	1	2	4	[8]	$(35, 7^*)$	2	1		1			
8	1	1	3	5	[10]	$(36, 9^*)$	3				1		
9	1	1	4	6	[12]	$(39, 9^*)$	4					1	
11	1	2	2	5	[10]	$(28, 8^*)$	5		1	2			
15	1	2	3	6	[12]	$(27, 9^*)$		2		3			2
17	1	2	4	7	[14]	$(27, 12^*)$				4	2		
19	1	2	5	8	[16]	$(28, 14^*)$				5	3		
20	1	2	6	9	[18]	$(30, 12^*)$				6		2	
24	1	3	4	8	[16]	$(24, 12^*)$		3	3				
26	1	3	5	9	[18]	$(24, 15^*)$					4		
28	1	3	7	11	[22]	$(25, 20^*)$					8		
29	1	3	8	12	[24]	$(27, 15^*)$						3	
31	1	4	5	10	[20]	$(23, 13^*)$		4					
33	1	4	6	11	[22]	$(22, 20^*)$			5		5		
34	1	4	9	14	[28]	$(24, 24^*)$					9		
35	1	4	10	15	[30]	$(25, 20^*)$						4	
37	1	5	7	13	[26]	$(21, 24^*)$					6		
38	1	5	12	18	[36]	$(14, 18^*)$						5	
40	1	6	8	15	[30]	$(21, 24^*)$					7		
41	1	6	14	21	[42]	$(24, 24^*)$						6	
43	2	2	3	7	[14]	$(19, 11^*)$	6		2				
47	2	3	4	9	[18]	$(16, 14^*)$			4	7			3
51	2	3	5	10	[20]	$(16, 14^*)$		5					
53	2	3	7	12	[24]	$(16, 20^*)$					11		
55	2	3	8	13	[26]	$(16, 23^*)$					10		
56	2	3	10	15	[30]	$(18, 18^*)$						7	
58	2	4	5	11	[22]	$(14, 19^*)$			6				
60	2	5	6	13	[26]	$(13, 23^*)$			7				
62	2	5	9	16	[32]	$(13, 29^*)$					14		
63	2	5	14	21	[42]	$(15, 27^*)$						9	
64	2	6	7	15	[30]	$(13, 23^*)$			9				
69	3	4	5	12	[24]	$(12, 18^*)$			8				
71	3	4	7	14	[28]	$(12, 18^*)$		6					
73	3	4	10	17	[34]	$(11, 31^*)$					13		
74	3	4	11	18	[36]	$(12, 30^*)$					12		
75	3	4	14	21	[42]	$(13, 26^*)$						8	
78	3	5	11	19	[38]	$(10, 35^*)$					15		
79	3	5	16	24	[48]	$(12, 30^*)$						10	
82	4	5	6	15	[30]	$(10, 20^*)$							4
84	4	5	7	16	[32]	$(9, 27^*)$			10				
85	4	5	13	22	[44]	$(9, 39^*)$					16		
86	4	5	18	27	[54]	$(10, 35^*)$						11	
88	4	6	7	17	[34]	$(8, 31^*)$			11				
91	5	6	8	19	[38]	$(7, 35^*)$			12				
92	5	6	22	33	[66]	$(9, 39^*)$						12	
93	5	7	8	20	[40]	$(8, 28^*)$							
94	7	8	10	25	[50]	$(6, 39^*)$							

6.4. The Three-Vector Chain IV_3: $\mathbf{k}_4 = (M,\, N,\, M+L,\, N+L)$. In this case (see Table 9), we have the dimension $d = 2M + 2N + 2L$, the eldest vector $\mathbf{k}_{\rm eld} = (1,1,1,1)$, and the invariant monomials are $(2,0,0,2) + (0,2,2,0)$. This three-vector chain includes the following vectors form the two-vector construction:

$$\begin{aligned} VII:\quad & m\cdot(2,1,1,0) + n\cdot(0,1,1,2) = (2m, m+n, m+n, 2n) \rightarrow \\ & M = 2m \leqslant 4, \\ & N = m+n \leqslant 4, \\ & L = n-m \geqslant 0. \end{aligned} \tag{6.25}$$

$$\begin{aligned} X:\quad & m\cdot(1,1,0,0) + n\cdot(0,0,1,1) = (m, m, n, n) \rightarrow \\ & M = m \leqslant 2, \\ & N = m \leqslant 2, \\ & L = n-m \geqslant 0. \end{aligned} \tag{6.26}$$

$$\begin{aligned} XII:\quad & m\cdot(3,2,1,0) + n\cdot(0,1,2,3) = (3m, 2m+n, m+2n, 3n) \rightarrow \\ & M = 3m, \\ & N = 2m+n, \\ & L = 2n-2m, \\ & (m,n) = (1,2),\ (2,1)\,;\ (1,1),\ (1,4),\ (4,1),\ (2,5),\ (5,2). \end{aligned} \tag{6.27}$$

$$\begin{aligned} XXI:\quad & m\cdot(1,2,3,0) + n\cdot(1,2,0,3) = (m+n, 2m+2n, 3m, 3n) \rightarrow \\ & M = m, \\ & N = 2m, \\ & L = m, \\ & (m,n) = (1,1), (1,2),\ (2,1);\ (1,5),\ (5,1),\ (4,5),\ (5,4). \end{aligned} \tag{6.28}$$

$$\begin{aligned} XXII:\quad & m\cdot(1,0,2,1) + n\cdot(0,1,0,1) = (m, n, 2m, m+n) \rightarrow \\ & M = m \leqslant [\mathrm{dim}]\{(0,1,0,1)\} = 2, \\ & N = n \leqslant [\mathrm{dim}]\{(1,0,2,1)\} = 4, \\ & L = m. \end{aligned} \tag{6.29}$$

Table 9. The 8 $K3$ hypersurfaces in the IV_3 chain: $\mathbf{k} = (M, N, M+L, N+L) = = M \cdot (1,0,1,0) + N \cdot (0,1,0,1) + L \cdot (0,0,1,1)$

ℵ	M	N	$M+L$	$N+L$	$[d]$	(Δ, Δ^*)	VII	X	XII	XXI	$XXII$
–	–	–	–	–	–	$J(\Delta)$	7	9	5	7	7
–	–	–	–	–	–	$\pi(\Delta^*)$	7	5	9	7	7
–	–	–	–	–	–	$\pi(\Delta)$	–	–	$5'$	$7'$	–
–	–	–	–	–	–	$J(\Delta^*)$	–	–	$9'$	$7'$	–
1	1	1	1	1	[4]	$(35, 5^*)$	1	1	1	–	–
4	1	1	2	2	[6]	$(30, 6^*)$	–	2	–	1	1
10	1	2	2	3	[8]	$(24, 8^*)$	2	–	–	–	–
13	1	2	3	4	[10]	$(23, 11^*)$	–	–	2	–	2
16	1	2	4	5	[12]	$(24, 12^*)$	–	–	–	2	3
44	2	3	3	4	[12]	$(15, 9^*)$	3	–	–	3	–
45	2	3	4	5	[14]	$(13, 16^*)$	–	–	3	–	4
66	3	4	5	6	[18]	$(10, 17^*)$	–	–	4	4	–

7. THE DUAL $K3$ ALGEBRA FROM FOUR-DIMENSIONAL EXTENDED VECTORS

As discussed in the Introduction, the enumeration of $K3$ reflexive polyhedra obtained at level zero from pairs of projective vectors (Section 5) and triples (Section 6) is not quite complete. The one remaining example, corresponding to $\mathbf{k}_4 = (7, 8, 9, 12)$, can be found using the intersection–projection and duality properties outlined in Section 3, as we now discuss. This method can be used to build projective-vector chains using the rich projective structure of $K3$ vectors. For example, one can construct a chain with, as youngest vector, $\mathbf{k}_4 = (7, 8, 10, 25)$, which is dual to the eldest vector $\mathbf{k}_4 = (1, 1, 1, 3)$ contained in the triple chain III_3. Similarly, one can consider other cases, e.g., building a chain with youngest vector $\mathbf{k}_4 = (5, 6, 8, 11)$, contained in the triple chain II_3.

7.1. The Dual π Projective-Vector Structure of $K3$ Hypersurfaces. We obtained in Section 6, as an interesting application of the $K3$ algebra, all the $1 + (4 \times 2) + 22$ invariant monomials of the 22 double-intersection $K3$ chains via the triple intersections of $K3$ extended vectors. These invariant monomials correspond to particular directions relative to the reflexive polyhedra, which can be used to find the projection structures of the vectors. In particular, they can be used to find all the projective vectors which have no planar-intersection structure at all. Because of duality, their polyhedra have sufficient invariant directions that the projections on the corresponding perpendicular planes give reflexive planar polyhedra. Examples include the youngest vectors which are dual to the eldest vectors as well as other relations in the corresponding chain, e.g., as we shall see, the remaining $K3$ vector (7,8,9,12) is dual to (1,1,1,1), (7,8,10,25) is dual to (1,1,1,3), etc.

To understand this more deeply, we consider triple chains built using a special subalgebra of the four-dimensional extended vectors: $\mathbf{k}_3^{ex(i)} = (0,0,0,1)$, $(0,0,1,1)$, $(0,1,1,1)$, $(0,1,1,2)$, and $(0,1,2,3)$, with all possible permutations. We consider triples $\mathbf{k}_3^{ex(i,j,l)}$ of these vectors with the property that each pair $(i,j),(j,l),(l,i)$ gives a reflexive planar polyhedron:

$$[\mathbf{k}_3^{ex(i)}]\bigcap[\mathbf{k}_3^{ex(j)}] = [\mathbf{k}_3]. \tag{7.1}$$

We note that the triple intersections of these triples of extended vectors always define an invariant direction, $\boldsymbol{\pi}$. In some cases, the triple intersection contains just two monomial vectors, and $\boldsymbol{\pi}$ is simply defined by their difference:

$$[\mathbf{k}_3^{ex(i)}]\bigcap[\mathbf{k}_3^{ex(j)}]\bigcap[\mathbf{k}_3^{ex(r)}] \Rightarrow \boldsymbol{\pi}_N = \{\boldsymbol{\mu} - \boldsymbol{\mu}_0\}, \tag{7.2}$$

where $\boldsymbol{\mu}_0 = (1,1,1,1)$ is the basic monomial $z^{\boldsymbol{\mu}_0+\mathbf{1}} = x\cdot y\cdot z\cdot u$. These cases are listed in Table 10.

These pairs of invariant monomials correspond to directions $\boldsymbol{\pi}_i=\boldsymbol{\mu}_i-\boldsymbol{\mu}_0$ in the exponent/monomial hyperspace given by the following vectors $\boldsymbol{\mu}_N$,

Table 10. Triples of $\mathrm{k}_3{}^{ex}$ vectors giving invariant directions $\boldsymbol{\pi}_N = \boldsymbol{\mu}_N - \boldsymbol{\mu}_0$ defined by pairs of monomials. Also indicated are the sizes of the corresponding polyhedra Δ and the two-vector chains to which they belong

$\boldsymbol{\pi}_N^{(\alpha)}$	$\mathbf{k}_3^{ex(i)}$	$\mathbf{k}_3^{ex(j)}$	$\mathbf{k}_3^{ex(p)}$	$\Delta_{J_{ij}}$	$\Delta_{J_{jp}}$	$\Delta_{J_{pi}}$	inv. monom	$\boldsymbol{\mu}_N$
$\boldsymbol{\pi}_1^{(1)}$	$(0,0,1,1)$	$(1,2,0,1)$	$(1,2,1,0)$	7_{XXII}	9_{VI}	7_{XXII}	$x^3\cdot z\cdot u$	$(3,0,1,1)$
$\boldsymbol{\pi}_1^{(2)}$	$(0,0,1,1)$	$(1,2,0,3)$	$(1,2,3,0)$	7_{XVI}	7_{XXI}	7_{XVI}	$x^3\cdot z\cdot u$	$(3,0,1,1)$
$\boldsymbol{\pi}_2^{(1)}$	$(0,1,1,1)$	$(1,0,1,1)$	$(1,1,0,1)$	10_{II}	10_{II}	10_{II}	u^3	$(0,0,0,3)$
$\boldsymbol{\pi}_2^{(2)}$	$(0,1,1,1)$	$(1,0,1,1)$	$(1,3,0,2)$	10_{II}	4_{III}	7_{XVII}	u^3	$(0,0,0,3)$
$\boldsymbol{\pi}_2^{(3)}$	$(0,1,1,1)$	$(1,0,3,2)$	$(1,3,0,2)$	7_{XVII}	7_{XXI}	7_{XVII}	u^3	$(0,0,0,3)$
$\boldsymbol{\pi}_2^{(4)}$	$(0,1,1,1)$	$(3,0,1,2)$	$(3,1,0,2)$	4_{III}	7_{XIX}	4_{III}	u^3	$(0,0,0,3)$
$\boldsymbol{\pi}_3^{(1)}$	$(1,1,1,0)$	$(0,1,2,1)$	$(2,1,0,1)$	8_{XIII}	9_{VII}	8_{XIII}	$y^3\cdot u$	$(0,3,0,1)$
$\boldsymbol{\pi}_3^{(2)}$	$(1,1,1,0)$	$(0,1,2,1)$	$(2,1,0,3)$	8_{XIII}	6_{XIV}	4_{III}	$y^3\cdot u$	$(0,3,0,1)$
$\boldsymbol{\pi}_3^{(3)}$	$(1,1,1,0)$	$(0,1,2,3)$	$(2,1,0,3)$	4_{III}	7_{XX}	4_{III}	$y^3\cdot u$	$(0,3,0,1)$
$\boldsymbol{\pi}_3^{(4)}$	$(0,1,2,1)$	$(1,2,3,0)$	$(2,1,0,3)$	7_{XVIII}	5_{XII}	6_{XIV}	$y^3\cdot u$	$(0,3,0,1)$
$\boldsymbol{\pi}_4^{(1)}$	$(0,1,1,2)$	$(1,0,1,2)$	$(1,2,1,0)$	9_{VI}	9_{VII}	5_{VIII}	y^4	$(0,0,4,0)$
$\boldsymbol{\pi}_4^{(2)}$	$(0,1,1,2)$	$(1,2,1,0)$	$(2,0,1,1)$	5_{VIII}	5_{VIII}	5_{VIII}	y^4	$(0,0,4,0)$
$\boldsymbol{\pi}_5^{(1)}$	$(1,0,1,2,)$	$(1,2,0,3)$	$(1,2,3,0)$	5_{IX}	7_{XXI}	6_{XIV}	$x^4\cdot y$	$(4,1,0,0)$

$N = 1, 2, 3, 4, 5$:

$$\begin{aligned} \boldsymbol{\mu}_1 &= (3,0,1,1), \\ \boldsymbol{\mu}_2 &= (0,0,0,3), \\ \boldsymbol{\mu}_3 &= (0,3,0,1), \\ \boldsymbol{\mu}_4 &= (0,0,4,0), \\ \boldsymbol{\mu}_5 &= (4,1,0,0), \end{aligned} \tag{7.3}$$

as can be seen in Table 10.

In other cases, the triple intersections contain three points which form a degenerate linear polyhedron, which also defines a unique direction $\boldsymbol{\pi}$ determined by three points, one of which ($\boldsymbol{\mu}_0$) corresponds to the origin:

$$[\mathbf{k}_3^{ex(i)}] \bigcap [\mathbf{k}_3^{ex(j)}] \bigcap [\mathbf{k}_3^{ex(r)}] \Rightarrow \boldsymbol{\pi}_N = \{\boldsymbol{\mu}_+ - \boldsymbol{\mu}_0\} = \{\boldsymbol{\mu}_0 - \boldsymbol{\mu}_-\}, \tag{7.4}$$

as seen in Table 11.

It is easy to see that five of the invariant monomials from Table 10 produce a reflexive three-dimensional polyhedron. For example, from $\boldsymbol{\mu}_2$, $\boldsymbol{\mu}_3$, $\boldsymbol{\mu}_4$, and $\boldsymbol{\mu}_5$ one obtains the following exceptional vector whose associated polyhedron has no intersection substructure:

$$\begin{aligned} \boldsymbol{\mu}_\alpha \cdot \mathbf{k}_4 &= d = k_1 + k_2 + k_3 + k_4, \quad \alpha = 0,2,3,4,5, \\ \mathbf{k}_4 &= (7,8,9,12)[d = 36], \end{aligned} \tag{7.5}$$

Table 11. Triples of k_3^{ex} vectors defining directions $\boldsymbol{\pi}_N$ determined by three invariant monomials

$\boldsymbol{\pi}_N^{(\alpha)}$	$\mathbf{k}_3^{ex(i)}$	$\mathbf{k}_3^{ex(j)}$	$\mathbf{k}_3^{ex(p)}$	$\Delta_{J_{ij}}$	$\Delta_{J_{jp}}$	$\Delta_{J_{pi}}$	$\boldsymbol{\mu}_+$	$\boldsymbol{\mu}_-$
$\boldsymbol{\pi}_6^{(1)}$	$(0,0,1,1)$	$(1,1,0,1)$	$(1,1,1,0)$	9_{XI}	10_{II}	9_{XI}	$(0,2,1,1)$	$(2,0,1,1)$
$\boldsymbol{\pi}_6^{(2)}$	$(0,0,1,1)$	$(1,1,0,2)$	$(1,1,2,0)$	9_V	9_{VII}	9_V	$(0,2,1,1)$	$(2,0,1,1)$
$\boldsymbol{\pi}_7^{(1)}$	$(0,1,1,1)$	$(1,0,1,1)$	$(1,1,0,2)$	10_{II}	8_{XIII}	8_{XIII}	$(0,0,1,2)$	$(2,2,1,0)$
$\boldsymbol{\pi}_7^{(2)}$	$(0,1,1,1)$	$(1,0,2,1)$	$(1,1,0,2)$	8_{XIII}	5_{VIII}	8_{XIII}	$(0,0,1,2)$	$(2,2,1,0)$
$\boldsymbol{\pi}_7^{(3)}$	$(0,1,1,1)$	$(1,0,2,1)$	$(1,2,0,3)$	8_{XIII}	6_{XIV}	7_{XVII}	$(0,0,1,2)$	$(2,2,1,0)$
$\boldsymbol{\pi}_7^{(4)}$	$(0,1,2,1)$	$(1,0,2,1)$	$(1,1,0,2)$	9_{VI}	5_{VIII}	5_{VIII}	$(0,0,1,2)$	$(2,2,1,0)$
$\boldsymbol{\pi}_8^{(1)}$	$(0,1,1,2)$	$(1,0,1,2)$	$(1,1,0,2)$	9_{VI}	9_{VI}	9_{VI}	$(0,0,0,2)$	$(2,2,2,0)$
$\boldsymbol{\pi}_8^{(2)}$	$(0,1,1,2)$	$(1,0,1,2)$	$(1,2,0,3)$	9_{VI}	5_{IX}	7_{XVIII}	$(0,0,0,2)$	$(2,2,2,0)$
$\boldsymbol{\pi}_8^{(3)}$	$(0,1,1,2)$	$(1,0,2,3)$	$(1,2,0,3)$	7_{XVIII}	7_{XX}	7_{XVIII}	$(0,0,0,2)$	$(2,2,2,0)$
$\boldsymbol{\pi}_8^{(4)}$	$(0,1,1,2)$	$(2,0,1,3)$	$(2,1,0,3)$	5_{IX}	7_{XIX}	5_{IX}	$(0,0,0,2)$	$(2,2,2,0)$

where we used the constraint

$$\boldsymbol{\mu}_0 = \frac{1}{4} \cdot (\boldsymbol{\mu}_2 + \boldsymbol{\mu}_3 + \boldsymbol{\mu}_4 + \boldsymbol{\mu}_5). \tag{7.6}$$

Thus duality enables us to identify the missing 95th $K3$ vector, which was not generated previously in our systematic study of the two- and three-vector chains. We recall that they contain totals of 90 and 91 vectors, respectively, of which only 94 were distinct.

Similarly, using these invariant monomials, one can find the rest of the exceptional $\mathbf{k}_4$ vectors, $(3,5,6,7)$, $(3,6,7,8)$, $(5,6,7,9)$ which were not included in the triple chains, together with $(3,4,5,6)$. They have intersection polyhedra that are not linear. These other exceptional $\mathbf{k}_4$ vectors are defined as follows

$$\begin{gathered} \boldsymbol{\mu}_\alpha \cdot \mathbf{k}_4 = d, \quad \alpha = 0,1,2,3,3', \\ \mathbf{k}_4 = (3,5,6,7)[d=21], \end{gathered} \tag{7.7}$$

where again the following constraint has been used

$$\begin{aligned} \boldsymbol{\mu}_0 &= \frac{1}{4} \cdot (\boldsymbol{\mu}_1 + \boldsymbol{\mu}_2 + \boldsymbol{\mu}_3 + \boldsymbol{\mu}_3') = \\ &= (3,1,0,1) + (0,0,0,3) + (1,0,3,0) + (0,3,1,0), \end{aligned}$$

and

$$\begin{gathered} \boldsymbol{\mu}_\alpha \cdot \mathbf{k}_4 = d, \quad \alpha = 0,1,2,3,4, \\ \mathbf{k}_4 = (3,6,7,8)[d=24], \end{gathered} \tag{7.8}$$

with the constraint:

$$\begin{aligned} \boldsymbol{\mu}_0 &= \frac{1}{4} \cdot (\boldsymbol{\mu}_1 + \boldsymbol{\mu}_2 + \boldsymbol{\mu}_3 + \boldsymbol{\mu}_4) = \\ &= (3,0,1,1) + (0,0,0,3) + (1,0,3,0) + (0,4,0,0). \end{aligned}$$

We also find

$$\begin{gathered} \boldsymbol{\mu}_\alpha \cdot \mathbf{k}_4 = d, \quad \alpha = 2,3,3',5, \\ \mathbf{k}_4 = (5,6,7,9)[d=27], \end{gathered} \tag{7.9}$$

where the following constraint also has been used

$$\begin{aligned} \boldsymbol{\mu}_0 &= \frac{1}{4} \cdot (\boldsymbol{\mu}_2 + \boldsymbol{\mu}_3 + \boldsymbol{\mu}_3' + \boldsymbol{\mu}_5) = \\ &= (0,0,0,3) + (0,3,0,1) + (0,1,3,0) + (4,0,1,0), \end{aligned}$$

and

$$\begin{aligned} \boldsymbol{\mu}_\alpha \cdot \mathbf{k}_4 = d, \quad \alpha = 1, 2, 3, 3', \\ \mathbf{k}_4 = (3, 4, 5, 6)[d = 18], \end{aligned} \tag{7.10}$$

where the following constraint also has been used

$$\begin{aligned} &\boldsymbol{\mu}_0 = \frac{1}{4} \cdot (\boldsymbol{\mu}_1 + \boldsymbol{\mu}_2 + \boldsymbol{\mu}_3 + \boldsymbol{\mu}_3') = \\ &= (3, 1, 1, 0) + (0, 0, 0, 3) + (1, 0, 3, 0) + (0, 3, 0, 1). \end{aligned}$$

7.2. Projective Chains of $K3$ Spaces Constructed from $\boldsymbol{\pi}_N$ Vectors. Using the invariant directions found in the previous Subsection, one can construct new triple chains:

$$p \cdot [\mathbf{k}_4]_{\boldsymbol{\pi}_N} = m \cdot \mathbf{k}^{ex(i)} + n \cdot \mathbf{k}^{ex(j)} + r \cdot \mathbf{k}^{ex(l)} \tag{7.11}$$

each corresponding to a direction $\boldsymbol{\pi}$ determined by an intersection of invariant monomial pairs. Each good projective vector in such a chain, determined by an invariant direction, contains the monomial/projective direction in its polyhedron. With respect to this direction, the polyhedron is projected onto a «good» planar reflexive polyhedron. If the projective vector appears in several different chains, its polyhedron will have «good» projections corresponding to each of these chains. This property can be used to make a classification by their projections of the projective vectors and their reflexive polyhedra. One finds that 78 projective $K3$ vectors out of 95 have such projective property. Taking into account the rest of the vectors which already were known from double-intersection $J = \Pi$-symmetric chains, one can recover all 95 projective $K3$ vectors.

The distribution of the 3-dimensional set of positive-integer numbers m, n, r depends on the dimension of the three extended vectors $d^{(i)} = \sum_\alpha \{\mathbf{k}_3^{ex(i)}\}_\alpha$, $i = 1, 2, 3$, participating in the construction of the chain, can have some «blank spots», corresponding to «false vectors» which do not correspond to any reflexive polyhedron. The origin of this phenomenon is connected with the structure of Calabi–Yau algebra, i.e., some of the projective vectors have different expansions (double-, triple-,...) in terms of the extended vectors. So, for example, if a vector is *forbidden* in two-vector expansions, it should also be forbidden in triple-, etc., expansions, which is what we call a false vector. The self-consistency of the algebra entails the absences of some combinations of integer numbers m, n, r, even though all of them are below their maximum values. We already have met and discussed this phenomenon in the classification of triple-vector chains.

Table 12. Extended vectors $\mathbf{k}_4$ in the chain $\boldsymbol{\pi}_2^{(1)}$ with $\Pi = 4$ with: $Q \cdot \mathbf{k} = (N+ +L, M+L, M+N, M+N+L) = M \cdot (0,1,1,1) + N \cdot (1,0,1,1) + L \cdot (1,1,0,1)$ **and** $d = 3M + 3N + 3L$**, whose youngest vector is** $\mathbf{k}_{\rm young} = (7,8,9,12)$

ℵ	$\mathbf{k}_4$	[det]	M	N	L	(Δ, Δ^*)	$\Pi - J^*$	Chain
95	$(7,8,9,12)$	[36]	5	4	3	$(5,35)$	$4-10$	–
89	$(5,6,7,9)$	[27]	4	3	2	$(6,30)$	$4-10$	III
80	$(3,6,7,8)$	[24]	5	2	1	$(9,21)$	$4-10$	III
76	$(3,5,6,7)$	[21]	4	2	1	$(9,21)$	$4-10$	III
66	$(3,4,5,6)$	[18]	3	2	1	$(10,17)$	$4-10$	III
65	$(3,3,4,5)$	[15]	2	2	1	$(12,12)$	$4-10$	III
44	$(2,3,3,4)$	[24]	2	1	1	$(7,26)$	$4-10$	III

As seen in Table 10, one can give examples of triple intersections giving just one good vector which has three different projections with $\Pi = 4$:

$$\begin{aligned}
&[\mathbf{k}_4]_{\boldsymbol{\pi}_1^{(2)}} \bigcap [\mathbf{k}_4]_{\boldsymbol{\pi}_2^{(2)}} \bigcap [\mathbf{k}_4]_{\boldsymbol{\pi}_3^{(4)}} \quad \Rightarrow \quad (3,5,6,7)[21], \\
&[\mathbf{k}_4]_{\boldsymbol{\pi}_1^{(2)}} \bigcap [\mathbf{k}_4]_{\boldsymbol{\pi}_2^{(2)}} \bigcap [\mathbf{k}_4]_{\boldsymbol{\pi}_4^{(2)}} \quad \Rightarrow \quad (3,6,7,8)[24], \\
&[\mathbf{k}_4]_{\boldsymbol{\pi}_2^{(2)}} \bigcap [\mathbf{k}_4]_{\boldsymbol{\pi}_3^{(3)}} \bigcap [\mathbf{k}_4]_{\boldsymbol{\pi}_3^{(1)}} \quad \Rightarrow \quad (5,6,7,9)[27].
\end{aligned} \tag{7.12}$$

Moreover, the exceptional vector, which has four different projections with $\Pi = 4$, is given by the intersection of four such chains, i.e.:

$$[\mathbf{k}_4]_{\boldsymbol{\pi}_2^{(1)}} \bigcap [\mathbf{k}_4]_{\boldsymbol{\pi}_3^{(2)}} \bigcap [\mathbf{k}_4]_{\boldsymbol{\pi}_4^{(2)}} \bigcap [\mathbf{k}_4]_{\boldsymbol{\pi}_5^{(1)}} \quad \Rightarrow \quad (7,8,9,12)[36]. \tag{7.13}$$

To understand this in more detail, we consider one chain with projection $\Pi = 4$, which is determined by the invariant direction $\boldsymbol{\pi}_2^{(1)}$. The vectors of this chain are represented as linear combinations with positive-integer coefficients, M, N, L, of the following three projective vectors, taken from the third line in Table 10:

$$\begin{aligned}
\mathbf{k}_4(\boldsymbol{\pi}_2^{(1)}) &= M \cdot (0,1,1,1) + N \cdot (1,0,1,1) + L \cdot (1,1,0,1) = \\
&= (\,N + L,\, M + L,\, M + N,\, M + N + L\,).
\end{aligned} \tag{7.14}$$

The basis is constructed out of the exceptional invariant monomials determining the $\boldsymbol{\pi}$ directions. Projecting on the perpendicular plane gives us planar reflexive polyhedra, so the third basis vector

$$\mathbf{e}_3 = (-1,-1,-1,2) \;\Rightarrow\; (0,0,0,3). \tag{7.15}$$

is common to all the chains discussed in this Subsection.

Table 13. The $K3$ hypersurfaces in chain III with intersection $J = 4$: $\mathbf{k}(III) = = (3n, m, m+n, m+2n) = m \cdot (0,1,1,1) + n \cdot (3,0,1,2)$, $d = 3m + 6n$ with level $l = m + n$, $m_{\max} = 6, n_{\max} = 2$

ℵ	$\mathbf{k}_i$[dim]	$\Delta(J=4)$	$\Delta^*(\Pi=10)$	(Π, J^*)
12	$(3,1,2,3)[9]$	$23 = 4_L + 4_J + 15_R$	$8^* = 3^*_L + 4^*_J + 1^*_R$	$(10, 4^*)$
44	$(3,2,3,4)[12]$	$15 = 7_L + 4_J + 4_R$	$9^* = 4^*_L + 3^*_C + 2^*_R$	$(9,5^*);(7,7^*)$
25	$(6,1,3,5)[15]$	$21 = 16_L + 4_J + 1_R$	$15^* = 7^*_L + 7^*_J + 1^*_R$	$(7,7^*)$
65	$(3,3,4,5)[15]$	$12 = 4_L + 4_J + 4_R$	$12^* = 1^*_L + 10^*_J + 1^*_R$	$(4,10)$
66	$(3,4,5,6)[18]$	$10 = 2_L + 4_J + 4_R$	$17^* = 8^*_L + 3^*_C + 6^*_R$	$(7,7)$
76	$(3,5,6,7)[21]$	$9 = 1_L + 4_J + 4_R$	$21^* = 11^*_L + 3^*_C + 7^*_R$	$(4,10)$
80	$(3,6,7,8)[24]$	$9 = 1_L + 4_J + 4_R$	$21^* = 12^*_L + 3^*_C + 6^*_R$	$(4,10)$
89	$(6,5,7,9)[27]$	$6 = 1_L + 4_J + 1_R$	$30^* = 17^*_L + 3^*_C + 10^*_R$	$(4,10)$

Looking at the distribution of allowed integers, M, N, L, we see «blank spots» such as $M = N = L = 1$, corresponding to the «false vector» $(2,2,2,3)$, which is forbidden by the double-vector classification: it would require $m = 2$ in the chain $(2,2,2,3) = m \cdot (1,1,1,0) + n \cdot (0,0,0,1)$, but actually $m_{\max} = 1$ for this chain. Also, all the polyhedra corresponding to these projective vectors have the other invariant directions $\boldsymbol{\pi}_3^{(2)} \to (1,0,3,0)$ with $\Pi = 4$ and should produce the following triple-vector expansion chain:

$$\begin{aligned} \mathbf{k}_4(\boldsymbol{\pi}_3^{(2)}) &= M \cdot (0,1,1,1) + N \cdot (1,0,1,2) + L \cdot (3,2,1,0) = \\ &= (N + 3L,\ M + 2L,\ M + N + L,\ M + 2N). \end{aligned} \tag{7.16}$$

Projecting on the perpendicular plane to the vector

$$\boldsymbol{e}_3 = (0,-1,2,-1) \ \Rightarrow \ (1,0,3,0) \tag{7.17}$$

gives us planar reflexive polyhedron with 4 points. This chain is a little longer and contains other projective vectors. Similarly, one can find using the other projective directions, $\boldsymbol{\pi}_4^{(\alpha)}$ and $\boldsymbol{\pi}_5^{(1)}$, two new triple expansion chains. Together these four invariant directions, $\boldsymbol{\pi}_i^{(\alpha)}$, $i = 2,3,4,5$, with the constructions of the corresponding triple projective chains contain 40 projective vectors (see Table 1).

One can compare the projection set, $\boldsymbol{\pi}_2^{(1)}$ and $\Pi = 4$, with the double-vector-intersection chain with $J = 4$. It is interesting to note that six vectors from the projective chain shown in Table 12 also appear in the III-intersection chain with $J = 4$ shown in Table 13. Conversely, the chain shown in this latter Table has just two vectors: $(3,1,2,3), (1,3,5,6)$ that are not contained in Table 12. The intersection structure of the III chain shown in Table 13 is obtained from the following two vectors:

$$\begin{aligned}\mathbf{k}_4(III) &= m\cdot(0,1,1,1)+n\cdot(3,0,1,2)= \\ &= (\,3n,\,m,\;m\,+\,n,\,m\,+\,2n\,), \\ &\quad 1\leqslant m\leqslant 6,\quad 1\leqslant n\leqslant 2.\end{aligned} \tag{7.18}$$

The corresponding four invariant monomials are

$$\begin{aligned}\boldsymbol{\mu}_0^1 &= (0,0,0,3)\Rightarrow u^3, \\ \boldsymbol{\mu}_0^2 &= (1,0,3,0)\Rightarrow x\cdot z^3, \\ \boldsymbol{\mu}_0^3 &= (2,3,0,0)\Rightarrow x^2\cdot y^3, \\ \boldsymbol{\mu}_0^4 &= (1,1,1,1)\Rightarrow x\cdot y\cdot z\cdot u,\end{aligned} \tag{7.19}$$

and the corresponding basis can be chosen in the form

$$\begin{aligned}\mathbf{e}_1 &= (0,-m-n,m,0), \\ \mathbf{e}_2 &= (0,-1,2,-1), \\ \mathbf{e}_3 &= (-1,-1,-1,2).\end{aligned} \tag{7.20}$$

The canonical expression for the determinant of this lattice is

$$\det(\mathbf{e}_1,\mathbf{e}_2,\mathbf{e}_3,\mathbf{e}_0)=3\cdot m\,+\,6\cdot n=d, \tag{7.21}$$

where $\mathbf{e}_0\equiv(1,1,1,1)$.

7.3. Example of a $J,\Pi\,=\,10$ Double-Intersection Chain. To see another aspect of mirror symmetry and duality, consider the II chain with intersection $J(\Delta)=\Pi(\Delta)=10$ and $J(\Delta^*)=\Pi(\Delta^*)=4$ shown in Table 14. The decomposition of this chain is in terms of the following two vectors:

$$\begin{aligned}\mathbf{k_4} &= m\cdot(0,1,1,1)+n\cdot(1,0,1,1)= \\ &= (\,n,\,m,\;m\,+\,n,\,m\,+\,n\,), \\ &\quad 1\leqslant m\leqslant 3,\quad 1\leqslant n\leqslant 3.\end{aligned} \tag{7.22}$$

The basis of the lattice in which the polyhedral intersection with the set of positive-integer points corresponds to Table 14 is the following:

$$\begin{aligned}\mathbf{e}_1 &= (-m,n,0,0), \\ \mathbf{e}_2 &= (-1,-1,1,0), \\ \mathbf{e}_3 &= (-1,-1,0,1),\end{aligned} \tag{7.23}$$

and the corresponding determinant is

$$\det(\mathbf{e}_1,\mathbf{e}_2,\mathbf{e}_3,\mathbf{e}_0)=3\cdot m\,+\,3\cdot n=d, \tag{7.24}$$

Table 14. The $K3$ hypersurfaces in chain II with intersection $J = 10$: $\mathbf{k}(II) = (n, m, m+n, m+n) = m \cdot (0,1,1,1) + n \cdot (1,0,1,1)$ with $d = 3m+3n$, $q = 1$, $m_{\max} = 3, n_{\max} = 3$

$\aleph$	$\mathbf{k}_i$[dim]	$\Delta(J=10)$	$\Delta^*(\Pi=4)$	(Π, J^*)
4	$(1,1,2,2)[6]$	$30 = 10_L + 10_J + 10_R$	$6^* = 1^*_L + 4^*_J + 1^*_R$	$(10, 4^*)$
12	$(1,2,3,3)[9]$	$23 = 10_L + 10_J + 3_R$	$8^* = 3^*_L + 4^*_J + 1^*_R$	$(10, 4^*)$
21	$(1,3,4,4)[12]$	$21 = 10_L + 10_J + 1_R$	$9^* = 4^*_L + 4^*_J + 1^*_R$	$(10, 4^*)$
48	$(2,3,5,5)[15]$	$14 = 3_L + 10_J + 1_R$	$11^* = 4^*_L + 4^*_J + 3^*_R$	$(10, 4^*)$

where $\mathbf{e}_0 = (1,1,1,1)$ again. The ten corresponding invariant monomials are:

$$\begin{aligned}
\boldsymbol{\mu}_0^1 &= (3,3,0,0) \Rightarrow x^3 \cdot y^3,\\
\boldsymbol{\mu}_0^2 &= (2,2,1,0) \Rightarrow x^2 \cdot y^2 \cdot z,\\
\boldsymbol{\mu}_0^3 &= (1,1,2,0) \Rightarrow x \cdot y \cdot z^2,\\
\boldsymbol{\mu}_0^4 &= (0,0,3,0) \Rightarrow z^3,\\
\boldsymbol{\mu}_0^5 &= (2,2,0,1) \Rightarrow x^2 \cdot y^2 \cdot u,\\
\boldsymbol{\mu}_0^6 &= (1,1,1,1) \Rightarrow x \cdot y \cdot z \cdot u,\\
\boldsymbol{\mu}_0^7 &= (0,0,2,1) \Rightarrow z^2 \cdot u,\\
\boldsymbol{\mu}_0^8 &= (1,1,0,2) \Rightarrow x \cdot y \cdot u^2,\\
\boldsymbol{\mu}_0^9 &= (0,0,1,2) \Rightarrow z \cdot u^2,\\
\boldsymbol{\mu}_0^{10} &= (0,0,0,3) \Rightarrow u^3.
\end{aligned} \tag{7.25}$$

For the vector $\mathbf{k}_4 = (1,1,2,2)$, one can consider the basis

$$\begin{aligned}
\mathbf{e}_1 &= (-3,3,0,0),\\
\mathbf{e}_2 &= (-1,-1,1,0),\\
\mathbf{e}_3 &= (-1,-1,0,1)
\end{aligned} \tag{7.26}$$

with determinant 18, in which the dual pair of polyhedra:

$$\begin{aligned}
1_L \,+\, 10_J \,+\, 1_R &= 12,\\
4^*_L \,+\, 4^*_J \,+\, 4^*_R &= 12^*
\end{aligned} \tag{7.27}$$

both contain 12 points and 12 mirror points, respectively.

7.4. Example of a Chain with $\Pi = 5$ and Eldest Vector $\mathbf{k}_4 = (7,8,10,25)$. Now we present in Table 15 a projective chain with $\Pi = 5$, constructed from the invariant direction $\boldsymbol{\pi}_8^{(1)}$ with the invariant monomials $(0,0,0,2) + (2,2,2,0)$.

The 14 projective vectors of this chain are represented as linear combinations with positive-integer coefficients, $M, N, L, Q,\ Q = 2, 1,$ of the following three vectors:

$$\begin{aligned} Q \cdot \mathbf{k}_4(\boldsymbol{\pi}_8^{(1)}) \ &= \ M \cdot (0,1,1,2) + N \cdot (1,0,1,2) + L \cdot (1,1,0,2) = \\ &= \ (\, N \ + \ L,\, M \ + \ L,\, M \ + \ N,\, 2 \cdot M \ + \ 2 \cdot N \ + \ 2 \cdot L\,). \end{aligned} \tag{7.28}$$

Projecting on the perpendicular plane gives us planar reflexive polyhedra, so the third basis vector

$$\mathbf{e}_3 = (-1,-1,-1,1) \ \Rightarrow \ (0,0,0,2) \tag{7.29}$$

is common to all the chain discussed in this Subsection.

There can be constructed additional three chains, $\boldsymbol{\pi}_8^{(2,3,4)}$, with the same invariant direction, (0,0,0,2), (2,2,2,0), and the same youngest vector, but with the different triple intersections and therefore with the different projective chains. Together one can find inside all of four projective chains, $\boldsymbol{\pi}_8^{(\alpha)}$, $\alpha = 1, 2, 3, 4$, a total of 33 projective vectors (see Table 1).

Table 15. The $K3$ hypersurfaces in the $\boldsymbol{\pi}_8^{(1)}$ chain with projection $\Pi = 5$ related to the IX with $J = 5$: $Q \cdot \mathbf{k} = (N + L,\ M + L,\ M + N,\ 2M + 2N + 2L) = M\cdot(0,1,1,2) + N\cdot(1,0,1,2) + L\cdot(1,1,0,2)$ with $d = 4M + 4N + 4L$, $\mathbf{k}_{\rm eld} = (1,1,1,3)$ $\mathbf{k}_{\rm young} = (7,8,10,25)$, $Q = 2$ or 1

ℵ	$\mathbf{k}_4$	[det]	M	N	L	Q	(Δ, Δ^*)	$\Pi - J^*$	chain
94	$(7,8,10,25)$	[50]	11	9	5	2	$(6,39^*)$	$5-9$	–
93	$(8,7,5,20)$	[40]	2	3	5	1	$(8,28^*)$	$5-9$	–
91	$(5,6,8,19)$	[38]	9	7	3	2	$(7,35^*)$	$5-9$	IX
88	$(7,6,4,17)$	[34]	9	5	3	2	$(8,31^*)$	$5-9$	IX
84	$(4,5,7,16)$	[32]	4	3	1	1	$(9,27^*)$	$5-9$	IX
82	$(4,5,6,15)$	[30]	7	5	3	2	$(10,20^*)$	$5-9$	IX
69	$(3,4,5,12)$	[48]	3	2	1	1	$(7,35^*)$	$5-9$	IX
64	$(2,6,7,15)$	[30]	6	3	1	2	$(13,23^*)$	$5-9$	IX
60	$(2,5,6,13)$	[26]	9	3	1	2	$(13,23^*)$	$5-9$	IX
58	$(2,4,5,11)$	[22]	7	3	1	2	$(14,19^*)$	$5-9$	IX
47	$(2,3,4,9)$	[36]	5	3	1	2	$(9,27^*)$	$5-9$	IX
43	$(2,2,3,7)$	[14]	3	3	1	2	$(19,11^*)$	$5-9$	IX
11	$(1,2,2,5)$	[20]	3	1	1	2	$(15,15^*)$	$5-9$	IX
3	$(1,1,1,3)$	[12]	1	1	1	2	$(39,6^*)$	$5-9$	IX

It is interesting to note that the chain $\boldsymbol{\pi}_8^{(1)}$ has 11 $\mathbf{k}_4$ vectors with $\Pi = 5$ in common with the IX_J chain where $J = 5$, whose structure is obtained from the following two vectors:

$$\begin{aligned} \mathbf{k}_4(IX) \;&=\; m \cdot (0,1,1,2) + n \cdot (2,1,0,3) = \\ &=\; (\,2n,\, m\,+\,n,\, m,\, 2m\,+\,3n\,), \\ &\quad\; 1 \leqslant m \leqslant 6, \quad 1 \leqslant n \leqslant 4. \end{aligned} \tag{7.30}$$

The chain IX of $\mathbf{k}_4$ projective vectors with the structure $5_{J=\triangle} \leftrightarrow 9_{\Pi=\triangle}$ is presented in Table 16. The lattice determinant and the basis are given by the following expressions:

$$\begin{aligned} \mathbf{e}_1 \;&=\; (0,-m,m+n,0), \\ \mathbf{e}_2 \;&=\; (-1,2,-2,0), \\ \mathbf{e}_3 \;&=\; (-1,-1,-1,1), \end{aligned} \tag{7.31}$$

and

$$\det(\mathbf{e}_1,\mathbf{e}_2,\mathbf{e}_3,\mathbf{e}_0) = 4 \cdot m \,+\, 6 \cdot n = d, \tag{7.32}$$

where $\mathbf{e}_0 = (1,1,1,1)$.

The possible values of m and n for this chain are also determined by the dimensions of the extended vectors, $d(\mathbf{k}^{ex(i)}) = 6$ and $d(\mathbf{k}^{ex(j)}) = 4$, with the

Table 16. The $K3$ hypersurfaces in the chain IX: $\mathbf{k}$=$(2n, m{+}n, m, 2m{+}3n)$= $=\; m \cdot (0,1,1,2) \,+\, n \cdot (2,1,0,3)$ **with** $d = 4m + 6n$**,** $m_{\max} = 6, n_{\max} = 3$ **and** $\mathbf{k}_{\text{eld}} = (1,2,2,5)[10]$

N	$\mathbf{k}$[dim]	$\Delta(J = \underline{5})$	$\Delta^*(\Pi = 9)$	$(\Delta_J, \Delta^*{}_\Pi)$
11	$(2,2,1,5)[10]$	$28 = 7_L + 5_J + 16_R$	$8^* = 3^*_L + 4^*_C + 1^*_R$	$(10')$
43	$(2,3,2,7)[14]$	$19 = 7_L + 5_J + 7_R$	$11^* = 1_L + 9_J + 1_R$	$(5_\Pi, 9_J)$
24	$(4,3,1,8)[16]$	$24 = 3_L + 5_J + 16_R$	$12^* = 1_L + 5_J + 6_R$	$(5_\Pi, 9_J)$
33	$(6,4,1,11)[22]$	$22 = 1_L + 5_J + 16_R$	$20^* = 1_L + 5_J + 14_R$	$(7_\Pi \in 9_\Pi)$
47	$(2,4,3,9)[18]$	$16 = 7_L + 5_J + 4_R$	$14^* = 6_L + 7_J + 1_R$	$(7_\Pi \in 9_\Pi)$
58	$(2,5,4,11)[22]$	$14 = 7_L + 5_J + 2_R$	$19^* = 9_L + 9_J + 11_R$	$(5_\Pi, 9_J)$
60	$(6,5,2,13)[26]$	$13 = 1_L + 5_J + 7_R$	$23^* = 1_L + 9_J + 13_R$	$(5_\Pi, 9_J)$
69	$(4,5,3,12)[24]$	$12 = 3_L + 5_J + 4_R$	$18^* = 6_L + 7_J + 5_R$	$(7_\Pi \in 9_\Pi)$
64	$(2,7,6,15)[30]$	$13 = 7_L + 5_J + 1_R$	$23^* = 13_L + 9_J + 1_R$	$(5_\Pi, 9_J)$
84	$(4,7,5,16)[32]$	$9 = 3_L + 5_J + 1_R$	$27^* = 13_L + 9_J + 5_R$	$(5_\Pi, 9_J)$
88	$(6,7,4,17)[34]$	$8 = 1_L + 5_J + 2_R$	$31^* = 9_L + 9_J + 13_R$	$(5_\Pi, 9_J)$
91	$(6,8,5,19)[38]$	$7 = 9_L + 5_J + 1_R$	$35^* = 16_L + 7_J + 12_R$	$(5_\Pi, 9_J)$

additional constraint $n_{\max} = 3 < \dim(0,1,1,2)$ (see Table 16):

$$p \cdot \mathbf{k}_4(IX) \; = \; m \cdot (0,1,1,2) \, + \, n \cdot (2,0,1,3), \qquad p = 1 \; \to \; 1 \leqslant m \leqslant 6;, \; 1 \leqslant n \leqslant 3. \tag{7.33}$$

The 5 invariant monomials for this chain are the following:

$$\begin{aligned} \boldsymbol{\mu}_0^1 &= (1,4,0,0) \; \Rightarrow \; x \cdot y^4, \\ \boldsymbol{\mu}_0^2 &= (2,2,2,0) \; \Rightarrow \; x^2 \cdot y^2 \cdot z^2, \\ \boldsymbol{\mu}_0^3 &= (3,0,4,0) \; \Rightarrow \; x^3 \cdot z^4, \\ \boldsymbol{\mu}_0^4 &= (1,1,1,1) \; \Rightarrow \; x \cdot y \cdot z \cdot u, \\ \boldsymbol{\mu}_0^5 &= (0,0,0,2) \; \Rightarrow \; u^2. \end{aligned} \tag{7.34}$$

7.5. Example of a $J = \Pi = 9$ Chain. To see another aspect of mirror symmetry and duality, we now consider the chain VI with intersection $J(\Delta) = \Pi(\Delta) = 9$ and $J(\Delta^*) = \Pi(\Delta^*) = 5$ shown in Table 15, which is constructed from the extended vectors $\mathbf{k}^i = (0,1,1,2)$ and $\mathbf{k}^j = (1,0,1,2)$. In this case, duality gives very simple connections between the numbers of integer points in the dual polyhedron pair, as seen in Table 17.

The canonical basis for chain VI is:

$$\begin{aligned} \mathbf{e}_1 \; &= \; (-m, n, 0, 0), \\ \mathbf{e}_2 \; &= \; (-1, -1, 1, 0), \\ \mathbf{e}_3 \; &= \; (-1, -1, -1, 1) \end{aligned} \tag{7.35}$$

with the following restriction on the determinant

$$\det(\mathbf{e}_1, \mathbf{e}_2, \mathbf{e}_3, \mathbf{e}_0) = 4 \cdot m \, + \, 4 \cdot n = d, \tag{7.36}$$

where $\mathbf{e}_0 = (1,1,1,1)$.

Table 17. The $K3$ hypersurfaces in the chain VI: $\mathbf{k}(VI) = (n, m, m+n, 2m+2n) = = m \cdot (0,1,1,2) + n \cdot (1,0,1,2)$

N	$\mathbf{k}_4$	$\Delta(J=9)$	$\Delta^*(\Pi=5)$	$\Delta_\Pi, \Delta^*{}_J$
6	$(1,1,2,4)[8]$	$35 = 13_L + 9_{J,\Pi} + 13_R$	$7^* = 1^*_L + 5^*_{\Pi,J} + 1^*_R$	$(9_{\Pi,J}, 5_{J,\Pi})$
15	$(2,1,3,6)[12]$	$27 = 5_L + 9_{J,\Pi} + 13_R$	$9^* = 1^*_L + 5^*_{\Pi,J} + 4^*_R$	$(9_{\Pi,J}, 5_{J,\Pi})$
24	$(3,1,4,8)[16]$	$24 = 2_L + 9_{J,\Pi} + 13_R$	$12^* = 1^*_L + 5^*_{\Pi,J} + 6_R$	$(9_{\Pi,J}, 5_{J,\Pi})$
31	$(4,1,5,10)[20]$	$23 = 1_L + 9_{J,\Pi} + 13_R$	$13^* = 1^*_L + 5^*_{\Pi,J} + 7_R$	$(9_{\Pi,J}, 5_{J,\Pi})$
24	$(3,2,5,10)[20]$	$16 = 2_L + 9_{J,\Pi} + 5_R$	$14^* = 3^*_L + 5^*_{\Pi,J} + 6^*_R$	$(9_{\Pi,J}, 5_{J,\Pi})$
71	$(3,4,7,14)[28]$	$12 = 2_L + 9_{J,\Pi} + 1_R$	$18^* = 7^*_L + 5^*_{\Pi,J} + 6^*_R$	$(9_{\Pi,J}, 5_{J,\Pi})$

The possible values of m and n for this chain are determined by the dimensions of the extended vectors, without any unexpected puzzles:

$$\begin{aligned} p \cdot \mathbf{k}_4(VI) \ = \ m \cdot (0,1,1,2) + n \cdot (1,0,1,2), \\ p = 1 \ \rightarrow \ 1 \leqslant m \leqslant 4; \ \ 1 \leqslant n \leqslant 4, \end{aligned} \tag{7.37}$$

and the following:

$$\begin{aligned} \boldsymbol{\mu}_0^1 &= (4,4,0,0) &&\Rightarrow && x^4 \cdot y^4, \\ \boldsymbol{\mu}_0^2 &= (3,3,1,0) &&\Rightarrow && x^3 \cdot y^3 \cdot z, \\ \boldsymbol{\mu}_0^3 &= (2,2,2,0) &&\Rightarrow && x^2 \cdot y^2 \cdot z^2, \\ \boldsymbol{\mu}_0^4 &= (1,1,3,0) &&\Rightarrow && x \cdot y \cdot z^3, \\ \boldsymbol{\mu}_0^5 &= (0,0,4,0) &&\Rightarrow && z^4, \\ \boldsymbol{\mu}_0^6 &= (2,2,0,1) &&\Rightarrow && x^2 \cdot y^2 \cdot u, \\ \boldsymbol{\mu}_0^7 &= (1,1,1,1) &&\Rightarrow && x \cdot y \cdot z \cdot u, \\ \boldsymbol{\mu}_0^8 &= (0,0,2,1) &&\Rightarrow && z^2 \cdot u, \\ \boldsymbol{\mu}_0^9 &= (0,0,0,2) &&\Rightarrow && u^2. \end{aligned} \tag{7.38}$$

are the 9 invariant monomials $\Psi_{\rm inv}$ for this chain.

Analogously, one can consider the projective chain $\boldsymbol{\pi}_7^{(\alpha)}(\Pi = 5)$ with the youngest vector (5,6,8,11), and compare it with the double-intersection chain $VIII$, constructed from the extended vectors $\mathbf{k}(VIII) = m \cdot (0,1,1,2) + n \cdot (1,1,2,0)$; $(d = 4m + 4n.\ m_{\rm max} = 3, n_{\rm max} = 4)$, $\mathbf{k}_{\rm eld} = (1,2,3,2)$[8]. Among the 95 $K3$ projective vectors, 26 have such an invariant-direction structure, and therefore can be found in corresponding projective chains (see Table 1).

8. $K3$ HYPERSURFACES AND CARTAN–LIE ALGEBRA GRAPHS

We discuss in this Section more details of the emergence of Cartan–Lie algebra graphs in our construction of CY spaces.

8.1. Cartan–Lie Algebra Graphs and the Classification of Chains of Projective Vectors. As we commented already in the Introduction and in Section 2, the structure of the projective $\mathbf{k}_4$ vectors in 22 chains leads to interesting relations with the five classical regular dual polyhedron pairs in three-dimensional space: the one-dimensional point, two-dimensional line segment and three-dimensional tetrahedron, octahedron-cube and icosahedron-dodecahedron. There are also interesting correspondences with the Cartan–Lie algebra CLA graphs for the five types of groups in the $\mathrm{ADE}_{6,7,8}$ series: see Figure 8. The $\mathrm{CLA}_{J,\Pi}$ graphs, which can be seen in the polyhedra of the corresponding $\mathbf{k}_4$ projective vectors, follow

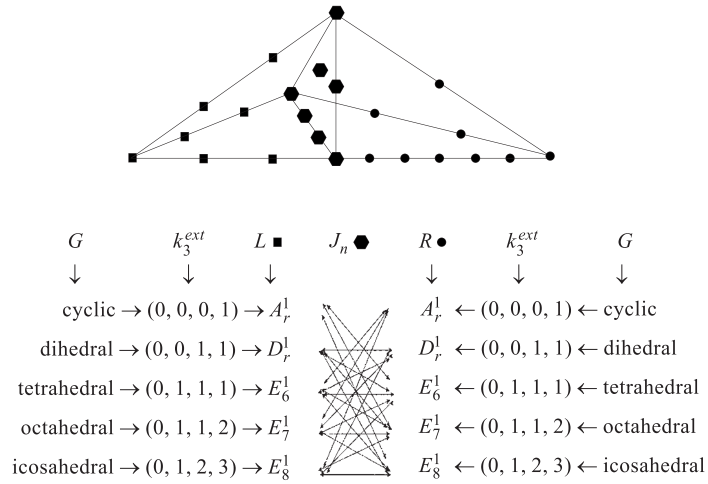

Fig. 8. Illustration of the Cartan–Lie algebra diagram classification of the $22(=[13+1]+8^*)$ chains of $K3$ polyhedra shown in Table 18. Here G denotes the cyclic, dihedral, tetrahedron, octahedron-cube, and icosahedron-dodecahedron subgroups of $SU(2)$, L/R denote left/right integer points and CLA_J diagrams, J_n — the type of intersection, and the $\mathbf{k}_3$ are all the possible planar vectors. We find $r_{\max L}=17$ or $r_{\max R}=17$ for the A_r^1 series, and $r_{\max L}=16$ or $r_{\max R}=16$ for the D_r^1 series. In the example shown here, one can see the polyhedron with the projective vector: $\mathbf{k}_4=(1,1,3,4)$[9]

completely the structure of the five possible extended vectors:

$$\begin{aligned}
\mathbf{k}_C^{ext} &= (0,0,0,1) \quad \leftrightarrow \quad A_r,\\
\mathbf{k}_D^{ext} &= (0,0,1,1) \quad \leftrightarrow \quad D_r,\\
\mathbf{k}_T^{ext} &= (0,1,1,1) \quad \leftrightarrow \quad E_6,\\
\mathbf{k}_O^{ext} &= (0,1,1,2) \quad \leftrightarrow \quad E_7,\\
\mathbf{k}_I^{ext} &= (0,1,2,3) \quad \leftrightarrow \quad E_8.
\end{aligned} \tag{8.1}$$

We give in Table 18 the ADE structures and the CD_J diagrams of all the eldest $K3$ projective vectors from the 22 double chains. An illustration is given in Figure 8, and the rest of this Section discusses the examples of chains XV to XIX, illustrating the power of our systematic approach.

8.2. The $K3$ Chain XV with Graphs in the $E_8^{(1)}-A_r^{(1)}$ Series. Here we give the list of $\mathbf{k}_4$ vectors which can be constructed from the Weierstrass vectors $\mathbf{k}_3\equiv(1,2,3)$ and $\mathbf{k}_1=(1)$, shown as chain XV in Table 19. The number of $\mathbf{k}_4$ vectors in this chain is determined by the positive-integer numbers: $m=1, n\leqslant 6$, according to the dimensions of the corresponding component $\mathbf{k}^i$.

Table 18. The eldest vectors $(m = n = 1)$ for all the 22 chains of $K3$ hypersurfaces, and the corresponding Cartan–Lie algebra diagrams CLA_J

N	$\mathbf{k}_i$(eldest)	Structure	max $\Delta(J)$	CLA_J	min $\Delta^*(\Pi)$
I	$(1,1,1,1)[4]$	$(0,1,1,1)_{e6}+(1,0,0,0)_a$	$35=10_{e6}+10_{J=\triangle}+15_a$	$E_6^{(1)} \leftrightarrow A_{12}^{(1)}$	$5^*=1^*_{e6}+3^*_C+1^*_a$
II	$(1,1,2,2)[6]$	$(0,1,1,1)_{e6}+(1,0,1,1)_{e6}$	$30=10_{e6}+10_{J=\Pi=\triangle}+10_{e6}$	$E_6^{(1)} \leftrightarrow E_6^{(1)}$	$6^*=1^*_{e6}+4^*_{\Pi=J=\triangle}+1^*_{e6}$
III	$(3,1,2,3)[9]$	$(0,1,1,1)_{e6}+(3,0,1,2)_{e8}$	$23=4_{e6}+4_{J=\triangle}+15_{e8}$	${G_2}^{(1)} \leftrightarrow E_8^{(1)}$	$8^*=3^*_{e6}+4^*_{J=\triangle}+1^*_{e8}$
IV	$(1,1,1,2)[5]$	$(0,1,1,2)_{e7}+(1,0,0,0)_a$	$34=13_{e7}+9_{J=\triangle}+12_a$	$E_7^{(1)} \leftrightarrow A_9^{(1)}$	$6^*=1^*_{e6}+4^*_C+1^*_a$
V	$(1,1,1,3)[6]$	$(0,1,1,2)_{e7}+(1,0,0,1)_d$	$39=13_{e7}+9_{J=\triangle}+17_d$	$E_7^{(1)} \leftrightarrow D_{10}^{(1)}$	$6^*=1^*_{e7}+4^*_C+1_d$
VI	$(1,1,2,4)[8]$	$(0,1,1,2)_{e7}+(1,0,1,2)_{e7}$	$35=13_{e7}+9_{J=\Pi=\triangle}+13_{e7}$	$E_7^{(1)} \leftrightarrow E_7^{(1)}$	$7^*=1^*_{e7}+5^*_{\Pi=\triangle}+1^*_{e7}$
VII	$(1,1,1,1)[4]$	$(0,1,1,2)_{e7}+(2,1,1,0)_{e7}$	$35=13_{e7}+9_{J=\triangle}+13_{e7}$	$E_7^{(1)} \leftrightarrow E_7^{(1)}$	$5^*=1^*_L+3^*_C+1^*_R$
$VIII$	$(1,2,3,2)[8]$	$(0,1,1,2)_{e7}+(1,1,2,0)_{e7}$	$24=12_{e7}+5_{J=\triangle}+7_{e7}$	$E_7^{(1)} \leftrightarrow F_4^{(1)}$	$8^*=3^*_{e7}+4^*_C+1^*_{e7}$
IX	$(2,2,1,5)[10]$	$(0,1,1,2)_{e7}+(2,1,0,3)_{e8}$	$28=7_{e7}+5_{J=\triangle}+16_{e8}$	$F_4^{(1)} \leftrightarrow E_8^{(1)}$	$8^*=3^*_{e7}+4^*_C+1^*_{e8}$
X	$(1,1,1,1)[4]$	$(0,0,1,1)_d+(1,1,0,0)_d$	$35=13_d+9_{J=\square}+13_d$	$D_8^{(1)} \leftrightarrow D_8^{(1)}$	$5^*_{\Pi=\diamond}=1^*_d+3^*_C+1^*_d$
XI	$(1,1,1,2)[5]$	$(0,0,1,1)_d+(1,1,0,1)_{e6}$	$34=15_d+9_{J=\square}+10_{e6}$	$D_8^{(1)} \leftrightarrow E_6^{(1)}$	$6^*=1^*_d+4^*_C+1^*_{e6}$
XII	$(1,1,1,1)[4]$	$(0,1,2,3)_{e8}+(3,2,1,0)_{e8}$	$13=4_{e8}+5_{J=\Pi=\square}+4_{e8}$	$G_2^{(1)} \leftrightarrow G_2^{(1)}$	$11^*=1^*_{e8}+9^*_{\Pi=J=\square}+1^*_{e8}$
$XIII$	$(1,1,2,3)[7]$	$(0,1,1,1)_{e6}+(1,0,1,2)_{e7}$	$31=10_{e6}+8_{J=\Pi=\square}+13_{e7}$	$E_6^{(1)} \leftrightarrow E_7^{(1)}$	$8^*=1^*_{e6}+6^*_{\Pi,J}+1^*_{e7}$
XIV	$(1,1,1,2)[5]$	$(0,1,1,2)_{e6}+(2,1,3,0)_{e8}$	$18=7_{e6}+6_{J=\Pi=\square}+5_{e8}$	$F_4^{(1)} \leftrightarrow G_2^{(1)}$	$10^*=1^*_{e6}+8^*_{\Pi=J=\square}+1^*_{e8}$
$XXII$	$(1,2,1,2)[6]$	$(0,1,1,2)_{e7}+(1,1,0,0)_d$	$30=13_{e7}+7_{J=\Pi=\square}+10_d$	$E_7^{(1)} \leftrightarrow D_7$	$6^*=1^*_{e7}+4^*_J+1^*_d$
XV	$(1,1,2,3)[7]$	$(0,1,2,3)_{e8}+(1,0,0,0)_a$	$31=16_{e8}+7_{J=\triangle}+8_a$	$E_8^{(1)} \leftrightarrow A_6^{(1)}$	$8^*=1^*_{e8}+6^*_C+1^*_a$
XVI	$(1,1,2,4)[8]$	$(0,1,2,3)_{e8}+(1,0,0,1)_d$	$35=16_{e8}+7_{J=\triangle}+12_d$	$E_8^{(1)} \leftrightarrow D_8$	$7^*=1^*_{e8}+5^*_C+1^*_{e8}$
$XVII$	$(1,1,3,4)[9]$	$(0,1,2,3)_{e8}+(1,0,1,1)_{e6}$	$33=16_{e8}+7_{J=\Pi=\triangle}+10_{e6}$	$E_8^{(1)} \leftrightarrow E_6^{(1)}$	$9^*=1^*_{e8}+7^*_{\Pi=J=\triangle}+1^*_{e6}$
$XVIII$	$(1,1,3,5)[10]$	$(0,1,2,3)_{e8}+(1,0,1,2)_{e7}$	$36=16_{e8}+7_{J=\Pi=\triangle}+13_{e7}$	$E_8^{(1)} \leftrightarrow E_7^{(1)}$	$9^*=1^*_{e8}+7^*_{\Pi=J=\triangle}+1^*_{e7}$
XIX	$(1,1,4,6)[12]$	$(0,1,2,3)_{e8}+(1,0,2,3)_{e8}$	$39=16_{e8}+7_{J=\Pi=\triangle}+16_{e8}$	$E_8^{(1)} \leftrightarrow E_8^{(1)}$	$9^*=1^*_{e8}+7^*_{\Pi=J=\triangle}+1^*_{e8}$
XX	$(1,1,1,3)[6]$	$(0,1,2,3)_{e8}+(2,1,0,3)_{e8}$	$21=7_{e8}+7_{J=\Pi=\triangle}+7_{e8}$	$F_4^{(1)} \leftrightarrow F_4^{(1)}$	$9^*=1^*_{e8}+7^*_{\Pi=J=\triangle}+1^*_{e8}$
XXI	$(3,2,4,3)[12]$	$(0,1,2,3)_{e8}+(3,1,2,0)_{e8}$	$15=4_{e8}+7_{J=\Pi=\triangle}+4_{e8}$	$G_2^{(1)} \leftrightarrow G_2^{(1)}$	$9^*=1^*_{e8}+7^*_{\Pi=J=\triangle}+1^*_{e8}$

Table 19. The $K3$ hypersurfaces in the chain XV: $\mathbf{k} = (m, 2\cdot m, 3\cdot m, n) = m\cdot(1,2,3,0) + n\cdot(0,0,0,1)$: $d = 6m+n$, $m_{\max} = 1, n_{\max} = 6$, $\mathbf{k}_{\text{eld}} = (1,2,3,1)[7]$

$\aleph$	m, n	$\mathbf{k}[d]$	$\Delta(J=7)$	Group	$\Delta^*(\Pi=7)$
5	$1,1$	$(1,2,3,1)[7]$	$31 = 8_L + 7_J + 16_R$	$A^{(1)}_{6\ L}$	$8^* = 1^*_L + 6^*_C + 1^*_R$
10	$1,2$	$(1,2,3,2)[8]$	$24 = 10_L + 7_J + 7_R$	$A^{(1)}_{7\ L}$	$8^* = 3^*_L + 4^*_C + 1^*_R$
12	$1,3$	$(1,2,3,3)[9]$	$23 = 12_L + 7_J + 4_R$	$A^{(1)}_{8\ L}$	$8^* = 4^*_L + 3^*_C + 1^*_R$
13	$1,4$	$(1,2,3,4)[10]$	$23 = 14_L + 7_J + 2_R$	$A^{(1)}_{9\ L}$	$11^* = 3^*_L + 3^*_C + 1^*_R$
14	$1,5$	$(1,2,3,5)[11]$	$24 = 16_L + 7_J + 1_R$	$A^{(1)}_{10\ L}$	$13^* = 9^*_L + 3^*_C + 1^*_R$
15	$1,6$	$(1,2,3,6)[12]$	$27 = 19_L + 7_J + 1_R$	$A^{(1)}_{11\ L}$	$9^* = 5^*_L + 3^*_C + 1^*_R$

The basis for this chain, see Figure 9, can be written in the the following form:

$$\begin{aligned} \mathbf{e}_1 &= (-n, 0, 0, m), \\ \mathbf{e}_2 &= (-2, 1, 0, 0), \\ \mathbf{e}_3 &= (-3, 0, 1, 0). \end{aligned} \tag{8.2}$$

The determinant of this canonical basis coincides, of course, with the dimensions of the $\mathbf{k}_4$ vectors:

$$\det(\mathbf{e}_1, \mathbf{e}_2, \mathbf{e}_3, \mathbf{e}_0) = 6\cdot m + 1\cdot n = d, \tag{8.3}$$

where $\mathbf{e}_0 = (1,1,1,1)$. The decomposition of this chain is again determined by the dimension of the extended vectors $d(\mathbf{k}^{ex(i)}) = k_1^{ex(i)} + k_2^{ex(i)} + k_3^{ex(i)} + k_4^{ex(i)}$, as seen in Table 19:

$$\begin{aligned} \mathbf{k}_4(XV) = m\cdot(1,2,3,0) \quad &+ \quad n\cdot(0,0,0,1), \\ m = 1, \qquad & \quad 1 \leqslant n \leqslant 6. \end{aligned} \tag{8.4}$$

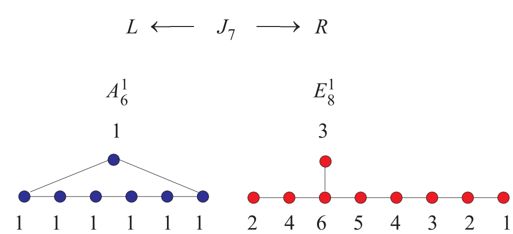

Fig. 9. The $A^{(1)}_{6\ L} - E^{(1)}_{8\ R}$ graph from the eldest $(1,2,3,1)[7]$ polyhedron in chain XV: $31 = 8_L + 7_J + 16_R$

The seven invariant monomials corresponding to this chain are:

$$\begin{aligned}
\boldsymbol{\mu}_0^1 &= (6,0,0,1) \quad \Rightarrow \quad x^6 \cdot u, \\
\boldsymbol{\mu}_0^2 &= (4,1,0,1) \quad \Rightarrow \quad x^4 \cdot y \cdot u, \\
\boldsymbol{\mu}_0^3 &= (2,2,0,1) \quad \Rightarrow \quad x^2 \cdot y^2 \cdot u, \\
\boldsymbol{\mu}_0^4 &= (0,3,0,1) \quad \Rightarrow \quad y^3 \cdot u, \\
\boldsymbol{\mu}_0^5 &= (3,0,1,1) \quad \Rightarrow \quad x^3 \cdot z \cdot u, \\
\boldsymbol{\mu}_0^6 &= (1,1,1,1) \quad \Rightarrow \quad x \cdot y \cdot z \cdot u, \\
\boldsymbol{\mu}_0^7 &= (0,0,2,1) \quad \Rightarrow \quad z^2 \cdot u.
\end{aligned} \tag{8.5}$$

Considering the dual pairs for these vectors, one can see that the singularities of the eldest vector $\mathbf{k}_4 = (1,2,3,1)$ correspond to some graphs of the ${A_6^{(1)}}_L - {E_8^{(1)}}_R$ series, as seen in Figure 9. For instance, if one looks at the integer points in the edges of the polyhedron on the left (right) side of the intersection by the hyperplane $\mathbf{k}^i = (0,1,2,3)$, one sees graphs with ${A_6^{(1)}}_L$ and ${E_8^{(1)}}_R$ Lie algebras. Going to the last minimal $\mathbf{k} = (1,2,3,6)$ of this chain, we find that the right graph degenerates and left points reproduce $A_{11}^{(1)}$ with the maximum possible rank in this chain. Thus, the six $\mathbf{k}$ vectors in this chain produce the following graphs in the A series: $A_6^{(1)}, A_7^{(1)}, A_8^{(1)}, A_9^{(1)}, A_{10}^{(1)}, A_{11}^{(1)}$.

8.3. The $K3$ Chain XVI with Graphs in the $E_8^{(1)} - D_r$ Series. The basis for the chain shown in Table 20 is

$$\begin{aligned}
\mathbf{e}_1 &= (-m, n, 0, 0), \\
\mathbf{e}_2 &= (0, -2, 1, 0), \\
\mathbf{e}_3 &= (-1, -1, -1, 1),
\end{aligned} \tag{8.6}$$

with

$$\det(\mathbf{e}_1, \mathbf{e}_2, \mathbf{e}_3, \mathbf{e}_0) = 6 \cdot m + 2 \cdot n = d, \tag{8.7}$$

where $\mathbf{e}_0 = (1,1,1,1)$ again. The decomposition of this chain is completely determined by the dimensions of the vectors shown in Table 20:

$$\begin{aligned}
p \cdot \mathbf{k}_4(XVI) \quad &= \quad m \cdot (0,1,2,3) + n \cdot (1,0,0,1), \\
p = 1^* \quad &\rightarrow \quad 1 \leqslant m \leqslant 2;\ 1 \leqslant n \leqslant 6, \\
p = 2 \quad &\rightarrow \quad m = n = 2.
\end{aligned} \tag{8.8}$$

Table 20. The $K3$ hypersurfaces in the chain XVI: $\mathbf{k} = (n, m, 2m, 3m+n) = m\cdot(0,1,2,3)+n\cdot(1,0,0,1)$: $(d = 6m+2n)$, $m_{\max} = 2, n_{\max} = 6$, $\mathbf{k}_{\rm eld} = (1,1,2,4)[8]$

ℵ	$\mathbf{k}[d]$	$\Delta(J=7)$	Group	$\Delta^*(\Pi=7)$	$(\Pi(\Delta), J(\Delta^*))$
6	$(1,1,2,4)[8]$	$35 = 16_L + 7_J + 12_R$	D_{8R}	$7^* = 1_L^* + 5_C^* + 1_R^*$	$(9, 5^*)$
11	$(2,1,2,5)[10]$	$28 = 7_L + 7_J + 14_R$	D_{9R}	$8^* = 1_L^* + 4_C^* + 3_R^*$	$(10, 4^*)$
15	$(3,1,2,6)[12]$	$27 = 4_J + 7_J + 16_R$	D_{10R}	$9^* = 1_L^* + 4_C^* + 4_R^*$	$(9, 5^*)$
17	$(4,1,2,7)[14]$	$27 = 2_L + 7_J + 18_R$	D_{11R}	$12^* = 1_L^* + 4_C^* + 7_R^*$	$(7, 7^*)$
19	$(5,1,2,8)[16]$	$28 = 1_L + 7_J + 14_R$	D_{12R}	$14^* = 1_L^* + 4_C^* + 9_R^*$	$(7, 7^*)$
20	$(6,1,2,9)[18]$	$30 = 1_L + 7_J + 22_R$	D_{13R}	$12^* = 1_L^* + 4_C^* + 7_R^*$	$(7, 7^*)$
47	$(3,2,4,9)[18]$	$16 = 4_L + 7_J + 5_R$	—	$14^* = 3_L^* + 5_C^* + 6_R^*$	$(7, 7^*)$
58	$(5,2,4,11)[22]$	$14 = 1_L + 7_J + 6_R$	—	$19^* = 3_L^* + 4_C^* + 12_R^*$	$(5, 9^*)$

The seven invariant monomials corresponding to this chain are the following:

$$\begin{aligned}
\boldsymbol{\mu}_0^1 &= (2,6,0,0) \quad \Rightarrow \quad x^2\cdot y^6,\\
\boldsymbol{\mu}_0^2 &= (2,4,1,0) \quad \Rightarrow \quad x^2\cdot y^4\cdot z,\\
\boldsymbol{\mu}_0^3 &= (2,2,2,0) \quad \Rightarrow \quad x^2\cdot y^2\cdot z^2,\\
\boldsymbol{\mu}_0^4 &= (2,0,3,0) \quad \Rightarrow \quad x^2\cdot z^3,\\
\boldsymbol{\mu}_0^5 &= (1,3,0,1) \quad \Rightarrow \quad x\cdot y^3\cdot u,\\
\boldsymbol{\mu}_0^6 &= (1,1,1,1) \quad \Rightarrow \quad x\cdot y\cdot z\cdot u,\\
\boldsymbol{\mu}_0^7 &= (0,0,0,2) \quad \Rightarrow \quad u^2.
\end{aligned} \tag{8.9}$$

The example of the ${E_8^{(1)}}_L - D_{8R}$ graph associated with the eldest $(1,1,2,4))[8]$ polyhedron in Table 20 is shown in Figure 10.

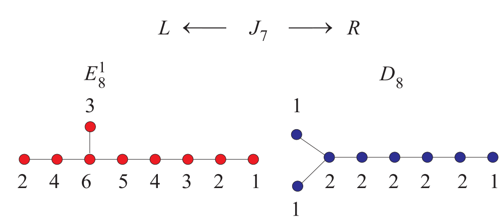

Fig. 10. The ${E_8^{(1)}}_L - D_{8R}$ graph from the eldest $(1,1,2,4)[8]$ polyhedron in the chain XVI: $33 = 16_L + 7_J + 10_R$

8.4. The $J = \Pi$ Symmetric Chain $XVII$ with Exceptional Graph $E_6 \times E_8$. We show in Table 21 the projective vectors constructed from $\mathbf{k}_3^{ex} = (0,1,1,1)$ and $\mathbf{k}_3^{ex} = (1,0,2,3)$. In this case, the number of points in the maximal polyhedron with $m = n = 1$ can easily be calculated: $33 = (10)_L + (7)_{\rm int} + (16)_R$. The «right» $15_R + 1_R$ points form the graph for the affine $E_8^{(1)}$ Lie algebra, as shown in Figure 11:

$$\begin{aligned} 6 = 1+1+1+1+1+1 \quad &\Rightarrow \quad \{(P_{x_0})_1 + (P_{x_1})_2 + (P_{x_2})_3 + \\ &+ \quad (P_{x_3})_4 + (P_{x_4})_5 + (P_{x_5})_6\}, \\ 3 = 3 \quad &\Rightarrow \quad \{(P_{x_6,x_6',x_6''})_3\}, \\ 6 = 4+2 \quad &\Rightarrow \quad \{(P_{x_7,x_7',x_7'',x_7'''})_4 + (P_{x_8,x_8'})_2\}. \end{aligned} \tag{8.10}$$

The «left» points in this polyhedron, $9_L + 1_L$, correspond to the $E_6^{(1)}$ affine series with the Coxeter numbers:

$$\begin{aligned} 3 = 1+1+1 \quad &\Rightarrow \quad \{(P_{x_1})_1 + (P_{x_2})_2 + (P_{x_3})_3\}, \\ 3 = 2+1 \quad &\Rightarrow \quad \{(P_{x_4,x_4'})_2 + (P_{x_0})_1\}, \\ 3 = 2+1 \quad &\Rightarrow \quad \{(P_{x_5,x_5'})_2 + (P_{x_6})_1\}. \end{aligned} \tag{8.11}$$

Table 21. The $K3$ hypersurfaces in the chain $XVII$: $\mathbf{k} = (n, m, m+2n, m+3n) = m \cdot (0,1,1,1) + n \cdot (1,0,2,3)$: $d = 3m + 6n$, $\max(m,n) = (6,3)$

$\aleph$	$\mathbf{k}[d]$	Δ	Δ^*
7	$(1,1,3,4)[9]$	$33 = 10_L + 7_{J=\Pi} + 16_R$	$9^* = 1_L^* + 7_{\Pi=J}^* + 1_R^*$
16	$(1,2,4,5)[12]$	$24 = 10_L + 7_{J=\Pi} + 7_R$	$12^* = 4_L^* + 7_{\Pi=J}^* + 1_R^*$
25	$(1,3,5,6)[15]$	$21 = 10_L + 7_{J=\Pi} + 4_R$	$15^* = 7_L^* + 7_{\Pi=J}^* + 1_R^*$
32	$(1,4,6,7)[18]$	$19 = 10_L + 7_{J=\Pi} + 2_R$	$20^* = 12_L^* + 7_{\Pi=J}^* + 1_R^*$
36	$(1,5,7,8)[21]$	$18 = 10_L + 7_{J=\Pi} + 1_R$	$24^* = 16_L^* + 7_{\Pi=J}^* + 1_R^*$
39	$(1,6,8,9)[24]$	$18 = 10_L + 7_{J=\Pi} + 1_R$	$24^* = 16_L^* + 7_{\Pi=J}^* + 1_R^*$
18	$(2,1,5,7)[15]$	$26 = 3_L + 7_{J=\Pi} + 16_R$	$17^* = 1_L^* + 7_{\Pi=J}^* + 9_R^*$
27	$(3,1,7,10)[21]$	$24 = 1_L + 7_{J=\Pi} + 16_R$	$24^* = 1_L^* + 7_{\Pi=J}^* + 16_R^*$
52	$(2,3,7,9)[21]$	$14 = 3_L + 7_{J=\Pi} + 4_R$	$23^* = 7_L^* + 7_{\Pi=J}^* + 9_R^*$
54	$(3,2,8,11)[24]$	$15 = 1_L + 7_{J=\Pi} + 7_R$	$27^* = 4_L^* + 7_{\Pi=J}^* + 16_R^*$
61	$(2,5,9,11)[27]$	$11 = 1_L + 7_{J=\Pi} + 3_R$	$32^* = 9_L^* + 7_{\Pi=J}^* + 16_R^*$
72	$(3,4,10,13)[30]$	$10 = 1_L + 7_{J=\Pi} + 2_R$	$35^* = 12_L^* + 7_{\Pi=J}^* + 16_R^*$
77	$(3,5,11,14)[33]$	$9 = 1_L + 7_{J=\Pi} + 1_R$	$39^* = 16_L^* + 7_{\Pi=J}^* + 16_R^*$

For $m_{\max} = d(\mathbf{k}(1,2,3)) = 6$ and $n_{\min} = 1$, the corresponding polyhedron contains 18 points: $18 = (10)_L + (7)_{\text{int}} + (1)_R$. Conversely, for $m_{\min} = 1$ and $n_{\max} = 3 = \dim(\mathbf{k}(1,1,1))$, the self-dual vector $\mathbf{k} = (3,1,7,10)$ has 24 integer points: $24 = (1)_L + (7)_{\text{int}} + (16)_R$. Finally, the polyhedron with $m = 5$ and $n = 3$ contains the minimal possible number of integer points, namely $9 = (1)_L + (7)_{\text{int}} + (1)_R$. This minimal vector $(3,5,11,14)[33]$ is the dual conjugate of the vector $\mathbf{k} = (1,1,4,6)[12]$.

The canonical basis of the chain shown in Table 21 is:

$$\begin{aligned} \mathbf{e}_1 &= (-m, n, 0, 0), \\ \mathbf{e}_2 &= (-2, -1, 1, 0), \\ \mathbf{e}_3 &= (-1, 0, -1, 1), \end{aligned} \tag{8.12}$$

with

$$\det(\mathbf{e}_1, \mathbf{e}_2, \mathbf{e}_3, \mathbf{e}_0) = 3 \cdot m + 6 \cdot n = d, \tag{8.13}$$

where $\mathbf{e}_0 = (1,1,1,1)$. The possible values of m and n for this chain are determined in the standard way from the dimensions of the extended vectors, $d(\mathbf{k}^{ex(j)}) = 6$ and $d(\mathbf{k}^{ex(i)}) = 3$, as seen in Table 21:

$$\begin{aligned} p \cdot \mathbf{k}_4(XVII) &= m \cdot (0,1,1,1) + n \cdot (1,0,2,3), \\ p = 1^* &\rightarrow 1 \leqslant m \leqslant 6,\ 1 \leqslant n \leqslant 3, \\ p = 2 &\rightarrow m = n = 2, \\ p = 3 &\rightarrow m = n = 3. \end{aligned} \tag{8.14}$$

The seven invariant monomials corresponding to this chain are the following:

$$\begin{aligned} \boldsymbol{\mu}_0^1 &= (6,3,0,0,) \Rightarrow x^6 \cdot y^3, \\ \boldsymbol{\mu}_0^2 &= (4,2,1,0,) \Rightarrow x^4 \cdot y^2 \cdot z, \\ \boldsymbol{\mu}_0^3 &= (2,1,2,0,) \Rightarrow x^2 \cdot y \cdot z, \\ \boldsymbol{\mu}_0^4 &= (0,0,3,0,) \Rightarrow z^3, \\ \boldsymbol{\mu}_0^5 &= (3,2,0,1,) \Rightarrow x^3 \cdot y^2 \cdot u, \\ \boldsymbol{\mu}_0^6 &= (1,1,1,1,) \Rightarrow x \cdot y \cdot z \cdot u, \\ \boldsymbol{\mu}_0^7 &= (0,1,0,2,) \Rightarrow y \cdot u^2 \end{aligned} \tag{8.15}$$

and the corresponding $E_6^{(1)}{}_L - E_8^{(1)}{}_R$ graph associated with the eldest $(1,1,3,4)$ [9] polyhedron in chain $XVII$ is shown in Table 22 and Figure 11.

Table 22. The group singularities of the dual pairs of elliptic polyhedra in chain $XVII$

$P^3(\mathbf{k})$	$H(\Delta)$	$H(\Delta^*)$	$G_L(\Delta)$	$G_R(\Delta)$	$G_L(\Delta^*)$	$G_R(\Delta^*)$
$(1,1,3,4)$	$m_1+m_2+m_3=0$	$m_1^*=0$	E_6	E_8	$SU(1)$	$SU(1)$
$(1,2,4,5)$	$m_1+m_2+m_3=0$	$m_1^*=0$	E_6	F_4	G_2	$SU(1)$
$(1,3,5,6)$	$m_1+m_2+m_3=0$	$m_1^*=0$	E_6	G_2	F_4	$SU(1)$
$(1,4,6,7)$	$m_1+m_2+m_3=0$	$m_1^*=0$	E_6	$SU(2)$	E_7	$SU(1)$
$(1,5,7,8)$	$m_1+m_2+m_3=0$	$m_1^*=0$	E_6	$SU(1)$	E_8	$SU(1)$
$(1,6,8,9)$	$m_1+m_2+m_3=0$	$m_1^*=0$	E_6	$SU(1)$	E_8	$SU(1)$

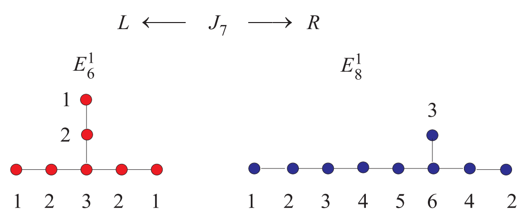

Fig. 11. The $E_6^{(1)}{}_L - E_8^{(1)}{}_R$ graph associated with the eldest $(1,1,3,4)[9]$ polyhedron in chain XVII: $33 = 10_L + 7_J + 16_R$

8.5. The $J = \Pi$ Symmetric Chain $XVIII$ with Exceptional Graph $E_7 \times E_8$. This chain can be built from the vectors $\mathbf{k}_4^{ex^i} = (0,1,1,2)$ and $\mathbf{k}_4^{ex^j} = (1,0,2,3)$, with positive integers $m \leqslant 6$ and $n \leqslant 4$. The maximal $(m = n = 1)$ polyhedron in this chain is again completely determined by the dimensions 4 and 6 of the projective vectors $\mathbf{k}_4^{ex^i}$ and $\mathbf{k}_4^{ex^j}$, respectively:

$$36 = (13)_L + (7)_{J=\Pi} + (16)_R. \tag{8.16}$$

The «right» $15_R + 1_R$ and «left» $12_L + 1_L$ points produce the graphs for the affine $E_8^{(1)}$ and $E_7^{(1)}$ Lie algebras, respectively, as seen in Figure 12. The vector $\mathbf{k} = (3,4,9,14)[28]$ is self-dual with $E_8^{(1)}$ graphs for the dual polyhedron pair. The «minimal» vector $\mathbf{k}$ gives the following set of integer lattice points in the polyhedron:

$$(1)_L + (7)_{\text{int}} + (1)_R = 9. \tag{8.17}$$

The canonical basis for the chain shown in Table 23 is:

$$\begin{aligned} \mathbf{e}_1 &= (-m, n, 0, 0), \\ \mathbf{e}_2 &= (-2, -1, 1, 0), \\ \mathbf{e}_3 &= (-1, -1, -1, 1), \end{aligned} \tag{8.18}$$

Table 23. The $K3$ hypersurfaces in the chain $XVIII$: $\mathbf{k} = (n, m, m+2n, 2m+3n) = = m \cdot (0,1,1,2) + n \cdot (1,0,2,3)$: $d = 4m + 6n$, $m_{\max} = 6, n_{\max} = 4$

ℵ	$\mathbf{k}[d]$	Δ	Δ^*
8	$(1,1,3,5)[10]$	$36 = 13_L + 7_{J=\Pi} + 16_R$	$9^* = 1^*_L + 7^*_{\Pi=J} + 1^*_R$
17	$(1,2,4,7)[14]$	$27 = 13_L + 7_{J=\Pi} + 7_R$	$12^* = 4^*_L + 7^*_{\Pi=J} + 1^*_R$
26	$(1,3,5,9)[18]$	$24 = 13_L + 7_{J=\Pi} + 4_R$	$15^* = 7^*_L + 7^*_{\Pi=J} + 1^*_R$
33	$(1,4,6,11)[22]$	$22 = 13_L + 7_{J=\Pi} + 2_R$	$20^* = 12^*_L + 7^*_{\Pi=J} + 1^*_R$
37	$(1,5,7,13)[26]$	$21 = 13_L + 7_{J=\Pi} + 1_R$	$24^* = 16^*_L + 7^*_{\Pi=J} + 1^*_R$
40	$(1,6,8,15)[30]$	$21 = 13_L + 7_{J=\Pi} + 1_R$	$24^* = 16^*_L + 7^*_{\Pi=J} + 1^*_R$
19	$(2,1,5,8)[16]$	$28 = 5_L + 7_{J=\Pi} + 16_R$	$14^* = 1^*_L + 7^*_{\Pi=J} + 6^*_R$
28	$(3,1,7,11)[22]$	$25 = 2_L + 7_{J=\Pi} + 16_R$	$20^* = 1^*_L + 7^*_{\Pi=J} + 12^*_R$
34	$(4,1,9,14)[28]$	$24 = 1_L + 7_{J=\Pi} + 16_R$	$24^* = 1^*_L + 7^*_{\Pi=J} + 16^*_R$
55	$(3,2,8,13)[26]$	$16 = 2_L + 7_{J=\Pi} + 7_R$	$23^* = 4^*_L + 7^*_{\Pi=J} + 12^*_R$
53	$(2,3,7,12)[24]$	$16 = 5_L + 7_{J=\Pi} + 4_R$	$20^* = 7^*_L + 7^*_{\Pi=J} + 6^*_R$
74	$(4,3,11,18)[36]$	$12 = 1_L + 7_{J=\Pi} + 4_R$	$30^* = 7^*_L + 7^*_{\Pi=J} + 16^*_R$
73	$(3,4,10,17)[34]$	$11 = 2_L + 7_{J=\Pi} + 2_R$	$31^* = 12^*_L + 7^*_{\Pi=J} + 12^*_R$
62	$(2,5,9,16)[32]$	$13 = 5_L + 7_{J=\Pi} + 1_R$	$29^* = 16^*_L + 7^*_{\Pi=J} + 6^*_R$
78	$(3,5,11,19)[38]$	$10 = 2_L + 7_{J=\Pi} + 1_R$	$35^* = 16^*_L + 7^*_{\Pi=J} + 12^*_R$
85	$(4,5,13,22)[44]$	$9 = 1_L + 7_{J=\Pi} + 1_R$	$39^* = 16^*_L + 7^*_{\Pi=J} + 16^*_R$

with

$$\det(\mathbf{e}_1, \mathbf{e}_2, \mathbf{e}_3, \mathbf{1}) = 4 \cdot m + 6 \cdot n = d. \tag{8.19}$$

The possible values of m and n for this chain fill up the dimensions of the extended vectors $d(\mathbf{k}^{ex(j)}) = 6$ and $d(\mathbf{k}^{ex(i)}) = 4$, as seen in Table 23:

$$\begin{aligned} p \cdot \mathbf{k}_4(XVIII) &= m \cdot (0,1,1,2) + n \cdot (1,0,2,3), \\ p = 1^* &\rightarrow 1 \leqslant m \leqslant 6,\ 1 \leqslant n \leqslant 4, \\ p = 2 &\rightarrow m = n = 2, \\ p = 3 &\rightarrow m = n = 3, \\ p = 4 &\rightarrow m = n = 4. \end{aligned} \tag{8.20}$$

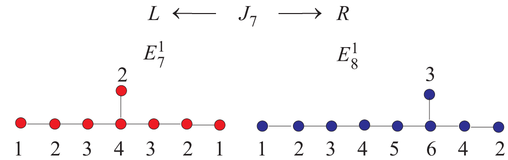

Fig. 12. The $E_7^{(1)}{}_L - E_8^{(1)}{}_R$ graphs associated with the $(1,1,3,5)[10]$ polyhedron in chain $XVIII$: $36 = 13_L + 7_J + 16_R$

Table 24. The group singularities of the dual pairs of elliptic polyhedra in chain $XVIII$

$P^3(\mathbf{k})$	$H(\Delta)$	$H(\Delta^*)$	$G_L(\Delta)$	$G_R(\Delta)$	$G_L(\Delta^*)$	$G_R(\Delta^*)$
$(1,1,3,5)$	$m_1+m_2+2m_3=0$	$m_1^*=0$	E_7	E_8	$SU(1)$	$SU(1)$
$(1,2,4,7)$	$m_1+m_2+2m_3=0$	$m_1^*=0$	E_7	F_4	G_2	$SU(1)$
$(1,3,5,9)$	$m_1+m_2+2m_3=0$	$m_1^*=0$	E_7	G_2	F_4	$SU(1)$
$(1,4,6,11)$	$m_1+m_2+2m_3=0$	$m_1^*=0$	E_7	$SU(2)$	E_7	$SU(1)$
$(1,5,7,13)$	$m_1+m_2+2m_3=0$	$m_1^*=0$	E_7	$SU(1)$	E_8	$SU(1)$
$(1,6,8,15)$	$m_1+m_2+2m_3=0$	$m_1^*=0$	E_7	$SU(1)$	E_8	$SU(1)$

The seven invariant monomials corresponding to this chain are the following:

$$\begin{aligned}
\boldsymbol{\mu}_0^1 &= (6,4,0,0,) &\Rightarrow&\quad x^6\cdot y^4,\\
\boldsymbol{\mu}_0^2 &= (4,3,1,0,) &\Rightarrow&\quad x^4\cdot y^3\cdot z,\\
\boldsymbol{\mu}_0^3 &= (2,2,2,0,) &\Rightarrow&\quad x^2\cdot y^2\cdot z^2,\\
\boldsymbol{\mu}_0^4 &= (0,1,3,0,) &\Rightarrow&\quad y\cdot z^3,\\
\boldsymbol{\mu}_0^5 &= (3,2,0,1,) &\Rightarrow&\quad x^3\cdot y^2\cdot u,\\
\boldsymbol{\mu}_0^6 &= (1,1,1,1,) &\Rightarrow&\quad x\cdot y\cdot z\cdot u,\\
\boldsymbol{\mu}_0^7 &= (0,1,0,2,) &\Rightarrow&\quad y\cdot u^2.
\end{aligned} \tag{8.21}$$

The $E_7^{(1)}{}_L - E_8^{(1)}{}_R$ graph associated with the eldest $(1,1,3,5))[10]$ polyhedron in chain $XVIII$ can be seen in Table 24 and Figure 12.

8.6. Chain XIX with $(7_J, 7_\Pi)$ Weierstrass Triangle Fibrations. We now consider the chain XIX of $\mathbf{k}_4$ projective vectors with E_{8L} and E_{8R} graphs. This chain starts from the $m=n=1$ polyhedron, which is left-right symmetric with respect to the intersection $P^2(1,2,3)$. This polyhedron $P^3(1,1,4,6)$ contains $39 = 16_L + (7)_{J=\Pi} + 16_R$ integer points: see Table 25 and Figure 13. The minimal vector $\mathbf{k} = (5,6,22,33)[66]$ is the dual conjugate of the eldest vec-

Table 25. The $K3$ hypersurfaces in the $J = \Pi$ symmetric chain XIX with $\mathbf{k} = (n, m, 2m + 2n, 3m + 3n) = m \cdot (0,1,2,3) + n \cdot (1,0,2,3)$: $d = 6m + 6n$, $m_{\max} = 6, n_{\max} = 6$, $\mathbf{k}_{\text{eld}} = (1,1,4,6)[12]$

$\aleph$	$\mathbf{k}_4$	$\Delta(J = \Pi = 7)$	$\Delta^*(\Pi = J = 7)$
9	$(1,1,4,6)[12]$	$39 = 16_L + 7_{J=\Pi} + 16_R$	$9^* = 1^*_L + 7^*_{\Pi=J} + 1^*_R$
20	$(1,2,6,9)[18]$	$30 = 16_L + 7_{J=\Pi} + 7_R$	$12^* = 4^*_L + 7^*_{\Pi=J} + 1^*_R$
29	$(1,3,8,12)[24]$	$27 = 16_L + 7_{J=\Pi} + 4_R$	$15^* = 7^*_L + 7^*_{\Pi=J} + 1^*_R$
35	$(1,4,10,15)[30]$	$25 = 16_L + 7_{J=\Pi} + 2_R$	$20^* = 12^*_L + 7^*_{\Pi=J} + 1^*_R$
38	$(1,5,12,18)[36]$	$24 = 16_L + 7_{J=\Pi} + 1_R$	$24^* = 16^*_L + 7^*_{\Pi=J} + 1^*_R$
41	$(1,6,14,21)[42]$	$24 = 16_L + 7_{J=\Pi} + 1_R$	$24^* = 16^*_L + 7^*_{\Pi=J} + 1^*_R$
56	$(2,3,10,15)[30]$	$18 = 7_L + 7_{J=\Pi} + 4_R$	$18^* = 7^*_L + 7^*_{\Pi=J} + 4_R$
75	$(3,4,14,21)[42]$	$13 = 4_L + 7_{J=\Pi} + 2_R$	$26^* = 12^*_L + 7^*_{\Pi=J} + 7_R$
63	$(2,5,14,21)[42]$	$15 = 7_L + 7_{J=\Pi} + 1_R$	$27^* = 16^*_L + 7^*_{\Pi=J} + 4^*_R$
79	$(3,5,16,24)[48]$	$12 = 4_L + 7_{J=\Pi} + 1_R$	$30^* = 16^*_L + 7^*_{\Pi=J} + 7^*_R$
86	$(4,5,18,27)[54]$	$10 = 2_L + 7_{J=\Pi} + 1_R$	$35^* = 16^*_L + 7^*_{\Pi=J} + 12^*_R$
92	$(5,6,22,33)[66]$	$9 = 1_L + 7_{J=\Pi} + 1_R$	$39^* = 16^*_L + 7^*_{\Pi=J} + 16^*_R$

tor $\mathbf{k} = (1,1,4,6)[12]$, the vector $\mathbf{k} = (1,6,14,21)[42]$ is self-dual, and its dual pair of $K3$ polyhedra yield the self-dual $E_8^{(1)}$ graph.

The basis of the chain shown in Table 25 is the following:

$$
\begin{aligned}
\mathbf{e}_1 &= (-m, n, 0, 0),\\
\mathbf{e}_2 &= (-2, -2, 1, 0), w \\
\mathbf{e}_3 &= (-1, -1, -1, 1),
\end{aligned}
\tag{8.22}
$$

with

$$
\det(\mathbf{e}_1, \mathbf{e}_2, \mathbf{e}_3, \mathbf{e}_0) = 6 \cdot m + 6 \cdot n = d, \tag{8.23}
$$

where $\mathbf{e}_0 = (1,1,1,1)$. The possible values of m and n for this chain are completely determined by the dimensions of the vectors $d(\mathbf{k}^{ex(j)}) = 6$ and $d(\mathbf{k}^{ex(i)}) =$ $= 6$ (see Table 25):

$$
\begin{aligned}
p \cdot \mathbf{k}_4(XIX) &= m \cdot (0,1,2,3) + n \cdot (1,0,2,3),\\
p = 1^* \quad &\rightarrow \quad 1 \leqslant m \leqslant 6,\ 1 \leqslant n \leqslant 6,\\
p = 2 \quad &\rightarrow \quad m = n = 2,\\
p = 3 \quad &\rightarrow \quad m = n = 3,\\
p = 4 \quad &\rightarrow \quad m = n = 4,\\
p = 6 \quad &\rightarrow \quad m = n = 6.
\end{aligned}
\tag{8.24}
$$

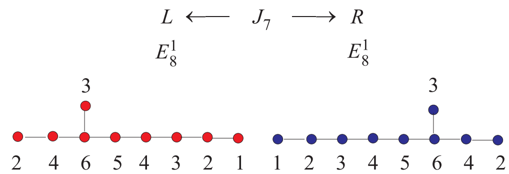

Fig. 13. The ${E_8^{(1)}}_L - {E_8^{(1)}}_R$ graph obtained from the eldest $(1,1,4,6)[12]$ polyhedron in chain XIX: $39 = 16_L + 7_J + 16_R$

Table 26. The group singularities of the dual pairs of elliptic polyhedra in chain XIX

$P^3(\mathbf{k})$	$H(\Delta)$	$H(\Delta^*)$	$G_L(\Delta)$	$G_R(\Delta)$	$G_L(\Delta^*)$	$G_R(\Delta^*)$
$(1,1,4,6)$	$m_1 + 2m_2 + 3m_3 = 0$	$m_1^* = 0$	E_8	E_8	$SU(1)$	$SU(1)$
$(1,2,6,9)$	$m_1 + 2m_2 + 3m_3 = 0$	$m_1^* = 0$	E_8	F_4	G_2	$SU(1)$
$(1,3,8,12)$	$m_1 + 2m_2 + 3m_3 = 0$	$m_1^* = 0$	E_8	G_2	F_4	$SU(1)$
$(1,4,10,15)$	$m_1 + 2m_2 + 3m_3 = 0$	$m_1^* = 0$	E_8	$SU(2)$	E_7	$SU(1)$
$(1,5,12,18)$	$m_1 + 2m_2 + 3m_3 = 0$	$m_1^* = 0$	E_8	$SU(1)$	E_8	$SU(1)$
$(1,6,14,21)$	$m_1 + 2m_2 + 3m_3 = 0$	$m_1^* = 0$	E_8	$SU(1)$	E_8	$SU(1)$

The seven invariant monomials corresponding to this chain are the following:

$$
\begin{aligned}
\boldsymbol{\mu}_0^1 &= (6,6,0,0) \quad \Rightarrow \quad x^6 \cdot y^6, \\
\boldsymbol{\mu}_0^2 &= (4,4,1,0) \quad \Rightarrow \quad x^4 \cdot y^4 \cdot z, \\
\boldsymbol{\mu}_0^3 &= (2,2,2,0) \quad \Rightarrow \quad x^2 \cdot y^2 \cdot z^2, \\
\boldsymbol{\mu}_0^4 &= (0,1,3,0) \quad \Rightarrow \quad y \cdot z^3, \\
\boldsymbol{\mu}_0^5 &= (3,3,0,1) \quad \Rightarrow \quad x^3 \cdot y^3 \cdot u, \\
\boldsymbol{\mu}_0^6 &= (1,1,1,1) \quad \Rightarrow \quad x \cdot y \cdot z \cdot u, \\
\boldsymbol{\mu}_0^7 &= (0,0,0,2) \quad \Rightarrow \quad u^2.
\end{aligned}
\tag{8.25}
$$

Using these invariant monomials and basis, the CY equations for all the $\mathbf{k}(l = m + n)$ projective vectors of this chain can be written in the following form:

$$
F(\mathbf{z})_{m,n} = \sum_{j=1}^{j=7} \mathbf{z}^{\boldsymbol{\mu}_0^j} \{ \sum_{p=1}^{p=\Pi_{jL}} a_{\boldsymbol{\mu}_0^j}^{pL} \cdot \mathbf{z}^{n_{pL} \cdot (-\mathbf{e}_1)} + \sum_{p=1}^{p=\Pi_{jR}} a_{\boldsymbol{\mu}_0^j}^{pR} \cdot \mathbf{z}^{-n_{pR} \cdot (-\mathbf{e}_1)} \},
\tag{8.26}
$$

where the basis vector $\mathbf{e}_1 = (m, -n, 0, 0)$. The ${E_8^{(1)}}_L - {E_8^{(1)}}_R$ graph obtained from the eldest $(1,1,4,6)[12]$ polyhedron in chain XIX is shown in Table 26 and Figure 13.

9. PERSPECTIVES ON THE FURTHER CLASSIFICATION OF CY_3 AND $K3$ SPACES

Although a fuller study of CY_3 spaces lies outside the scope of this paper, a preliminary study is of interest here, for the following reason. In addition to the 95 $K3$ spaces (Table 1) related to the zeroes of single polynomials discussed in previous Sections, others can be found by «higher-level» constructions as the intersections of the loci of zeroes of quasi-homogeneous polynomials, which are obtainable from CY_3 spaces, as we now discuss.

When going on to consider the general construction of $\mathbf{k}_5$ projective vectors in CP^4 that describe CY_3 hypersurfaces, we start from the 95 simple extensions of these $K3$ vectors as well as 5 multiple extensions of lower-dimensional vectors, together with all their possible permutations. In accordance with the previous five forms of extended vectors, one finds the following sets and permutations: quadruply-extended basic vectors with the cyclic C_5 group of permutations:

$$\mathbf{k}_1^{ex} = (0,0,0,0,1), \quad |C_5| = 5, \tag{9.1}$$

triply-extended composite vectors with the dihedral D_5 group of permutations

$$\mathbf{k}_2^{ex} = (0,0,0,1,1), \quad |D_5| = 10, \tag{9.2}$$

the following doubly-extended composite vectors with the D_5', A_5', and A_5 groups of permutations

$$\mathbf{k}_3^{ex} = (0,0,1,1,1), \quad |D_5'| = 10, \tag{9.3}$$
$$\mathbf{k}_3^{ex} = (0,0,1,1,2), \quad |A_5'| = 30, \tag{9.4}$$
$$\mathbf{k}_3^{ex} = (0,0,1,2,3), \quad |A_5| = 60, \tag{9.5}$$

we recall that the alternating group of permutations A_5 can be identified with the icosahedral symmetry group I. All the other extended $\mathbf{k}_5$ vectors can be obtained similarly from 95 $K3$ vectors, utilising the symmetric group S_5 or some subgroups. The full set of extended $\mathbf{k}_5$ vectors is displayed in Table 27. As noted in its caption, the total number of extended vectors is 10 270.

As an illustration how our method may be used to classify CY_3 manifolds, we now describe briefly how to obtain the complete list of $\mathbf{k}_5$ vectors with $K3$ intersections, which we find to be distributed in 4242 chains. To build the chains for CY_3 which have a double-vector structure, each of which is parametrized by a pair of positive integers, one should find the «good» pairs of «extended» vectors (i.e., those whose intersection gives a reflexive $K3$ hypersurface), which involves checking all the $10\ 270 \times 10\ 271/2 = 52\ 731\ 315$ possible pairs of vectors from Table 27. It was just such a search by computer that led to the 4242 double

Table 27. The 100 distinct types of five-dimensional «extended» projective vectors used to construct CY_3 spaces, listed together with the orders of their permutation groups. Including these permutations, the total number of extended vectors is 10 270

ℵ	$\mathbf{k}_{5ex}^{(i)}$	G(perm)	ℵ	$\mathbf{k}_{5ex}{}^{(i)}$	G(perm)
i	(0, 0, 0, 0, 1)	5	46	(0, 2, 3, 4, 7)	120
ii	(0, 0, 0, 1, 1)	10	47	(0, 2, 3, 4, 9)	120
iii	(0, 0, 1, 1, 1)	10	48	(0, 2, 3, 5, 5)	60
iv	(0, 0, 1, 1, 2)	30	49	(0, 2, 3, 5, 7)	120
v	(0, 0, 1, 2, 3)	60	50	(0, 2, 3, 5, 8)	120
1	(0, 1, 1, 1, 1)	5	51	(0, 2, 3, 5, 10)	120
2	(0, 1, 1, 1, 2)	20	52	(0, 2, 3, 7, 9)	120
3	(0, 1, 1, 1, 3)	20	53	(0, 2, 3, 7, 12)	120
4	(0, 1, 1, 2, 2)	30	54	(0, 2, 3, 8, 11)	120
5	(0, 1, 1, 2, 3)	60	55	(0, 2, 3, 4, 7)	120
6	(0, 1, 1, 2, 4)	60	56	(0, 2, 3, 10, 15)	120
7	(0, 1, 1, 3, 4)	60	57	(0, 2, 4, 5, 9)	120
8	(0, 1, 1, 3, 5)	60	58	(0, 2, 4, 5, 11)	120
9	(0, 1, 1, 4, 6)	60	59	(0, 2, 5, 6, 7)	120
10	(0, 1, 2, 2, 3)	60	60	(0, 2, 5, 6, 13)	120
11	(0, 1, 2, 2, 5)	60	61	(0, 2, 5, 9, 11)	120
12	(0, 1, 2, 3, 3)	60	62	(0, 2, 5, 9, 16)	120
13	(0, 1, 2, 3, 4)	120	63	(0, 2, 5, 14, 21)	120
14	(0, 1, 2, 3, 5)	120	64	(0, 2, 6, 7, 15)	120
15	(0, 1, 2, 3, 6)	120	65	(0, 3, 3, 4, 5)	60
16	(0, 1, 2, 4, 5)	120	66	(0, 3, 4, 5, 6)	120
17	(0, 1, 2, 4, 7)	120	67	(0, 3, 4, 5, 7)	120
18	(0, 1, 2, 5, 7)	120	68	(0, 3, 4, 5, 8)	120
19	(0, 1, 2, 5, 8)	120	69	(0, 3, 4, 5, 12)	120
20	(0, 1, 2, 6, 9)	120	70	(0, 3, 4, 7, 10)	120
21	(0, 1, 3, 4, 4)	60	71	(0, 3, 4, 7, 14)	120
22	(0, 1, 3, 4, 5)	120	72	(0, 3, 4, 10, 13)	120
23	(0, 1, 3, 4, 7)	120	73	(0, 3, 4, 10, 17)	120
24	(0, 1, 3, 4, 8)	120	74	(0, 3, 4, 11, 18)	120
25	(0, 1, 3, 5, 6)	120	75	(0, 3, 4, 14, 21)	120
26	(0, 1, 3, 5, 9)	120	76	(0, 3, 5, 6, 7)	120
27	(0, 1, 3, 7, 10)	120	77	(0, 3, 5, 11, 14)	120
28	(0, 1, 3, 7, 11)	120	78	(0, 3, 5, 11, 19)	120
29	(0, 1, 3, 8, 12)	120	79	(0, 3, 5, 16, 24)	120
30	(0, 1, 4, 5, 6)	120	80	(0, 3, 6, 7, 8)	120
31	(0, 1, 4, 5, 10)	120	81	(0, 4, 5, 6, 9)	120
32	(0, 1, 4, 6, 7)	120	82	(0, 4, 5, 6, 15)	120
33	(0, 1, 4, 6, 11)	120	83	(0, 4, 5, 7, 9)	120
34	(0, 1, 4, 9, 14)	120	84	(0, 4, 5, 7, 16)	120
35	(0, 1, 4, 10, 15)	120	85	(0, 4, 5, 13, 22)	120
36	(0, 1, 5, 7, 8)	120	86	(0, 4, 5, 18, 27)	120
37	(0, 1, 5, 7, 13)	120	87	(0, 4, 6, 7, 11)	120
38	(0, 1, 5, 12, 18)	120	88	(0, 4, 6, 7, 17)	120
39	(0, 1, 6, 8, 9)	120	89	(0, 5, 6, 7, 9)	120
40	(0, 1, 6, 8, 15)	120	90	(0, 5, 6, 8, 11)	120
41	(0, 1, 6, 14, 21)	120	91	(0, 5, 6, 8, 19)	120
42	(0, 2, 2, 3, 5)	60	92	(0, 5, 6, 22, 33)	120
43	(0, 2, 2, 3, 7)	60	93	(0, 5, 7, 8, 20)	120
44	(0, 2, 3, 3, 4)	60	94	(0, 7, 8, 10, 25)	120
45	(0, 2, 3, 4, 5)	120	95	(0, 7, 8, 9, 12)	120

chains mentioned above, together with their eldest vectors. For more complete information about these chains, see [37].

These chains give many CY_3 projective vectors, but not all. The complete list also includes the «good» triples which have elliptic fibres. This requires looking for good triples among the following five types of five-dimensional extended vectors:

$$\begin{array}{ll} 1. & (0,0,0,0,1) \Rightarrow 5, \\ 2. & (0,0,0,1,1) \Rightarrow 10, \\ 3. & (0,0,1,1,1) \Rightarrow 10, \\ 4. & (0,0,1,1,2) \Rightarrow 30, \\ 5. & (0,0,1,2,3) \Rightarrow 60, \end{array} \tag{9.6}$$

where the number after the arrow on each line of (9.7) corresponds to the number of permutations in each case. We have found 259 such good triples, together with their eldest vectors, corresponding to 259 elliptic chains. The union of the $K3$ and elliptic projective vectors still does not yield the full dual set of $\mathbf{k_5}$ projective vectors. We must also construct another set of chains using quadruples from among the following multiply-extended vectors:

$$\begin{array}{ll} 1. & (0,0,0,0,1) \Rightarrow 5, \\ 2. & (0,0,0,1,1) \Rightarrow 10. \end{array} \tag{9.7}$$

The number of CY_3 chains found in this way is just six.

In addition to these 4242 double, 259 triple and 6 quadruple CY_3 chains (to be compared with the 22 double and 4 triple $K3$ chains found previously), one must find all the vectors whose intersection contains only one central interior point (to be compared with the exceptional $K3$ vector $(7,8,9,12)$). We have found just two such examples in the case of CY_3, namely $(41,48,51,52,64)$ and $(51,60,64,65,80)$, again using the intersection-projection duality technique. The eldest vectors for all the CY_3 projective vector chains we have found can be obtained from [37].

In the cases of dimension higher than three, the concept of intersection–projection duality is richer, and leads to one important and by now well-known consequence [7,33], namely the isomorphism between different homology groups for dual pairs of CY_d manifolds M, M^*, and specifically the following relation:

$$H^{p,q}(M) \sim H^{d-p,q}(M^*) \tag{9.8}$$

for $0 \leqslant p,q \leqslant d$. We leave a more complete discussion of duality of CY_3 spaces to future work, limiting our discussion here of their ramifications for the classification of $K3$.

Our construction based on the 10270 extended vectors obtained from the $100(=95+5)$ types of projective vectors in lower dimensions $n=1,2,3,4$ shown in Table 27 yielded all the 4242 $(259,...)$ eldest vectors representing CY_3 spaces with $K3$ (elliptic, ...) fibers. However, this method of construction simultaneously provides a new *higher-level* list of $K3$ spaces defined by planar polyhedra. To explain this, let us first assign to all $K3$ spaces defined by n-dimensional projective vectors *level zero*, and denote them by Π_0. Then, *level one* $K3$ spaces consist of all the «good» intersections* of two $(n+1)$-dimensional extended vectors, denoted by Π_1. This yields a list of reflexive polyhedra that is more complete than the previous list of polyhedra obtained from n-dimensional projective vectors, i.e., $\Pi_0 \subseteq \Pi_1$. Continuing, one may define the set of all «good» intersections of *level two*, Π_2, by considering the intersections of three $(n+2)$-dimensional extended vectors, and similarly for the higher levels $3,4,...$:

$$\Pi_0 \subseteq \Pi_1 \subseteq \Pi_2 \subseteq ... \subseteq \Pi_{\text{last}} \tag{9.9}$$

until this process gives us no new reflexive polyhedra. Since the number of distinct reflexive polyhedra in any dimension is finite, e.g., the maximal number of integer points for planar polyherdra is 10, for $K3$ polyhedra it is 39, etc., there exists a maximum last level, after which one cannot find any new types of polyhedra.

Following this approach in the simple case of CY_1 spaces, we recall that we found three planar polyhedra (triangles) at level zero, determined by the three projective vectors $(1,1,1)$, $(1,1,2)$ and $(1,2,3)$. At level one, constructing the 22 chains of $K3$ projective vectors via the 22 «good» intersections of the five types of four-dimensional extended vectors, we now find 7 new planar polyhedra in 9 of the 22 two-vector $K3$ chains, differing from the previous three triangles by the numbers of vertices (V,V^*) and/or by the numbers of integer points (N,N^*) and/or by the areas of these planar polyhedra, as shown in Table 28. To look for further new polyhedra at level 2, one should consider the five following types of vectors: $(1),(1,1),(1,1,1),(1,1,2)$, and $(1,2,3)$, extended to five dimensions. Taking into account all the 50 possible permutations, and looking for the «good» triple intersections, we find among the 259 «good» planar reflexive polyhedra mentioned above just three distinct new polyhedra, which are exhibited in Table 29.

Extending this procedure, we found among the 4242 chains of CY_3 spaces with «good» intersections 730 new $K3$ polyhedra at level one, many with multiple realizations as in Tables 28 and 29. As an example how such new $K3$ spaces emerge, consider the following two-vector CY_3 chain: $m(0,1,1,4,6)+$

*In the sense that they give n-dimensional reflexive polyhedra.

Table 28. The 7 distinct new planar polyhedra, representing new CY_1 spaces, that are found as double intersections involving 9 of the 22 two-vector $K3$ chains. Two realizations each are given for 2 of the new polyhedra

ℵ	$\mathbf{k}_{4ex}^{(i)}$	$\mathbf{k}_{4ex}^{(i)}$	N, N^*	V, V^*
1	$(0,0,1,1)$	$(1,1,0,0)$	$9,5^*$	$4,4^*$
	$(0,0,1,1)$	$(1,1,0,1)$	$9,5^*$	$4,4^*$
2	$(0,0,1,1)$	$(1,2,0,1)$	$7,7^*$	$4,4^*$
3	$(0,1,1,1)$	$(1,0,1,2)$	$8,6^*$	$4,4^*$
4	$(0,1,1,1)$	$(3,0,1,2)$	$4,10^*$	$3,3^*$
5	$(0,1,1,2)$	$(1,1,2,0)$	$5,9^*$	$3,3^*$
	$(0,1,1,2)$	$(2,0,1,3)$	$5,9^*$	$3,3^*$
6	$(0,1,1,2)$	$(2,1,3,0)$	$6,8^*$	$4,4^*$
7	$(0,1,2,3)$	$(3,2,1,0)$	$5,9^*$	$4,4^*$

Table 29. The 3 distinct new planar polyhedra, representing new CY_1 spaces, that are obtainable as triple intersections of five-dimensional extended projective vectors, the sum of which gives the eldest CY_3 projective vector. Three realizations each are given for 2 of the new polyhedra

ℵ	$\mathbf{k}_{5ex}^{(i)}$	$\mathbf{k}_{5ex}^{(i)}$	$\mathbf{k}_{5ex}^{(i)}$	N, N^*	V, V^*
1	$(0,0,0,1,1)$	$(0,1,1,0,0)$	$(1,0,1,0,1)$	$8,6^*$	$5,5^*$
2	$(0,0,0,1,1)$	$(0,1,1,0,1)$	$(1,0,1,1,0)$	$7,7^*$	$5,5^*$
	$(0,0,0,1,1)$	$(0,1,1,0,1)$	$(1,1,2,0,0)$	$7,7^*$	$5,5^*$
	$(0,0,1,1,1)$	$(1,1,0,0,1)$	$(0,1,0,1,2)$	$7,7^*$	$5,5^*$
3	$(0,0,0,1,1)$	$(1,1,1,0,0)$	$(0,1,2,0,1)$	$6,8^*$	$5,5^*$
	$(0,0,0,1,1)$	$(0,1,2,0,1)$	$(2,1,0,1,0)$	$6,8^*$	$5,5^*$
	$(0,0,1,1,1)$	$(0,1,0,1,2)$	$(1,0,2,1,0)$	$6,8^*$	$5,5^*$

$+n(1,0,1,4,6)$. The maximum values of m and n are determined by the dimensions of these extended vectors, namely $d = 12$. This chain contains 46 different $\mathbf{k}_5$ projective vectors. The four-dimensional pentahedroid corresponding to the eldest vector in this chain is shown in Figure 14. As can be seen there, in addition to its 5 vertices, the pentahedroid has 10 one-dimensional edges, 10 two-dimensional triangular faces, and 5 three-dimensional tetrahedral facets.

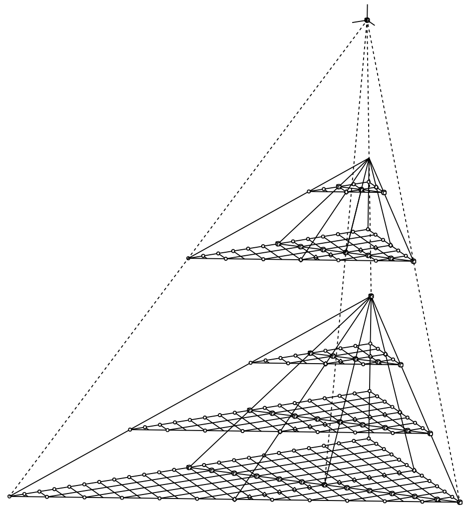

Fig. 14. The 4-dimensional pentahedroid corresponding to the CY_3 space specified by the eldest vector $\mathbf{k}_5 = (1, 1, 2, 8, 12)[24]$ in the two-vector chain $m(0, 1, 1, 4, 6)+$ $+n(1, 0, 1, 4, 6)$. The number of integer points in this pentahedroid is $N(S) = 335$, and the volume $S = 72$. $SL(4, Z)$ transformations produce an infinite number of polyhedroids, conserving the volume

This pentahedroid contains two realizations of the tetrahedron corresponding to $\mathbf{k}_4 = (1, 1, 4, 6)$, whose intersection contains an elliptic fibre corresponding to $\mathbf{k}_3 = (1, 2, 3)$.

A snapshot of the complete $m(0, 1, 1, 4, 6) + n(1, 0, 1, 4, 6)$ chain is shown in Figure 15, where the number of points N in each member of the chain is plotted as a function of $d = k_1 + k_2 + k_3 + k_4 + k_5$ for each of the allowed values of m. We note a systematic tendency for N to *decrease* as d increases. (The structure of the chain is, of course, symmetric under the interchange: $n \leftrightarrow m$). The corresponding plot for the dual polyhedra is shown in Figure 16: here we see that the number of points N^* *increases* as d increases.

To get another impression of the rich new structures emerging at levels one and above, we consider a «tetrahedron subalgebra» of our $K3$ algebra, i.e., we consider only those projective vectors corresponding to point- and segment-polyhedra, triangles and tetrahedra. With this restriction, we start from only 32 $K3$ projective vectors, corresponding to four-vertex tetrahedra and five of our previous extended vectors. In this way, the number of reflexive polyhedra at level one is reduced to just 632, consisting of 460 tetrahedra and 172 reflexive polyhedra with numbers of vertices between 5 and 10. In this list of 632 polyhedra, there are actually only 146 distinct new types of polyhedra, as shown in

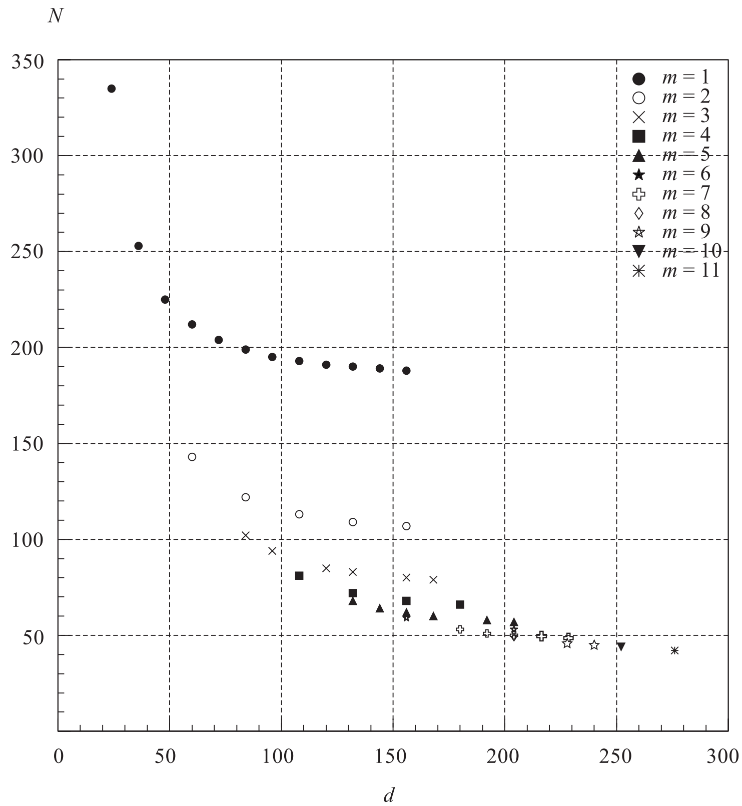

Fig. 15. The number of points N found in different members of the chain $m(0,1,1,4,6)+n(1,0,1,4,6)$, plotted as a function of $d = k_1 + k_2 + k_3 + k_4 + k_5$ for different values of m

Table 30. More information about them can be obtained from [37]: we leave their more detailed study to later work.

The method described here has a very simple geometrical interpretation. According to the chain structure, each CY_3 can have a complex internal structure, and correspondingly its vector can be extended as a sum of two $K3$, three elliptic, four two-component or five single-component extended vectors. Another nice feature of this chain structure is that it gives us complete information about the integer lattice which determines all the CY equations. Moreover, it also gives us the possibility of summarizing the singularity structure of CY_3 spaces. As we discussed in Section 8, the $K3$ polyhedron structure gives us a systematic way of classifying the corresponding Cartan–Lie algebra graphs. It will be interesting to make a full corresponding analysis for CY_3 hypersurfaces, taking duality into

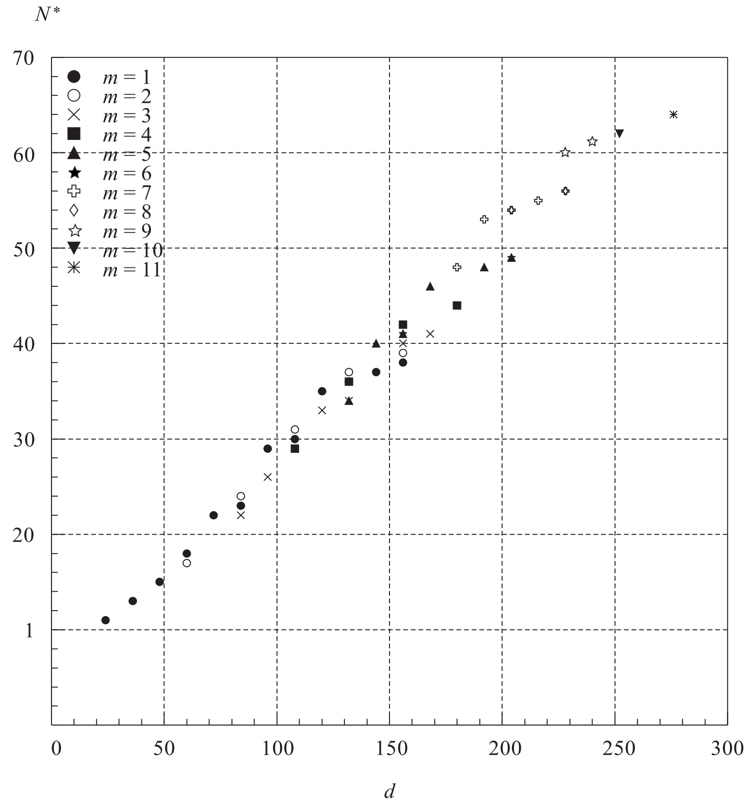

Fig. 16. The number of points N^* found in the polyhedra dual to the previous $m(0,1,1,4,6)+n(1,0,1,4,6)$ chain, plotted as a function of $d=k_1+k_2+k_3+k_4+k_5$ for different values of m

account. This method could also provide the full classification of Betti–Hodge topological numbers for CY_3 manifolds. Moreover, this algebraic method enables us to «walk» between different dimensions, e.g., to classify CY_4, $..._5$,... manifolds (Figure 1). The greatest limitations may be our abilities to analyze this algebra and/or the available computer resources.

A fuller analysis of our structural classification of the $\mathbf{k}_5$ vectors for CY_3 manifolds will be given in later work. An important aspect of this procedure is that we can study the structures of the positive-integer lattices which correspond to the $\mathbf{k}$ vectors, introducing the corresponding modular (for two-dimensional sublattices) and hypermodular (for 3-, 4- or higher-dimensional lattices) transformations. These yield duality groups that are more general than the well-known S, T and U dualities, including them as subgroups. Moreover, the study of the

Table 30. The 146 distinct new polyhedra, representing new $K3$ spaces, that are obtainable as double intersections of projective vectors in the «tetrahedron subalgebra» containing only point- and segment-polyhedra, triangles and tetrahedra. Many of these have several different realizations as double intersections: more details can be found in [37]

$\aleph$	N, N^*	V, V^*	Pic, Pic*	$\aleph$	N, N^*	V, V^*	Pic, Pic*	$\aleph$	N, N^*	V, V^*	Pic, Pic*
1	$31, 6^*$	$6, 5^*$	$2, 18^*$	51	$14, 19^*$	$7, 6^*$	$13, 8^*$	101	$22, 20^*$	$5, 5^*$	$10, 11^*$
2	$28, 9^*$	$7, 6^*$	$4, 16^*$	52	$26, 8^*$	$6, 5^*$	$4, 17^*$	102	$20, 16^*$	$5, 5^*$	$10, 13^*$
3	$29, 7^*$	$6, 5^*$	$4, 17^*$	53	$25, 14^*$	$6, 6^*$	$7, 13^*$	103	$24, 18^*$	$5, 5^*$	$9, 12^*$
4	$22, 8^*$	$6, 5^*$	$7, 16^*$	54	$15, 21^*$	$5, 5^*$	$12, 10^*$	104	$15, 21^*$	$4, 4^*$	$14, 10^*$
5	$31, 9^*$	$6, 5^*$	$3, 17^*$	55	$22, 16^*$	$6, 6^*$	$9, 11^*$	105	$21, 15^*$	$4, 4^*$	$10, 14^*$
6	$21, 12^*$	$7, 6^*$	$8, 13^*$	56	$12, 18^*$	$6, 7^*$	$13, 10^*$	106	$10, 26^*$	$5, 6^*$	$15, 7^*$
7	$17, 20^*$	$7, 7^*$	$11, 9^*$	57	$17, 13^*$	$6, 6^*$	$10, 13^*$	107	$10, 32^*$	$6, 6^*$	$16, 4^*$
8	$22, 14^*$	$6, 6^*$	$8, 13^*$	58	$24, 12^*$	$5, 5^*$	$7, 14^*$	108	$19, 14^*$	$5, 5^*$	$11, 13^*$
9	$24, 12^*$	$6, 5^*$	$7, 14^*$	59	$15, 15^*$	$4, 4^*$	$14, 12^*$	109	$16, 26^*$	$5, 5^*$	$13, 8^*$
10	$20, 12^*$	$6, 6^*$	$10, 13^*$	60	$20, 11^*$	$7, 6^*$	$9, 14^*$	110	$12, 27^*$	$5, 5^*$	$15, 7^*$
11	$20, 20^*$	$6, 6^*$	$10, 10^*$	61	$10, 20^*$	$5, 6^*$	$16, 9^*$	111	$15, 15^*$	$5, 5^*$	$12, 13^*$
12	$13, 14^*$	$6, 6^*$	$13, 11^*$	62	$11, 14^*$	$6, 6^*$	$14, 12^*$	112	$10, 23^*$	$6, 6^*$	$15, 7^*$
13	$26, 8^*$	$6, 5^*$	$5, 17^*$	63	$24, 18^*$	$5, 5^*$	$8, 12^*$	113	$6, 34^*$	$5, 6^*$	$18, 2^*$
14	$26, 7^*$	$6, 5^*$	$5, 17^*$	64	$16, 17^*$	$6, 6^*$	$11, 11^*$	114	$25, 11^*$	$5, 5^*$	$8, 15^*$
15	$18, 8^*$	$6, 5^*$	$9, 16^*$	65	$8, 26^*$	$5, 6^*$	$17, 5^*$	115	$15, 15^*$	$4, 4^*$	$13, 13^*$
16	$24, 10^*$	$6, 6^*$	$6, 15^*$	66	$14, 11^*$	$7, 6^*$	$12, 14^*$	116	$14, 16^*$	$5, 5^*$	$12, 13^*$
17	$11, 11^*$	$4, 4^*$	$15, 15^*$	67	$8, 26^*$	$6, 7^*$	$17, 3^*$	117	$9, 27^*$	$5, 5^*$	$16, 6^*$
18	$21, 17^*$	$7, 7^*$	$9, 11^*$	68	$21, 19^*$	$6, 6^*$	$10, 10^*$	118	$10, 26^*$	$6, 6^*$	$16, 6^*$
19	$14, 15^*$	$6, 6^*$	$12, 11^*$	69	$12, 12^*$	$4, 4^*$	$14, 14^*$	119	$22, 14^*$	$5, 5^*$	$9, 14^*$
20	$23, 11^*$	$5, 5^*$	$7, 15^*$	70	$10, 17^*$	$5, 6^*$	$15, 11^*$	120	$7, 31^*$	$5, 6^*$	$17, 3^*$
21	$10, 20^*$	$7, 7^*$	$15, 7^*$	71	$9, 15^*$	$4, 4^*$	$16, 12^*$	121	$15, 15^*$	$5, 5^*$	$13, 12^*$
22	$7, 23^*$	$5, 6^*$	$17, 5^*$	72	$8, 23^*$	$5, 6^*$	$16, 8^*$	122	$15, 15^*$	$4, 4^*$	$12, 14^*$
23	$10, 14^*$	$5, 6^*$	$15, 12^*$	73	$24, 12^*$	$6, 6^*$	$8, 14^*$	123	$19, 11^*$	$5, 5^*$	$10, 14^*$
24	$12, 12^*$	$6, 6^*$	$13, 13^*$	74	$19, 11^*$	$4, 4^*$	$11, 14^*$	124	$12, 18^*$	$6, 6^*$	$14, 10^*$
25	$6, 30^*$	$4, 4^*$	$18, 4^*$	75	$11, 19^*$	$4, 4^*$	$17, 10^*$	125	$11, 17^*$	$5, 5^*$	$14, 11^*$
26	$25, 11^*$	$6, 6^*$	$6, 14^*$	76	$19, 11^*$	$4, 4^*$	$10, 17^*$	126	$20, 14^*$	$6, 6^*$	$7, 14^*$
27	$12, 12^*$	$4, 4^*$	$16, 14^*$	77	$8, 24^*$	$5, 6^*$	$16, 7^*$	127	$14, 16^*$	$5, 5^*$	$13, 12^*$
28	$21, 9^*$	$4, 4^*$	$9, 17^*$	78	$31, 11^*$	$5, 5^*$	$5, 16^*$	128	$19, 17^*$	$5, 5^*$	$11, 12^*$
29	$15, 15^*$	$5, 6^*$	$11, 12^*$	79	$20, 22^*$	$5, 5^*$	$11, 10^*$	129	$12, 24^*$	$5, 5^*$	$15, 8^*$
30	$12, 12^*$	$4, 4^*$	$14, 16^*$	80	$26, 10^*$	$6, 5^*$	$3, 17^*$	130	$12, 20^*$	$6, 6^*$	$13, 10^*$
31	$31, 8^*$	$5, 5^*$	$4, 17^*$	81	$26, 10^*$	$5, 5^*$	$7, 16^*$	131	$12, 24^*$	$5, 5^*$	$14, 9^*$
32	$17, 11^*$	$6, 5^*$	$9, 16^*$	82	$19, 11^*$	$4, 4^*$	$10, 16^*$	132	$7, 26^*$	$5, 6^*$	$17, 5^*$
33	$20, 10^*$	$5, 5^*$	$9, 16^*$	83	$16, 14^*$	$5, 5^*$	$12, 14^*$	133	$11, 28^*$	$7, 7^*$	$15, 5^*$
34	$18, 12^*$	$5, 5^*$	$11, 14^*$	84	$14, 16^*$	$6, 6^*$	$12, 12^*$	134	$9, 33^*$	$5, 5^*$	$16, 4^*$
35	$15, 12^*$	$4, 4^*$	$13, 13^*$	85	$23, 13^*$	$5, 5^*$	$9, 14^*$	135	$14, 28^*$	$5, 5^*$	$14, 7^*$
36	$9, 21^*$	$4, 4^*$	$17, 9^*$	86	$23, 10^*$	$5, 5^*$	$8, 15^*$	136	$10, 29^*$	$6, 6^*$	$15, 5^*$
37	$25, 17^*$	$6, 6^*$	$8, 12^*$	87	$14, 16^*$	$6, 5^*$	$14, 11^*$	137	$11, 25^*$	$5, 5^*$	$15, 8^*$
38	$15, 21^*$	$5, 5^*$	$13, 10^*$	88	$12, 18^*$	$6, 6^*$	$15, 10^*$	138	$17, 26^*$	$6, 6^*$	$12, 8^*$
39	$17, 10^*$	$6, 5^*$	$11, 15^*$	89	$29, 13^*$	$5, 5^*$	$6, 15^*$	139	$15, 18^*$	$5, 5^*$	$13, 11^*$
40	$10, 23^*$	$6, 6^*$	$16, 7^*$	90	$17, 19^*$	$5, 5^*$	$12, 11^*$	140	$11, 19^*$	$5, 5^*$	$16, 10^*$
41	$13, 28^*$	$7, 7^*$	$14, 6^*$	91	$11, 19^*$	$4, 4^*$	$16, 10^*$	141	$20, 25^*$	$5, 5^*$	$11, 9^*$
42	$24, 21^*$	$5, 5^*$	$9, 11^*$	92	$14, 16^*$	$6, 6^*$	$13, 11^*$	142	$10, 26^*$	$5, 5^*$	$16, 7^*$
43	$9, 24^*$	$5, 5^*$	$17, 7^*$	93	$10, 24^*$	$6, 6^*$	$15, 6^*$	143	$11, 25^*$	$6, 6^*$	$15, 7^*$
44	$12, 30^*$	$6, 6^*$	$15, 5^*$	94	$8, 34^*$	$5, 6^*$	$17, 3^*$	144	$9, 33^*$	$5, 5^*$	$17, 4^*$
45	$21, 9^*$	$5, 5^*$	$8, 16^*$	95	$14, 16^*$	$5, 5^*$	$14, 12^*$	145	$11, 13^*$	$5, 5^*$	$14, 13^*$
46	$16, 11^*$	$6, 5^*$	$11, 13^*$	96	$16, 15^*$	$7, 6^*$	$12, 12^*$	146	$9, 36^*$	$5, 5^*$	$17, 3^*$
47	$11, 16^*$	$7, 7^*$	$13, 9^*$	97	$11, 31^*$	$5, 5^*$	$16, 5^*$				
48	$26, 10^*$	$6, 5^*$	$6, 15^*$	98	$9, 30^*$	$6, 7^*$	$16, 4^*$				
49	$18, 12^*$	$6, 5^*$	$11, 13^*$	99	$14, 10^*$	$6, 5^*$	$12, 15^*$				
50	$12, 22^*$	$6, 7^*$	$14, 8^*$	100	$9, 28^*$	$6, 7^*$	$16, 5^*$				

geometric properties of the one-dimensional complex torus, two-dimensional $K3$ hypersurfaces and Calabi–Yau manifolds with dimensions $d = 3, 4, ...$ gives insight into the possible rank and dimensions of the Lie algebras which may be important for the understanding of the nature of the symmetries used in high-energy physics.

Acknowledgements. G.V. thanks H.Dahmen, G.Harigel, L.Fellin, V.Petrov, A.Zichichi and the CERN Theory Division for support. We all thank F.Cindolo and A.Toukhtarov for technical help and support. The work of D.V.N. was supported in part by DOE grant No. DE-FG-0395ER40917.

REFERENCES

1. **Schwarz J.** — Nucl. Phys. Proc. Suppl., 1997, v.B55, p.1;
Polchinski J. — String Duality: A Colloquium, Rev. Mod. Phys., 1996, v.68, p.1245; TASI Lectures on D-Branes, NSF-ITP-96-145; hep-th/9611050;
Sen A. — Unification of String Dualities, Nucl. Phys. Proc. Suppl., 1997, v.58, p.5; An Introduction to Nonperturbative String Theory, MRI-PHY-P980235; hep-th/9802051;
Duff M. — M-Theory (The theory formerly known as strings), Int. J. Mod. Phys., 1996, v.A11, p.5623;
Townsend P. — Four Lectures on M-Theory, DAMTP-R-96-58; hep-th/9612121;
Douglas M. — Superstring Dualities, Dirichlet Branes and the Small Scale Structure of Space, RU-96-91; hep-th/9610041;
Förste S., Louis J. — Quaternions and M-Theory in Spaces with Boundaries, HEP-UK-0002; hep-th/9612198;
Vafa C. — Lectures on Strings and Dualities, HUTP-97-A009; hep-th/9702201;
Ibáñez L.E., Uranga A. — $D = 6, N = 1$ String Vacua and Duality, FTUAM-97-9; hep-th/9707075;
Gómez C., Hernández R. — Fields, Strings and Branes, IFT-UAM-CSIC-97-4; hep-th/9711102.
2. **Polchinski J.** — Dirichlet-Branes and Ramond-Ramond Charges, Phys. Rev. Lett., 1995, v.75, p.4724;
Townsend P. — D-Branes from M-Branes, Phys.Lett., 1995, v.B360, p.13;
Bachas C. — Lectures on D-Branes, CPHT-CL-615-0698; hep-th/9806199;
Bachas C. — Scales of String Theory, Class. Quant. Grav., 2000, v.17, p.1.
3. **Aldazabal G., Ibáñez L.E., Quevedo F.** — A D-Brane Alternative to the MSSM, FTUAM-2000-001; hep-ph/0001083;
Berglund P., Ellis J., Faraggi A., Nanopoulos D.V., Qiu Z. — Elevating the Free-Fermion $Z_2 \times Z_2$ Orbifold Model to a Compactification of F-Theory, ACT-12-98; hep-th/9812141;
Antoniadis I. — Mass Scales in String and M-Theory, CPHT-CL741; hep-th/9909212.
4. **Calabi E.** — On Kahler Manifolds with Vanishing Canonical Class, in: Algebraic Geometry and Topology, A Symposium in Honor of S. Lefshetz, 1955, Princeton University Press, Princeton, NJ, 1957;
Yau S.-T. — Calabi's Conjecture and Some New Results in Algebraic Geometry, Proc. Nat. Acad. Sci., 1977, v.74, p.1798;
Candelas P., Horowitz G., Strominger A., Witten E. — Nucl. Phys., 1985, v.B258, p.46;
Hübsch T. — Calabi–Yau Manifolds — A Bestiary for Physicists. World Scientific Pub. Co., Singapore, 1992.
5. **Satake I.** — On a Generalization of the Notion of Manifold, Proc. Nat. Acad. Sci. USA, 1956, v.42, p.359;

Dixon L., Harvey J.A., Vafa C., Witten E. — Strings on Orbifolds, Nucl. Phys., 1985, v.B261, p.678, and 1986, v.B274, p.285.

6. **Schwarz J.H.** — Introduction to M-Theory and AdS/CFT Duality, CALT-68-2204; hep-th/9812037 and references therein;
Duff M. — TASI Lectures on Branes, Black Holes and Anti-de Sitter Space, UM-TH-99-07; hep-th/9912164;
Greene B. — D-Brane Topology Changing Transitions, Nucl. Phys., 1998, v.B525, p.284;
Greene B., Lazaroiu C., Raugas M. — D-Branes on Non-Abelian Threefold Quotient Singularities, Nucl. Phys., 1999, v.B553, p.711.

7. **Batyrev V.** — Dual Polyhedra and Mirror Symmetry for Calabi–Yau Hypersurfaces in Toric Varieties, J. Algebraic Geom., 1994, v.3, p.493;
Batyrev V. — Variations of the Mixed Hodge Structure of Affine Hypersurfaces in Algebraic Tori, Duke Math. J., 1993, v.69, p.349;
Batyrev V., Cox D. — On the Hodge Structure of Projective Hypersurfaces in Toric Varieties, Duke Math. J., 1994, v.75, p.293.

8. **Aspinwall P.** — K3 Surfaces and String Duality, RU-96-98; hep-th/9611137;
Kreuzer M., Skarke H. — Classification of Reflexive Polyhedra in Three Dimensions, Adv. Theor. Math. Phys., 1998, v.2, p.847;
Nikulin V.V. — Surfaces of Type K3 with Finite Automorphism Group and Picard Group of Rank Three, Proc. Steklov Math. Inst.,1985, v.3, p.95;
Kreuzer M., Skarke H. — Reflexive Polyhedra, Weights and Toric Calabi–Yau Fibrations, HUB-EP-00/03, TUW-00/01, math.AG/0001106.

9. **Font A., Ibáñez L., Lüst D., Quevedo F.** — Strong-Weak Coupling Duality and Nonperturbative Effects in String Theory, Phys. Lett., 1990, v.B249, p.35;
Sen A. — Strong-Weak Coupling Duality in Four-Dimensional Field Theory, Int. J. Mod. Phys., 1994, v.A9, p.3707;
Hull C., Townsend P. — Unity of Superstring Dualities, Nucl. Phys., 1995, v.B438, p.109;
Duff M. — Strong/Weak Coupling Duality from the Dual String, Nucl. Phys., 1995, v.B442, p.47;
Townsend P. — The Eleven-Dimensional Supermembrane Revisited, Phys. Lett., 1995, v.B350, p.184;
Witten E. — String Theory Dynamics in Various Dimensions, Nucl. Phys., 1995, v.B443, p.85;
Sen A. — String-String Duality Conjecture in Six Dimensions and Charged Solitonic Strings, Nucl. Phys., 1995, v.B450, p.103;
Schwarz J., Sen A. — Nucl. Phys., 1994, v.B411, p.35.

10. **Alvarez-Gaume L., Zamora F.** — Duality in Quantum Field Theory (and String Theory), CERN-TH/97-257; hep-th/9709180.

11. **Dixon L.** — Some World-Sheet Properties of Superstring Compactifications on Orbifolds and Otherwise, in: Superstrings, Unified Theories, and Cosmology, 1987. World Scientific Pub. Co., Singapore, New Jersey, Hong Kong, 1988, p.67.

12. **Lerche W., Vafa C., Warner N.** — Chiral Rings in N=2 Superconformal Theories, Nucl. Phys., 1989, v.B324, p.251.

13. **Candelas P., Lynker M., Schimmrigk R.** — Calabi–Yau Manifolds in Weighted P_4, Nucl. Phys., 1990, v.B341, p.383.

14. **Roan S.** — The Mirror of Calabi–Yau Orbifold, Internat. J. Math., 1991, v.2, p.439.

15. **Aspinwall P., Greene B., Morrison D.** — The Monomial-Divisor Mirror Map, alg-geom/9309007.

16. **King B.** — Beyond the Quartic Equation. Birkhäuser, Boston, 1996;
Ribenboim P. — Fermat's Last Theorem. Springer-Verlag, New York, 1999.

17. **Lang S.** — Elliptic Functions. Addison-Wesley Pub. Co., Reading, Massachusetts, 1973.

18. **Bershadsky M., Johansen A., Pantev T., Sadov V., Vafa C.** — F-Theory, Geometric Engineering and $N = 1$ Dualities, Nucl. Phys., 1997, v.B505, p.153;
Katz S., Vafa C. — Geometric Engineering of $N = 1$ Quantum Field Theories, Nucl. Phys., 1997, v.B497, p.196;
Katz S., Vafa C. — Matter from Geometry, Nucl. Phys., 1997, v.B497, p.146;
Douglas M., Katz S., Vafa C. — Small Instantons, del Pezzo Surfaces and Type-II Theory, Nucl. Phys., 1997, v.B497, p.155.

19. **Duff M., Minasian R., Witten E.** — Evidence for Heterotic/Heterotic Duality, Nucl. Phys., 1996, v.B465, p.413;
Witten E. — Small Instantons in String Theory, Nucl. Phys., 1996, v.B460, p.541;
Polchinski J., Witten E. — Evidence for Heterotic — Type I String Duality, Nucl. Phys., 1996, v.B460, p.525;
Sethi S., Vafa C., Witten E. — Constraints on Low-Dimensional String Compactifications, Nucl. Phys., 1996, v.B480, p.213;
Horava P., Witten E. — Eleven-Dimensional Supergravity on a Manifold with Boundary, Nucl. Phys., 1996, v.B475, p.94;
Candelas P., Perevalov E., Rajesh G. — F-Theory Duals of Nonperturbative Heterotic $E_8 \times E_8$ Vacua in Six Dimensions, Nucl. Phys., 1997, v.B502, p.613;
Morrison D., Vafa C. — Compactifications of F-Theory on Calabi–Yau Threefolds–I, Nucl. Phys., 1996, v.B473, p.74;
Aldazabal G., Font A., Ibáñez L.E., Uranga A.M. — New Branches of String Compactifications and Their F-Theory Duals, Nucl. Phys., 1997, v.B492, p.119;
Klemm A., Lian B., Roan S-S., Yau S. — Calabi–Yau Fourfolds for M- and F-Theory Compactifications, Nucl. Phys., 1998, v.B518, p.515;
Aspinwall P., Katz S., Morrison D. — Lie Groups, Calabi–Yau Threefolds, and F-Theory, DUKE-CGTP-00-02, OSU-Math-2000-3; hep-th/0002012.

20. **Douglas M.** — Enhanced Gauge Symmetry in M-Theory, JHEP, 1997, 9707, p.004;
Greene B., Morrison D., Strominger A. — Black Hole Condensation and the Unification of String Vacua, Nucl. Phys., 1995, v.B451, p.109;
Strominger A. — Massless Black Holes and Conifolds in String Theory, Nucl. Phys., 1995, v.B451, p.96;
Strominger A. — Statistical Hair on Black Holes, Phys. Rev. Lett., 1996, v.77, p.3498;
Strominger A. — Black Hole Condensation and Duality in String Theory, Nucl. Phys. Proc. Suppl., 1996, v.46, p.204.

21. **Schlichenmaier M.** — An Introduction to Riemann Surfaces, Algebraic Curves and Moduli Spaces. Springer-Verlag, Berlin, Heildeberg, 1989.

22. **Shafarevich I.** — Basic Algebraic Geometry 1,2. Springer-Verlag, Berlin, 1994.

23. **Kostrikin A., Shafarevich I.** — Algebra. Springer-Verlag, Berlin, 1990.

24. **Dimka A.** — Singularities and Topology of Hypersurfaces. Springer-Verlag, Berlin, 1992.

25. **Barth W., Peters C., Van de Ven A.** — Compact Complex Surfaces. Springer-Verlag, Berlin, 1984.

26. **Miranda R.** — Smooth Models for Elliptic Threefolds, in: The Birational Geometry of Degenerations, R. Friedman and D.R. Morrison (eds.), Birkhäuser, Boston, 1983.

27. **Greene B., Plesser M.** — Duality in Calabi–Yau Moduli Spaces, Nucl. Phys., 1990, v.B338, p.38.

28. **Lamotke K.** — Regular Solids and Isolated Singularities, Advanced Lectures in Mathematics. Braunschweig, Wiesbaden, Vieweg, 1986.

29. **Cox D.** — Recent Developments in Toric Geometry, in: Proc. Sympos. Pure Math., v.62, Part 2, Amer. Math. Soc., Providence, RI, 1997; alg-geom/9606016.

30. **Du Val P.** — Homographies, Quaternions and Rotations. Clarendon Press, Oxford, 1964;
Dimca A. — Singularities and Topology of Hypersurfaces. Springer-Verlag, New York, 1992;
Barth W., Peters C., Van de Ven A. — Compact Complex Surfaces. Springer-Verlag, Berlin, Heidelberg, 1984.

31. **Parker Manning H.** — Geometry of Four Dimensions. Dover Pub. Inc., New York, 1956.

32. **Fulton W.** — Introduction to Toric Varieties. Princeton Univ. Press, Princeton, NJ, 1993.

33. **Greene B.R.** — String Theory on Calabi–Yau Manifolds, CU-TP-812; hep-th/9702155.

34. **Candelas P., Font A.** — Duality Between the Webs of Heterotic and Type II Vacua, Nucl. Phys., 1998, v.B511, p.295;
Candelas P., Perevalov E., Rajesh G. — Toric Geometry and Enhanced Gauge Symmetry of F-Theory/Heterotic Vacua, Nucl. Phys., 1997, v.B507, p.445;
Candelas P., Perevalov E., Rajesh G. — Matter from Toric Geometry, Nucl. Phys., 1998, v.B519, p.225;
Candelas P., Skarke H. — F-Theory, SO(32) and Toric Geometry, Phys. Lett., 1997, v.B413, p.63;
Perevalov E., Skarke H. — Enhanced Gauge Symmetry in Type II and F-Theory Compactifications: Dynkin Diagrams from Polyhedra, Nucl. Phys., 1997, v.B505, p.679;
Perevalov E. — On the Hypermultiplet Moduli Space of Heterotic Compactifications with Small Instantons; hep-th/9812253;
Skarke H. — String Dualities and Toric Geometry: An Introduction, UTTG-09-97; hep-th/9806059.

35. **Bershadsky M., Intriligator K., Kachru S., Morrison D.R., Sadov V., Vafa C.** — Geometric Singularities and Enhanced Gauge Symmetries, Nucl. Phys., 1996, v.B481, p.215.

36. **Tate J.** — Algorithm for Determining the Type of a Singular Fiber in an Elliptic Pencil, in: Modular Functions of One Variable IV, Lecture Notes in Math., v.476. Springer-Verlag, Berlin, 1975.

37. Files containing these lists are available on request from `Francesco.Anselmo@cern.ch`.